University of Coimbra

Faculty of Science and Technology

Department of Electrical and Computer Engineering

DESIGN, IMPLEMENTATION, PATH PLANNING, AND CONTROL OF A POLE CLIMBING ROBOT

PhD Thesis

Mahmoud Tavakoli

Coimbra, July 2010

University of Coimbra

Faculty of Science and Technology

Department of Electrical and Computer Engineering

DESIGN, IMPLEMENTATION, PATH PLANNING, AND

CONTROL OF A POLE CLIMBING ROBOT

Thesis submited:

to the Electrical and Computer Engineering Department of the Faculty of Science and Technology of the University of Coimbra in partial fulfillment of the requirements for the Degree of Doctor of Philosophy.

Mahmoud Tavakoli

Coimbra, July 2010

This thesis is realized under Supervision of

Professor Doctor Aníbal Traça de Almeida

Full Professor of the

Faculty of Science and Technology, University of Coimbra

and

Professor Doctor Lino José Forte Marques

Auxiliary Professor of the

Faculty of Science and Technology, University of Coimbra

This thesis is dedicated to my parents, Esmaeil and Mahnaz, and to my wife Leila.

Resumo

Os robôs de trepar estruturas têm inúmeras aplicações no campo da inspecção de estruturas tubulares tridimensionais construídas pelo Homem. A aplicação que mais se destaca é a inspecção periódica com recurso a sondas de testes não destrutivos (NDT) de forma a determinar o estado de degradação da estrutura bem como identificar possíveis defeitos nas soldaduras. Hoje em dia, as inspecções deste tipo são realizadas por técnicos especializados que se deslocam através das estruturas enquanto estas estão a ser utilizadas, normalmente transportando substâncias químicas perigosas. Este tipo das tarefas é designado na literatura inglesa como tarefas DDD (de *Dirty*, *Dangerous* and *Difficult* - Sujas, Perigosas e Difíceis).

Se um Robô for capaz de trepar estruturas tubulares 3D com curvas e ramificações, bem como realizar uma digitalização de toda a sua superfície exterior, então pode ser equipado com sondas NDT de forma a executar inspecções autónomas. Este cenário seria mais seguro, barato e provavelmente, mais rápido do que utilizando as técnicas actuais. A investigação na área dos robôs de trepar tem-se focado maioritariamente em robôs de trepar paredes (WCRs), sendo o número de trabalhos sobre robôs de trepar estruturas (PCRs) bastante reduzido. Isto deve-se à dificuldade acrescida no desenvolvimento de PCRs comparativamente aos WCRs, já que os PCRs necessitam de garras dedicadas e graus de liberdade adicionais. Dentro dos PCRs, há que distinguir os robôs simples, capazes de trepar apenas estruturas tubulares lineares daqueles capazes de lidar com curvas e ramificações. Esta tese trata do projecto e desenvolvimento de um robô industrial do tipo PCR, capaz de trepar e varrer estruturas 3D com um mínimo de graus de liberdade. Este robô é capaz de ultrapassar secções curvas e em T, sendo ainda capaz de varrer a estrutura com uma sonda de inspecção sem recorrer a um braço extra.

Abstract

Pole climbing robots have many applications in the inspection of human made 3D tubular structures. The most important application is performing periodical inspections by NDT probes in order to detect the progression of material degradation and welding defects.

Nowadays, NDT methods are applied by dextrous technicians in elevated structures, while dangerous chemicals run inside the pipes. These jobs can be categorized as DDD (or 3D) jobs (jobs that are Dirty, Dangerous, and Difficult). In the United States, wages for DDD jobs can be over 70,000 USD annually, even though there are lack of workers for such jobs.

If a robot is able to climb across 3D tubular structures with bends and branches and also scan all of its exterior surface, it might be equipped with NDT probes to perform autonomous inspections. This is safer, cheaper, and probably faster to do than using human workers.

Previous researches on climbing robots all around the world focused mostly on Wall Climbing Robots (WCRs) and only a few research works were performed on Pole Climbing Robots (PCRs). The reason is the higher difficulty in designing PCRs compared to WCRs, as WCRs use standard grippers like vacuum cups or magnets to stick to the surface, PCRs need dedicated grippers. Furthermore there are fundamental differences between simple PCRs that only climb from a straight pole and those that should pass bends and branches. This thesis presents the "Design, development and automation of an industrial pole climbing and manipulating robot with minimum possible degrees of freedom, which is able to overcome bends and T-junctions of a structure, manipulate across the structure, and scan all of its surface, without need to an extra arm."

Acknowledgment

I would like to thank Doctor Lino Marques and Doctor Aníbal Traça de Almeida for their supervision, support and encouragement; ISR-UC for the facilities provided and project financing and Foundation of Science and Technology for the scholarship SFRH / BD / 29883 / 2006 that they provided during my study; I would like to thank some of my colleagues Ali Marjovi, Svetlana Larionova, Grzegorz Tomaszewski, José Francisco, Pedro Oliveira, Pedro Sousa, Ricardo Faria, Gonçalo Cabrita and Joao Lucas for their supports on my project and for their friendship and Mitra Shahabi for the proofreading of this thesis. I would also like to thank my kind parents for their love and support from many kilometers away. I would like to especially thank my wife Leila, for all her love, patience, support and inspiration.

Contents

List of Figures

List of Tables

List of Abbreviation

2D   2 Dimensional.

3D   3 Dimensional.

AuRA   Autonomous Robot Architecture.

CAN   Controller Area Network.

DDD   Dirty, Dangerous, Difficult.

DOF   Degree(s) Of Freedom.

FOS   Factor Of Safety.

FSR   Force Sensitive Resistors.

GUI   Graphical User Interface.

I/O   Input-Output.

ISR-UC   Instituto de Sistemas e Robótica da Universidade de Coimbra.

JAUS   Joint Architecture for Unmanned Systems.

NDT   Non Destructive Test.

PAM   Pneumatic Artificial Muscle.

PCR   Pole Climbing Robot.

PCRs   Pole Climbing Robots.

PM   Pneumatic Muscle.

TCP/IP   Transmission Control Protocol/Internet Protocol.

USD   United States Dollar.

WCRs   Wall Climbing Robots.

Chapter 1

Introduction

1.1 Motivation

Climbing robots have received an increasing attention during the last decade due to their potential applications in the maintenance of tall buildings, agricultural harvesting, highways and bridge maintenance, shipyard production facilities, etc. Pole Climbing Robots (PCR), form a branch of climbing robots which are usually considered for inspection and maintenance of structures with circular cross section. In this section three different application areas of pole climbing robots are described:

- Inspection of pipelines in industrial plants

- Maintenance of lighting poles in highways

- Elevated observer in disasters and beacon for swarm robot rescue navigation

An important application area for PCRs is inspection and maintenance of pipelines. Oil refineries, nuclear plants, fertilizer plants, petrochemical plants, and cement plants need to monitor the condition of their equipment to detect the progression of material degradation and welding defects specially in their static pressure equipments, reservoirs, and pipes. Any failure in the mentioned plants may result in a disaster similar to what happened in Chernobyl in 1986 (Figure 1.1). Periodical tests are necessary to locate possible defection, and prevent failures. Many

Figure 1.1: Chernobyl disaster is considered as the worst nuclear power plant disaster in history.

NDT methods were developed for monitoring material degradation by employing appropriate techniques and equipments implemented by well trained technicians. Some examples are:

- **Ultrasonic wall thickness measurement** using digital thickness gauges to monitor reduction in thickness due to corrosion and erosion [Sit08].

- **Magnetic Particle Inspection** of welds in high pressure piping and vessels. The objective of testing is to detect cracks in the welding, heat affected zone, and adjacent parent material [Sit08].

- **A Liquid penetrant inspection** is a low cost and easy to perform method which looks for surface defects in a variety of nonferrous materials including some metals, plastics, rubber, and ceramics. It can also be very precise, revealing flaws such as cracks caused by fatigue, damage, strain, or improper manufacturing when these cracks are too small to be seen in a casual visual inspection. In a liquid penetrant inspection a dye is applied to the surface and the excess dye is wiped off. Then a developer is applied and dye which has adhered to cracks and other defects will activate the developer, revealing flaws in the surface of the material being tested [Sit08].
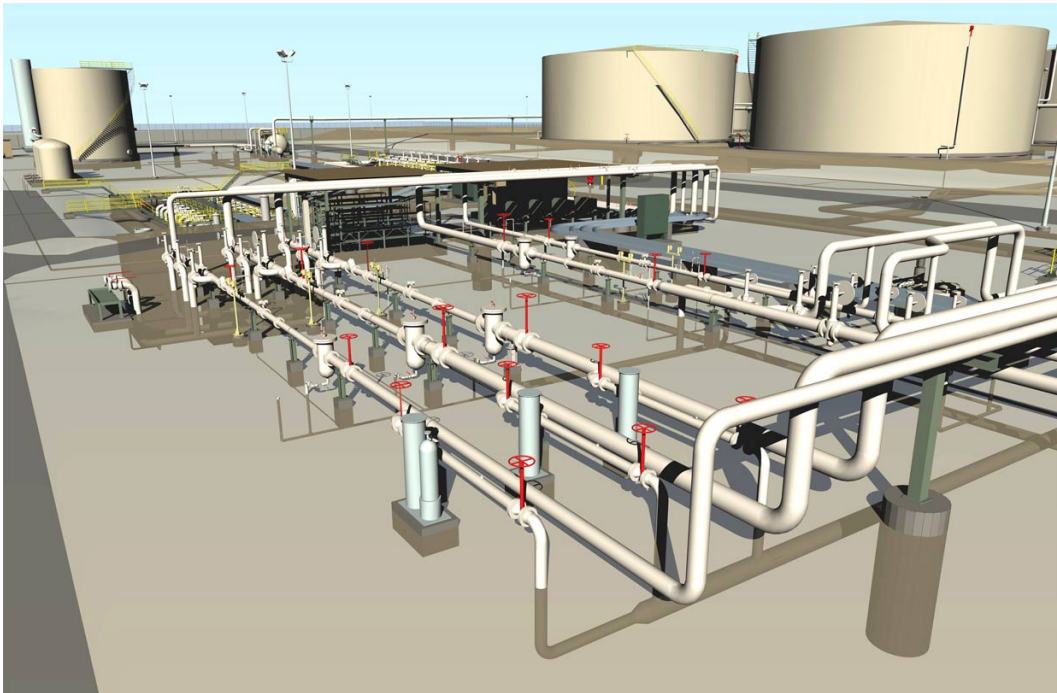
Figure 1.2: A typical piping model in an industrial plant.

- **Ultrasonic flaw detection** is used for pipe lines operating under combinations of high pressure and temperature, where the material failure due to the phenomena of creep starts from inner surface and proceeds to the pipe outer diameter giving way to direct leak path or sudden failure. Ultrasonic flaw detection detects initiation and progression of such cracks [Sit08].

To perform NDT methods, usually a probe should approach to the testing area. Figure 1.2 shows a typical piping installation which can be found in such plants. The inspection of such piping is very difficult, not only due to the height of the pipes, but also because of radioactive radiation on nuclear plants or chemical pollution in oil and gas industries. In the current approach for performing these tests, a human worker carries the probe to the test areas. This is not a problem until the job is done on the floor, but applying NDT in elevated structures, where dangerous chemicals or hot fluids run inside the pipes and the working area is polluted by chemicals, makes it extremely difficult and can be categorized in the 3D jobs (jobs that are Dirty, Dangerous, and

Figure 1.3: Inspection of pipelines in refineries is a difficult and dangerous job.

Difficult). In the United States, wages for 3D occupations can be over 70,000 USD annually, even though there are lack of workers who wish to do such jobs. On the other hand since these jobs are dangerous to human life, employers should buy a very expensive life insurance for their employees. Power line and lamp posts are other examples of tall structures, which need regular repairs and maintenance. Like the previous examples, these jobs also require skilled and fearless workers (See figure 1.3).

If a climbing robot has the ability of climbing from such structures and carrying the test probe to the test area, it will address this problem. If the robot can climb over such structures and scan the whole surface of the pipes, one can equip it with NDT probes and do the required testing automatically. This method is safer, cheaper, and probably faster to do than using human workers. This is the main application of PCRs.

The second application area of PCRs is maintenance of lighting poles in the highways, including simple tasks like washing the pole surface to more complicated missions such as changing the damaged lamp bulb with a new one.

The third application area for PCRs was discussed in a European project called GUARDIANS. GUARDIANS is a Group of Unmanned Autonomous Robots for Discovery and Information Acquisition, Navigating to detect chemicals and explosives. The GUARDIANS project developed a swarm of autonomous robots to survey, inspect and map two types of terrains, a partly destroyed urban area and a havocked country side. The swarm included mobile wheeled robots. During the experiments of the swarm, the project partners declared the need for an elevated observer as well as an elevated beacon. As the GUARDIANS swarm aims to explore areas after a disaster and provide quick information to authorities, installation of an observer and/or a beacon in an elevated structure is time consuming. But a PCR can climb from a lighting pole and carry the necessary equipments, providing beacon for communication between robots, which is not effected by local on land obstacles and can provide live video broadcast for authorities.

1.2 State of the art

During the last two decades, different types of climbing robots were developed either for climbing over flat or curved surfaces. In this section, first a short categorization of various climbing robots including wall climbing robots and in pipe robots will be presented. Then a deeper study

about pole climbing robots which have been developed will be presented.

In the category of wall climbing robots, to hold the robot attached to a smooth surface, suction cups [DT02, NH94, Rac02, RPRC01, YSD$^+$99] or magnets [CPA$^+$98, HNT91] have been used. Robots whose end-effectors match engineered features of the environment like fences, porous materials, or bars [BDM00, XBFK94, YHR01, AOT01] have been also developed.

Furthermore robots for climbing inside pipes or ducts have received an increasing attention due to their applications in pipe inspection. Most of the already developed in pipe robots [Neu94, RP97, HOMS99, OO05, RC05, RKL$^+$09, LMLW09] have similar mechanical structures. They use springs to push derived wheels to the internal circumference of the pipe. Recently developed in-pipe robots use linkages to overcome the bent sections and T-junctions.

During the last two decades, most of the research in the area of climbing robots focused on WCRs and in pipe robots and only a few number of PCRs were designed and developed. Generally, design and implementation of PCRs face more problems than those of WCRs and in-pipe robots. Many factors contribute to this. For instance using vacuum grippers on human made 3D structures like poles and scaffolds is not a good choice because the vacuum system can not work efficiently on curved surfaces. Another example is wheeled wall climbing robots. In such WCRs all wheels are on a single plane, but in continuous motion PCRs this is more problematic as the wheels should first encircle the pole and then adapt their diameter to the structure cross section and apply enough normal force to the wheels. It should be noted that design of in-pipe robots is quite different from PCRs as in-pipe robots take advantage of the internal circumference of pipes which is not the case for the PCRs.

Due to many problems associated with the design and development of PCRs, to the best of the author's knowledge less than 10 PCRs have been developed all around the world so far [BGP$^+$00a, ASAR03, RSAS00, TZVB05, BAH05, HH01, HKL$^+$09].

Previously developed PCRs can be categorized into two main design categories.

- Continuous motion PCRs

- Noncontinuous PCRs either with serial, parallel, or hybrid climbing mechanisms.

Continuous motion PCRs [BAH05, HH01] usually take advantage of a simple structure and are faster than step by step based robots, but they have lower maneuverability. This kind of robots are mostly appropriate for climbing over simple poles and performing simple tasks which do not require a manipulator, like washing poles [BAH05]. Figure 1.4 shows a continuous motion PCR developed in University of Tehran [YAH⁺04, MNA06]. This robot aims to wash the poles of highways. The robot uses three spring loaded wheels which encircle the structure. It can climb from straight poles rapidly and continuously. However it can not pass bends or T-junctions and is not able to perform in situ manipulations. The main advantages of continuous motion PCRs include:

- High climbing speed, provided by its continuous climbing mode using wheels.

- Simplicity of the design and implementation.

- Possibility of modular design using similar simple wheeled modules connected to each other through active or passive joints.

The main disadvantages of continuous motion PCRs include:

- Difficulties in passing bent sections: This design group can only pass bent sections of the structure if the robot contains a separate arm or if several continuous motion modules are connected together through active joints, (see [YAH⁺04] and [MNA06]).

- Inability of passing T-junctions: Due to the close structure of each module as it can be seen in [YAH⁺04, MNA06, LXGL07, HH01], it can not pass T-junctions of structures.

- Low maneuverability: To perform some manipulation around the pole, they need an extra articulated arm.
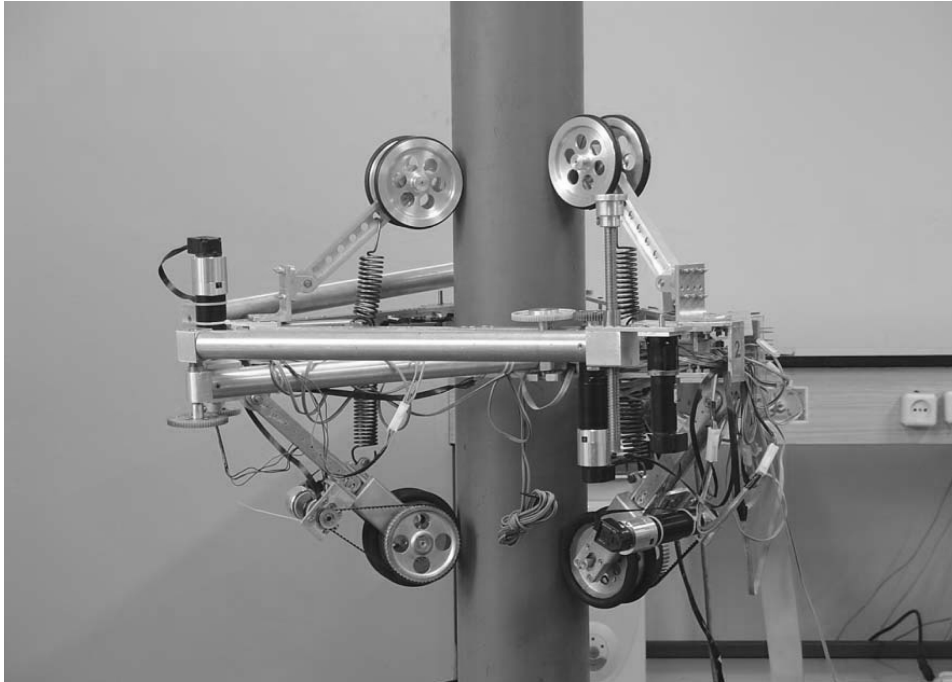
Figure 1.4: A continuous motion PCR developed in University of Tehran for cleaning the poles [YAH⁺04].

- Lack of safety in case of power failure: This is mainly due to the lack of separate climbing and gripping modules. Any failure of the climbing mechanism will be also a failure in the gripping mechanism. There exist passive mechanical locking mechanisms which make the system fault tolerant in case of power failures. For instance application of high ratio gear boxes on gripping mechanism increases the gripper inertia, and locks the grippers at its last pose, e.g. closed, in case of power failure. Such mechanisms might not be used on the continuous motion PCRs as there exist no separate climbing and gripping mechanisms.

A few step by step based PCRs with different types of grippers and climbing mechanisms have been also developed [BGP⁺00a, ASAR03, TZVB05]. But in this area many problems remain unsolved. For example most of the researches were addressing the climbing problem and less efforts were given to address the manipulation over the structure. For instance "ROMA" is a 75 kg pole climbing robot with a 6-DOF serial climbing mechanism[BGP⁺00b] (Figure 1.5)
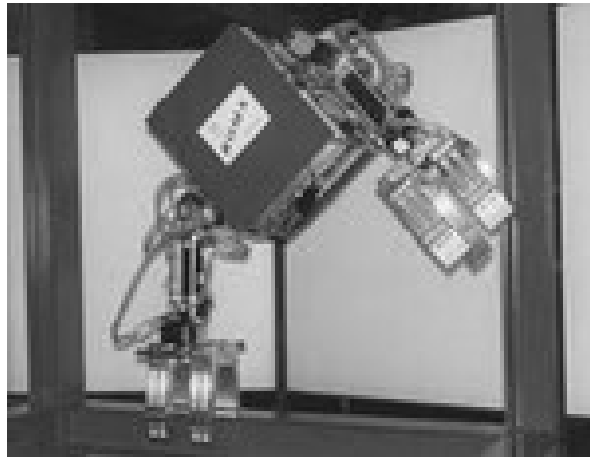
Figure 1.5: "ROMA" is a pole climbing robot with a 6-DOF serial climbing mechanism [BGP$^+$00b].

and the "Trepa" robot is a 6-DOF parallel climbing mechanism pole climbing robot [SARS05] (Figure 1.6). In both cases using a 6 degrees of freedom mechanism make the robots heavy. These studies did not report any analysis about the minimum necessary degrees of freedom for climbing over 3D structures. Excessive degrees of freedom increase the robot's weight without necessarily increasing its efficiency. Furthermore, even when a 6-DOF climbing mechanism is used, such mechanism can be also used for manipulation purposes over the structure. But in none of the previous cases manipulation was considered. For instance in the "Trepa" robot an additional arm is considered for manipulation (Figure 1.6). Another problem of the "Trepa" robot is its closed gripping structure which does not allow passing T-junctions which limits more its maneuverability. Except the fact that maneuverability and manipulation precision of the PCRs have not been studied because the preference was given to address the climbing problem itself, another fact contributing to lack of such studies might be the difficulties associated with the fine manipulation with large actuators.

Recently a quadrupedal PCR which can rapidly climb across straight poles was reported (See figure 1.7 [HKL$^+$09]). This robot takes advantage of a novel biologically inspired gripper. This robot may not be able to climb from metallic surfaces due to the claws-like grippers which are designed to penetrate into the soft materials, like wood. Furthermore the ability of passing the
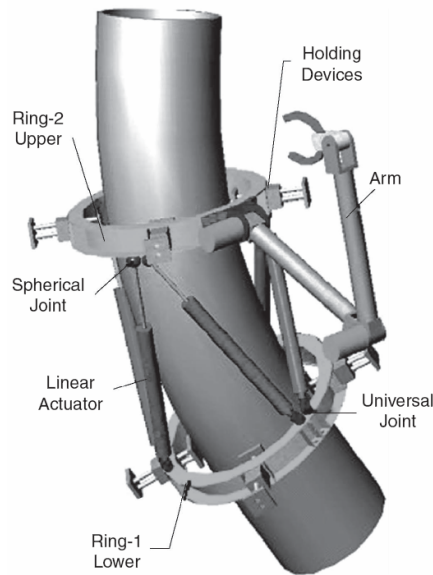
Figure 1.6: "Trepa" robot is a pole climbing robot with a 6-DOF parallel climbing mechanism [SARS05].

bent sections and T-junctions was not reported.

Even though each of the previously mentioned PCRs address some of the relative problems, but none of them considered the whole problem of climbing and manipulating over 3D structures comprehensively. Furthermore, they did not report optimization in the design process. Finally it should be also referred that the manipulation problem of the current PCRs can not be solved by simply adding an additional arm to an existing climbing mechanism as stated in [SARS05] (Figure 1.6) since the accurate positioning of an arm installed on a mobile base will be a problem which should be addressed.

Considering the few researches conducted on the area of pole climbing robots, the previously developed PCRs had one or more of the following problems unsolved:

- Not being able to pass bent sections or branches [BAH05, HH01].

- Having more DOF than necessary, resulting in heavier and slower mechanisms [BGP+00a].
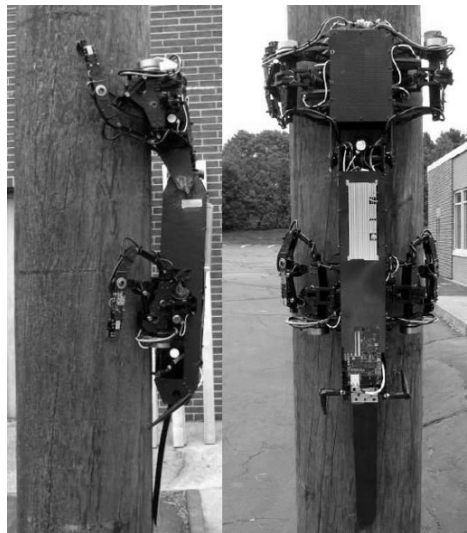
Figure 1.7: The biologically inspired pole climbing robot "RISE" can climb from straight structures with soft and non metallic materials [HKL$^+$09].

- Not being able to perform manipulation and practical operation on the pole, or needing an extra arm to do so [BAH05, ASAR03].

- Lack of analysis on the industrial pipings and not being designed for industrial applications[RSAS00].

1.3 Statement of the problem

To develop an industrial pole climbing robot, able to perform in situ manipulation for NDT in elevated industrial pipings of plants, the definition of the project objectives should consider the size and geometry of the piping in plants. Even though the development of a robot which can climb and manipulate across all kinds of piping and scaffolds with wide range of profile shapes and sizes is not possible due to the large variety of such structures, the wider range of structures that the robot handle, the better.

For a better perception of the problem, an analysis of existing structures is necessary. To develop an industrial PCR, one should consider all problems which are associated with navigation on piping of plants. Figures 1.2 and 1.8 show some examples of typical piping in plants. As it can

be seen the piping includes a range of cross section diameters, bends of 90° and 45°, T-junctions, step changes on cross section size, and also obstacles with large diameters.

Therefore, considering the existing piping and scaffolds in plants, the main objectives of the project are defined as:

- **Design and prototyping of an industrial pole climbing and manipulating robot with the minimum possible degrees of freedom which is able to pass bends and T-junctions, overcome step changes in the cross section, operate in a reasonable range of cross section diameters, scan all of the pole's exterior circumference, and perform in situ manipulation without need for an extra arm. Weight optimization, safety, modularity and simplicity of the design and control should be considered in the design process.**

Modularity grants the robot the ability of operating in a wider range of structures. For instance modular grippers can be developed for different ranges of cross section shapes and diameters, provided that the grippers can be replaced easily and quickly. Weight optimization, safety, tolerance to power failure, climbing speed, etc. are some other parameters which increase the usability of the robot. Such parameters along with an analysis of the problem is discussed more extensively in chapter 2.

1.4   Contributions

The main contribution of this thesis is design and implementation of a novel PCR able to climb and manipulate across industrial 3D structures. The following list describes the main contributions in the design, development and automation process of the 3DCLIMBER (the robot is named "3DCLIMBER") in detail.

- Design of a climbing robot which can pass bends and T-junctions and overcome regular
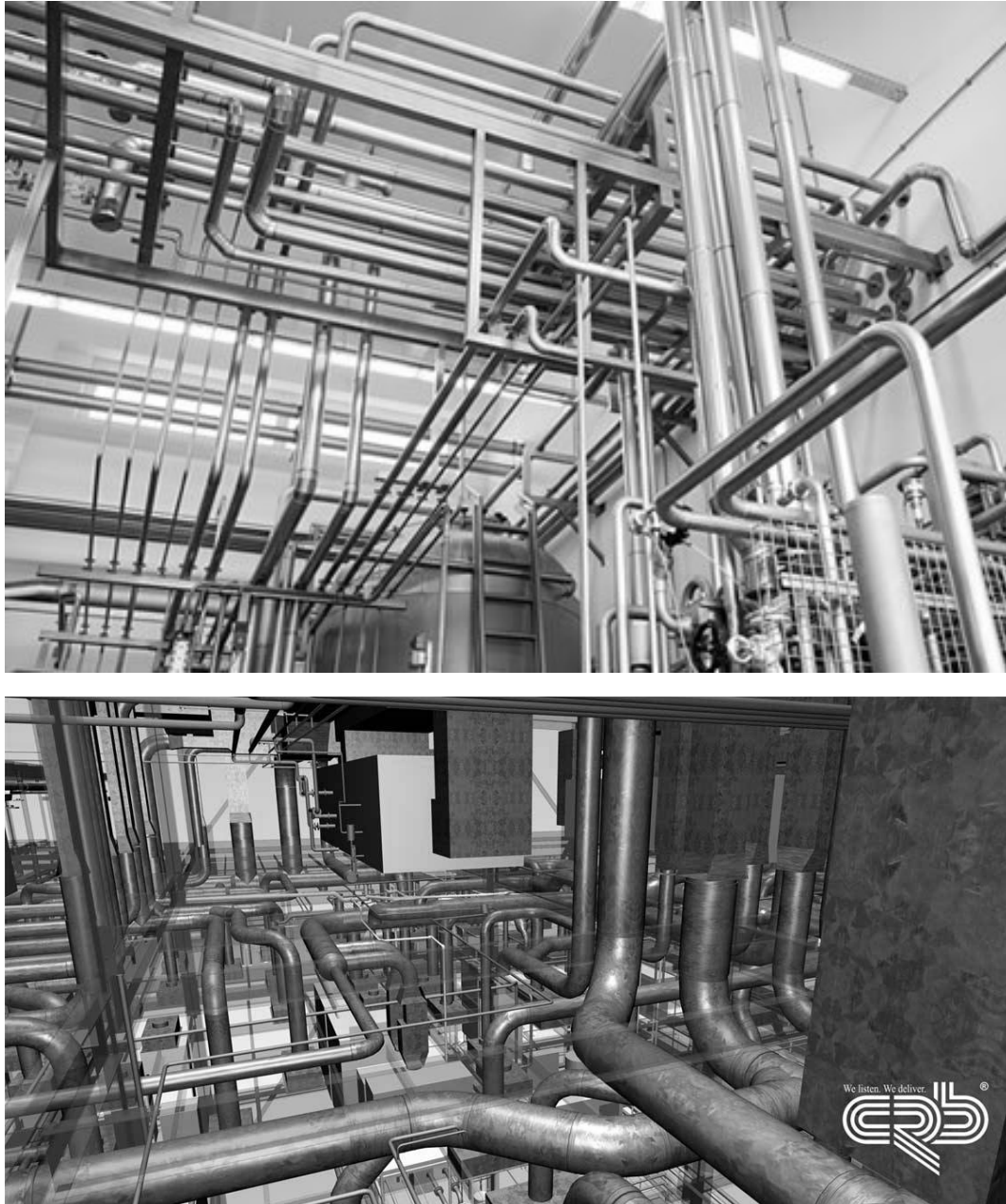
Figure 1.8: typical piping in industrial plants.

and step changes on the cross section size.

- Design and implementation of a climbing mechanism with minimum possible degrees of freedom which makes it possible to scan the whole exterior surface of the structure.

- Design and implementation of unique V-shaped grippers which have a self centering character eliminated the necessity of integration of additional sensors and complicated centering algorithms. Furthermore, design of an open gripping structure, allows full detachment from the structure and thus performance of manipulation across the structure. Being able to perform some manipulation on the structure without an extra arm, means that the robot is able to stay on the pole with only one gripper while the other gripper can detach from the pole and perform the necessary manipulation.

- Design and implementation of grippers which are tolerant to power failure allows the robot to stay on the structure without any active actuator. Even if after grasping the structure, the gripper actuator fails to operate for any reason, the robot will not detach from the structure or slip on it.

- Development and integration of necessary algorithms and low cost sensors for fine manipulation with the serial arm. These algorithms and sensors effectively reduced the positioning errors and can be used for similar articulated arms where the base of the arm is not fix and contains positioning errors.

To achieve all of the mentioned contributions, some innovative designs in the climbing and gripping mechanisms will be introduced.

Furthermore, designing a system involves analysis about the supporting technologies i.e. actuators. In this project two kinds of actuators (pneumatic muscles and electrical rotary actuators) have been analyzed and compared. It is important to mention that in this thesis more emphasis is given to the mechanical design of the robot due to the author's background in mechanical engineering.

1.5   Organization of the thesis

The next chapter specifies the robot mission, including a detailed definition of the project, the desired goals of the robot, and the definition of the type of structures that the robot should climb.

According to the defined mission and the specified structure, some conceptual designs for the robot are proposed in chapter 3, and the design which better fits the project goals is presented. Later in this chapter, a study which determines the minimum necessary degrees of freedom required for a robot to be able to perform all objectives of the project is presented. Then a conceptual design for the climbing mechanism of the robot is presented.

Chapter 4 contains a transition between conceptual and detailed design. Kinematic, workspace, singularity, Jacobean matrix, and dynamic analysis of the conceptual design are presented. All analyses were performed by considering parametric variables as length of the links, mass of the parts etc., as they were unknown in this stage.

Chapter 5 describes the detailed design, prototyping, and assembly of the robot. In all stages of the project from conceptual to detailed design, SolidWorks[web08] was used for 3D modeling of the designs. Using the model and the analysis performed in the previous phase, the lengths of the links were calculated and the actuators were selected. All of these analyses along with the detailed design of non standard parts, and selection process of the standard parts of the robot are presented in chapter 5. Then, a task space trajectory generating algorithm is presented. This algorithm uses the inverse kinematics equations to generate joint space trajectories for the actuators. The final step in the detailed design of the robot is validation of the design. Using the 3D model of the robot and the task space trajectory generation algorithm, a set of robot movements was simulated in Cosmos Motion[web08] and VisualNastran[sC08] simulation softwares. Results from simulation proved the concept and validated the calculated link lengths and the kinematics equations. Furthermore it helped in selecting nearly optimized actu-

ators and link lengths. Manufacturing, assembly, and the mechanical properties of the robot's prototype is presented in the last section of chapter 5.

The electrical architecture of the 3DCLIMBER, motor drivers and sensors utilized for automation of the robot are described in chapter 6. Then in chapter 7 path planning algorithms along with the control and the GUI are presented. Chapter 8 describes the testings and the results. Chapter 9 presents a study about possibility of integration of biologically inspired designs and actuators. To perform this study, another study was achieved to compare pneumatic muscles and rotary electrical actuators in terms of force/torque, weight, power, and size which is also presented.

Chapter 10 concludes the thesis and discusses the future works.

Chapter 2

The Robot Mission

"It is better to know some of the questions than all of the answers."

James Thurber

2.1 Introduction

The detailed and comprehensive definition of a project and its goals orients the project in the proper direction. To achieve this, **the working environment** of the robot (the 3D structure) and **the robot missions** should be well defined. Then we should develop a **robot** which can climb over the designed structure and perform the defined mission.

Furthermore, a robot may achieve a mission, but the quality of the performance should be also evaluated. For example, a mission can be defined as "the robot should reach the pose **P=(x,y,z, θ, γ, ϕ)**", but the quality of the performance can be determined by parameters such as the time that the robot spends to reach **P**, the precision, accuracy and repeatability of the action, etc. Therefore an evaluation method should be defined which receives such data as input and calculates a numerical index for quality of the performance. Although these methods are

17
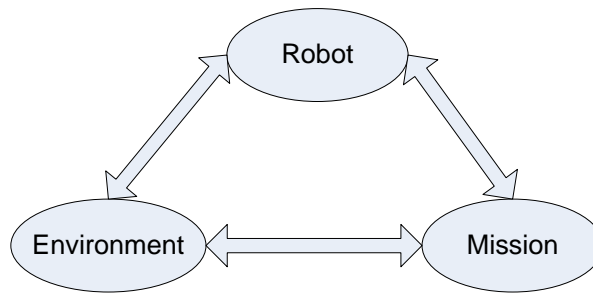
Figure 2.1: Entities involved in a benchmarking process.

used to compare the performance between the already developed robots, they are useful in the early stages of designing a robot. Therefore we defined an evaluation method to compare the performance of the previously developed robots in achievement of some specific tasks, to select the most appropriate mechanisms for the interests of the project. For a more comprehensive definition of the project, measures which help to assess the quality of the performance should be well defined.

This can be achieved by designing a benchmark for PCRs with the objective of pipe inspection in industrial plants. Definition of benchmarks for robotic applications consists of definition of 3 inter-related elements (figure 2.1), which are the robot, the environment, and the mission. A working environment should be fully defined, and then the robot mission should be defined based on the environment. Then the functionality of a robot can be measured according to the level of success in achievement of each task of the mission on the defined environment.
 Benchmarks are usually used to compare performance of different robots performing the same assignment. A benchmark is proposed here that can be used for this goal, but the standardization of a benchmark mainly depends on approval by several experts in this area and also employment of the benchmark by several research groups. On the other hand the measures which are defined in the proposed benchmark will be useful in future, to compare the robot's performance quality after improvements or application of different algorithms. It means to measure the robot performance in different phases of the project. For example if a mechanical system or a con-

trol algorithm does not produce the desired results, one may apply an alternative algorithm or replace an alternative system and then compare the performance of both methods against the designated benchmark.

In this chapter, a short definition of benchmarking will be presented and then a benchmark for PCRs with industrial applications will be proposed. Design and implementation of a 3D structure, definition of the robot missions and metrics for assessment of the robot performance will be also presented. As the objective of this project is to develop an industrial PCR which can make NDT inspections, the definition of the environment, mission, and measures will be according to this objective. It is important to mention that the missions defined in the benchmark are more comprehensive and more idealistic than the objectives of the 3DCLIMBER project, because the benchmark should consider further developments.

2.2 Benchmark

There is, in the robotics community, a growing awareness of the difficulty to compare in a rigorous quantitative way the many research results obtained in the many different application areas of the field. [BHdP09]. Though for pure theoretical articles this may not be the case, typically when researchers claim that their particular algorithm or system is capable of achieving some performance, those claims are intrinsically unverifiable, either because it is their unique system or because lack of experimental details, including working hypothesis [dP06a]. Benchmarking can principally reduce the research efforts by preventing ineffective researches and, as a result of benchmarking one can compare results from different robots and different methods. The importance of robotic benchmarking was discussed by Angel P. del Pobil in [dP06b]. Three essential aspects of benchmarks are: [HPC01]

1. Task: the robot has to perform a given mission.

2. Standard: the benchmark is accepted by a significant set of experts in the field.

3. Precise Definition: the task is described precisely, especially the execution environment, the mission goal, and limiting constraints.

According to dillmann [Dil04], the definition of these three aspects lacks one important feature of benchmarks, which is a numerical evaluation of the performance. Without that, it is only possible to decide whether or not a given system is able to perform a mission. What we need, in fact, is to "develop performance metrics" [JME01] for a given application [Dil04]. There are also disadvantages connected to the introduction of benchmarks. As soon as benchmarks enter the field and are widely respected, researchers and manufacturers are likely to compare and optimize their products to the benchmarks rather than to the real application areas. Whenever there exists a gap between the benchmark and the real world, optimization towards the benchmark test will not necessarily improve the system's performance in the real application [Dil04]. So it is important to consider real applications when designing a benchmark. To address this problem, the proposed benchmarks in this thesis are based on achievement of practical and useful tasks with industrial applications.

2.2.1   Working area of the robot (environment)

According to our previous experiences on design of climbing robots [TZVB05, TZV$^+$04], geometry and size of the structure can have a huge impact on complexity of the robot. Structures can vary from a simple straight pole, to poles with bends and branches, and even with changes on the cross section size. The proposed testing environment should be similar to real human made 3D structures (e.g., pipe structures which are used in petrochemical plants (figure 1.8)). Usually these kind of structures are not only a straight pole, but include bent sections and branches. On the other hand, robots which can just climb over straight poles are very different from those which can overcome bends and branches. They are less complicated in several technical aspects and thus can not be evaluated with the same benchmark designed for those PCRs which can pass bent and branches. Therefore the structure employed in the proposed benchmark includes bents and T-junctions. The angle of bent sections is also an important parameter. Usually in human

made plants, poles and tubes have 90° bends, while in few cases it can be between 90° to 135°. Therefore the bends of the structure are either 90° or 135°.

The size of the structure cross section can also affect the complexity level of the robot. The size of the structure can be defined in a certain range, but if the outer diameter of the cross section profile is very large (e.g. more than 400 mm), wall climbing robots with vacuum or magnet gripper can be used. In this case another benchmark might be proposed which is out of the domain of this thesis. Furthermore we should not consider structures designed specifically to facilitate the robot operation, instead the robot should be designed to operate in common real structures.

According to these considerations a structure was designed and built as shown in (figure 2.2). As it can be seen in the picture, the structure includes bent sections of 90° and 135° degrees. The outer diameter of the pipes is 219 mm and does not include engineered features on the surface (e.g. handles).

2.2.2 Definition of the mission

A mission is defined for the robot considering the defined environment. The mission is defined as:

"The robot should climb over a straight structure and should overcome bent sections and branches. The robot's manipulator should be able to reach to any position in the structure and scan all surface of the structure, since for practical application (e.g. NDT test of welding on the pipe) the robot should be able to reach every position on the structure." Finally the mission is divided to some submissions which are called tasks. The following set of standard tasks are defined:

- Start climbing from one side of the structure.

- Scanning the entire surface of the structure and finding the defected areas and publishing a report of that.

Figure 2.2: Developed structure for pole climbing robot benchmarking.

- Descending from the other side of the structure.

2.2.3   Metrics and quantitative evaluation

To evaluate the performance of robots in achievement of the defined mission on the defined environment, quantitative metrics for different parameters should be considered. Some parameters considered to be used for the performance evaluation of robots are:

- Fulfillment of the mission and quality of achievement.

- Speed of the robot (the total time to accomplish the mission).

- Fault tolerance of the robot.

- Self attachment to the pole.

- Ability to move on the floor.

- Level of autonomy.

As numerical values are necessary for comparison, a scoring system was developed to evaluate the performance of the robot against each parameter. So a 0 to 100 scaling system was considered and divided to some portions according to the importance of each parameter for our application.

Fulfillment of the mission and quality of performance

The fulfillment of the mission and quality of performance are the most important parameters of evaluation including 50 percent of the total score. If the robot can just climb from one side of the structure, scan some parts, and descend from the other side of the pole, it means that it fulfills the mission. The quality of performance can be measured by several methods. A suggestion can be distributing some defected weldings on the structure, and the robot should find and register the position of those defected weldings. This can be done by an ultrasonic NDT probe, which can be installed on the robot manipulator. The quantity of non detected items or wrongly detected items will determine the score. Table 2.1 shows a proposed example of a metrics table for evaluation of all parameters.

Speed of the robot

Speed of climbing is an important factor, because it is a fundamental parameter in industrial applications. Scoring can be easily defined according to the mission completion time.

Fault tolerance

As the robot should work at high altitudes, it is important to evaluate its performance in the case of power failures. Scoring method depends on the level of safety considered for such case. A power failure can occur in the controller's power supply or in the main power supply. The desirable situation is that the robot maintains its position on the pole in such cases of power failure and can locate itself after the failure cause is abolished.

Ability to move on the floor and self attachment to the pole

It would be quite interesting if the robot can move on the floor, with wheels or legs. In this case the robot can perform bigger missions. For instance it can start to test a set of structures, because it can move on floor and locate each structure independently. Moreover another parameter should be considered: The robot should be able to attach itself to the pole without the help of human.

Level of the automation

Level of the automation is also of great importance. The most autonomous robot is the one which can perform a mission without having the geometry and dimensions of the structure. It means that the robot also makes the "World Modeling". A robot can be considered semi-autonomous if it can perform the mission autonomously when it has the geometry and dimensions of the structure in advance (priori knowledge of the working area). A robot which is controlled manually e.g. by a joystick is considered non autonomous.

Other Parameters

Parameters like modular design, simplicity, creativity, etc. are also important and can be considered.

Evaluation Function

An evaluation function can be proposed as:

$PI = \sum_1^n (W_i P_i)$

Where PI is the performance index, P_i is the indicator of the performance quality of the ith parameter during achievement of a predefined mission and W_i is the weight factor, showing the importance of the ith parameter for the aims of the mission. W_is are determined based on the objectives of the project. For instance one can consider the following two different applications: first, Autonomous inspection of sophisticated pipelines, and second, cleaning and maintenance

Table 2.1: Metrics for evaluation of PCRs performance

Item	Evaluation Method	Total Scores
Fulfillment of the mission	The robot can climb over the structure from one side and descend from the other part.	30
Quality of performance	10 defected weldings should be recognized and their position should be registered. Each successful register gains 2 scores.	20
Speed of mission achievement	10 scores for the robot which achieves the mission in time	10
Fault tolerance	The robot gains 10 scores if the robot is tolerant to failure on main power and controller power. If it is tolerant just to one of them it gains 5 scores.	10
Ability to move on floor	Yes: 5 points, No: 0 Points	5
Self attachment to the pole	Yes: 5 points, No: 0 Points	5
Level of autonomy	Fully Autonomous: 10 points, Semi Autonomous: 5 points, Non autonomous: 0 points	10
Other parameters, Modular design simplicity, creativity	Without metrics	10

of lamp posts of highways. While "ability of overcoming branches" is necessary for the first application and a big weigh factor can be considered for it, it is not necessary for the second application and a zero weight factor can be assigned to it. Conversely, considering "climbing speed", the weight factor assigned to it for the second application should be bigger than the one for the first application.

2.3 The 3DCLIMBER

In the 3DCLIMBER project we aim to build an industrial PCR with good maneuverability skills. After a survey on the already developed PCRs, our objectives and possibilities and looking at the current available technologies, the following objectives were chosen for the 3DCLIMBER. The robot should:

- be able to climb from the designed structure.

- scan the whole surface of the structure.

- be fault tolerant according to the benchmark definition. So the robot should maintain its position on the pole in case of power failure, and can locate itself after the failure cause abolished.

- autonomously navigate across the structure, while having a priori knowledge of the structure. It means that the structure geometry would be provided to the robot beforehand, and the robot should be able to reach to any location in the structure autonomously.

- Modularity and simplicity should be considered in the design of the robot.

2.4 Conclusion

In this chapter a benchmark for evaluation of PCRs was proposed. The benchmark is designed for PCRs with industrial applications. The PCR benchmark was published as a book chapter in [TMdA08b]. A structure with tubular profile and bends and branches which is similar to piping in industrial plants was designed and implemented as the environment for the experiments. The mission, the benchmark parameters and the evaluation metrics were also defined. The benchmark contributed to a better and more precise definition of the project objectives, and a better perception of the problems and parameters which should be considered in the design of the robot.

Chapter 3

Conceptual Design
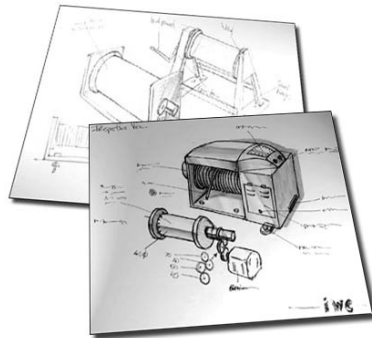
3.1 Introduction

Design is the process by which the needs of the customer or the marketplace are transformed into a product satisfying these needs. Figure 3.1 shows general systematic approaches of the design process and figure3.2 shows the approach used in the design process of the 3DCLIMBER. After identification of the problem, some designs for the 3DCLIMBER robot were proposed. A few of them will be described in the next section. Some designs are demonstrated by a 2D sketch, while others are demonstrated by a 3D model. All 3D models which can be seen in this thesis were modeled in Solidworks.
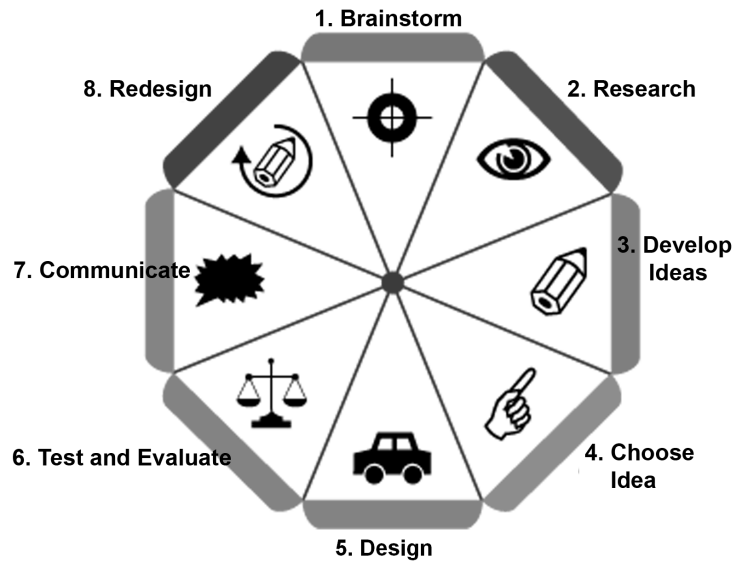
Figure 3.1: Systematic approach to design process.

In this chapter some of the conceptual designs which proposed during this project will be presented. Considering these concepts and previously developed PCRs in various research centers, PCRs were categorized into 4 design groups and the advantages and disadvantages of each group, in general, and also regarding the objectives of the project will be presented. Regarding these advantages and disadvantages, the best category which fits into the objectives of the project was selected. Also an analysis was performed in order to calculate the minimum degrees of freedom which is necessary for a robot to perform all required goals of the project. At the end of this chapter the final conceptual design will be presented.

It is worth mentioning that in the first phase of the conceptual design, it was tried not to take into account all objectives of the project. This is for not restricting the possible innovative designs which might be adaptable to fulfill the requirements of the project with some changes. Therefore, primarily some of the possible concepts for 3DCLIMBER will be described (even though some of them might not fulfill the project requirements) and then both previously developed robots and conceptual designs which were proposed in this chapter were categorized into 4 different design groups. Afterwards the adaptability of each design group to the requirements
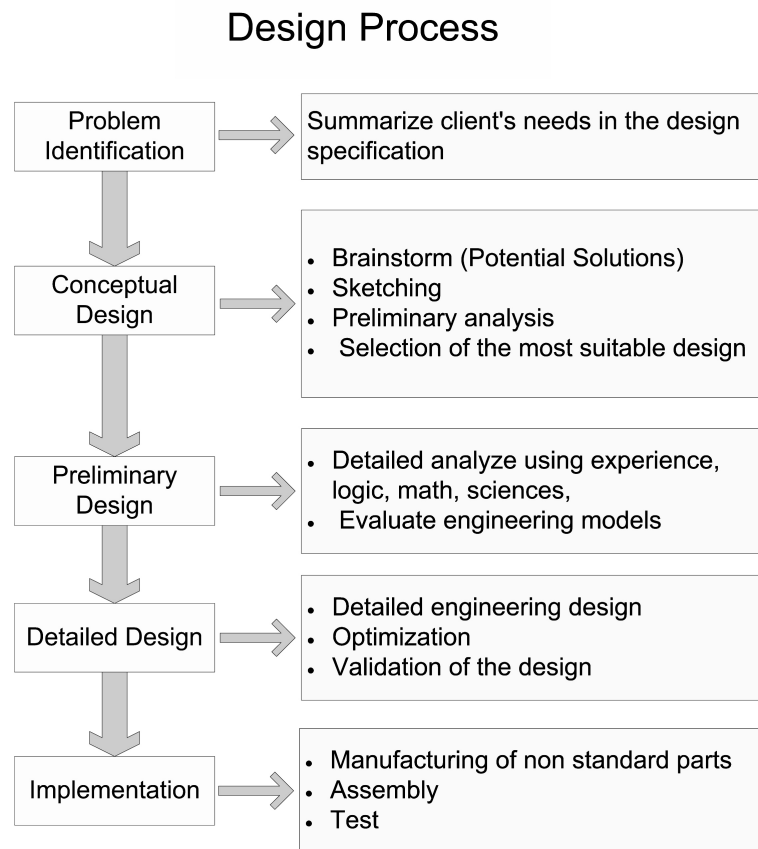
Design Process

Figure 3.2: Systematic approach utilized in the design process of 3DCLIMBER.

of the 3DCLIMBER project will be discussed.

3.2 Conceptual designs

Several conceptual designs for gripping and climbing modules of 3DCLIMBER were proposed and evaluated in the early stages of the project. Some designs were inspired by previously developed robots, but most of them were novel designs. In this section a short overview of the proposed designs will be presented. Each design may demonstrate a concept for the gripper of the robot, for the climbing module or for both.
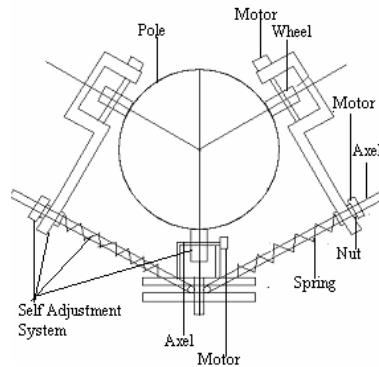
Figure 3.3: Tripod climbing robot.

3.2.1   Tripod climbing concept

Tripod climbing is a continuous motion concept. Figure 3.3 shows one module of this design which consists of one active and two passive wheels, and springs to push the wheels to the pole. One motor is employed to adjust the springs and to create enough force to grasp the pole by all wheels. In fact, gripping action can be done with one motor and a self adjustment system, which pushes all wheels to the pole, and climbing action can be done by another driven wheel. Using two modules, the robot will be able to pass bends, but it can not pass branches due to its closed structure. The main advantages of this conceptual design are simplicity, modularity, and high speed. The main drawbacks are the inability of passing T-junctions and the limited maneuverability. Therefore to manipulate across the structure, a separate robotic arm should be integrated.

3.2.2   Flexible gripper concept

Design of the gripper is one of the most important problems in pole climbing robots which should be addressed, as it should be able to withstand forces and torques generated by the robot weight. Wall climbing robots can take the advantage of magnetic or vacuum grippers which are not a good choice in pole climbing robots due to the curvature of the pole. Also, poles may have different section sizes and dimensions. None of the previously developed PCRs included a universal gripper appropriate for different section sizes and forms. While in continuous motion pole
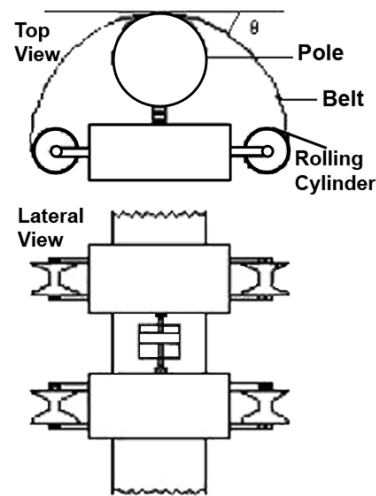
Figure 3.4: The flexible gripper concept can adapt to a big range of section sizes and shapes of the pole.

climbing robots, tires are responsible for both climbing and gripping actions, in non-continuous climbing robots, there exist separate climbing and gripping modules. Consequently gripping mechanisms and climbing structures can be designed and developed separately.

The flexible gripper concept introduces an interesting design for the gripper. The proposed gripper design is a flexible and universal design. As it is shown in figure 3.4, a flexible belt is rolled around 2 cylinders. One of the cylinders is equipped with a motor, which can establish enough tension in the belt and consequently provide the required friction for the gripping action. This gripping module can be used with all noncontinuous climbing mechanisms and is adaptable to different section sizes and shapes. The main drawback is the closed gripper structure, which makes it problematic to overcome T-junctions.

3.2.3 Belt-pushing continuous climbing concept

Inspired by the previously described belt gripper, a concept for a continuous motion robot is proposed. As it is shown in figure 3.5, a flexible belt is used to encircle the entire climbing mechanism. A cylinder for rolling the belt around it and a motor for driving the cylinder, estab-
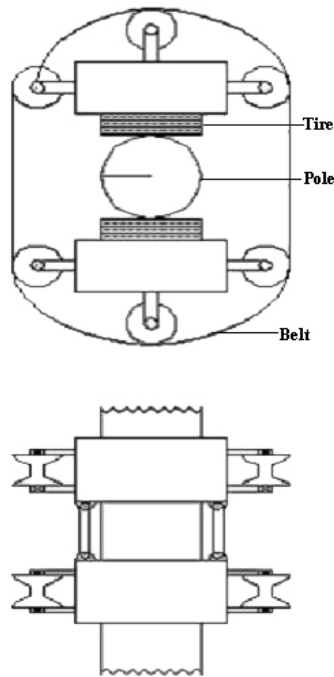
Figure 3.5: The belt pushing climbing concept can adapt to a big range of section sizes and shapes of the pole.

lish enough tension in the belt to provide the required normal force to push the tires to the pole. At least one of the tires should be active and driven by a motor. It is also possible to use several climbing modules, and connect them with an appropriate mechanisms to obtain the required DOF for overcoming bent sections.

All of the previously developed PCRs can travel along structures with a limited range of cross section size. If it is necessary to adapt them for structures with bigger diameters, the size and weight of the robot increases relatively. Consequently, the size of the climbing mechanism increases and thus the robot will be heavier. Belt pushing continuous climbing concept addresses this problem with a flexible belt concept in which the robot can climb over a wide range of poles. In contrast with previously developed robots, this concept would be very light for structures with big diameters.
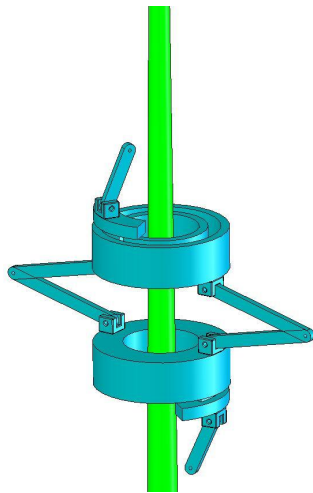
Figure 3.6: Step by step basis robot with a hybrid (serial-parallel) climbing configuration.
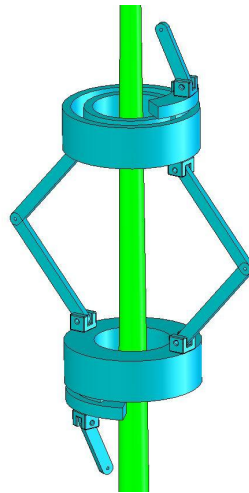
Figure 3.7: Step by step basis robot with a serial climbing configuration.

The main advantages of this design are ability of climbing over structures with big cross section, ability of climbing over a wide range of cross section sizes, simplicity, modularity, high speed, and ability of passing bends. The main drawback is that a robot built based on this design can not pass T-junctions.

3.2.4 Step by step based climbing concepts

Step by step based PCRs may take advantage of separate climbing and gripping modules. At least two gripping modules and a climbing mechanism form the PCR. The climbing mechanism can be a serial, a parallel or a hybrid (serial-parallel) configuration. At each time at least one of the grippers should grip the structure. We call this gripper "base of the robot". Meanwhile, the other gripper can detach from the structure and act as a manipulator. The climbing mechanism, on the other hand is the arm of the robot and should contain adequate degrees of freedom in order to perform all of the desired missions, e.g. NDT inspections. We proposed several concepts for the climbing mechanisms which can be seen in figures 3.6, 3.7, 3.8, and 3.9.

For all designs we took into account that the robot should be able to scan all area of the structure in order to do inspection. Thus, in all concepts we considered a straightforward mechanism for
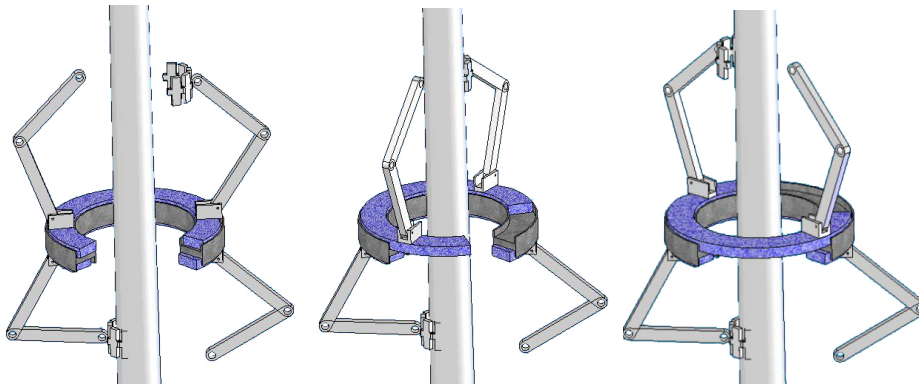
Figure 3.8: Step by step basis robot rotating around the pole.

rotation around the pole. On the other hand, different climbing configurations were purposed. Figure 3.6 demonstrates a hybrid (serial-parallel) climbing configuration. In fact two serial arms are paralleled in order to help the climbing action. Figure 3.7 shows a serial climbing configuration which consists of two 3-DOF planar serial arms and a rotation mechanism around the pole. It also proposes an innovative V-shaped gripper, which will be described later comprehensively. Figure 3.8 presents a biomimetic design, which consists 4 arms in order to climb from bents and branches, while it also takes advantage of a mechanism for rotation around the pole. A conceptual design for a gripper is demonstrated in figure 3.10. Some electromagnet modules connect to each other through passive joints. By activating the magnets of all modules, the gripper encircles the structure. The main advantages of this design are simplicity and adaptability to different cross section shapes and sizes. Another conceptual design for a gripper is demonstrated in figure 3.11. A motor drives two ballscrews and consequently a linear slider moves in the linear guide. V-shaped end effectors are applied as they can mechanically centralize themselves to the circular structures.

3.3   PCR design groups: adaptation with requirements

In addition to conceptual designs which were firstly proposed in this project, previously developed PCRs have been also analyzed. Categorization of the concepts and developed PCRs will
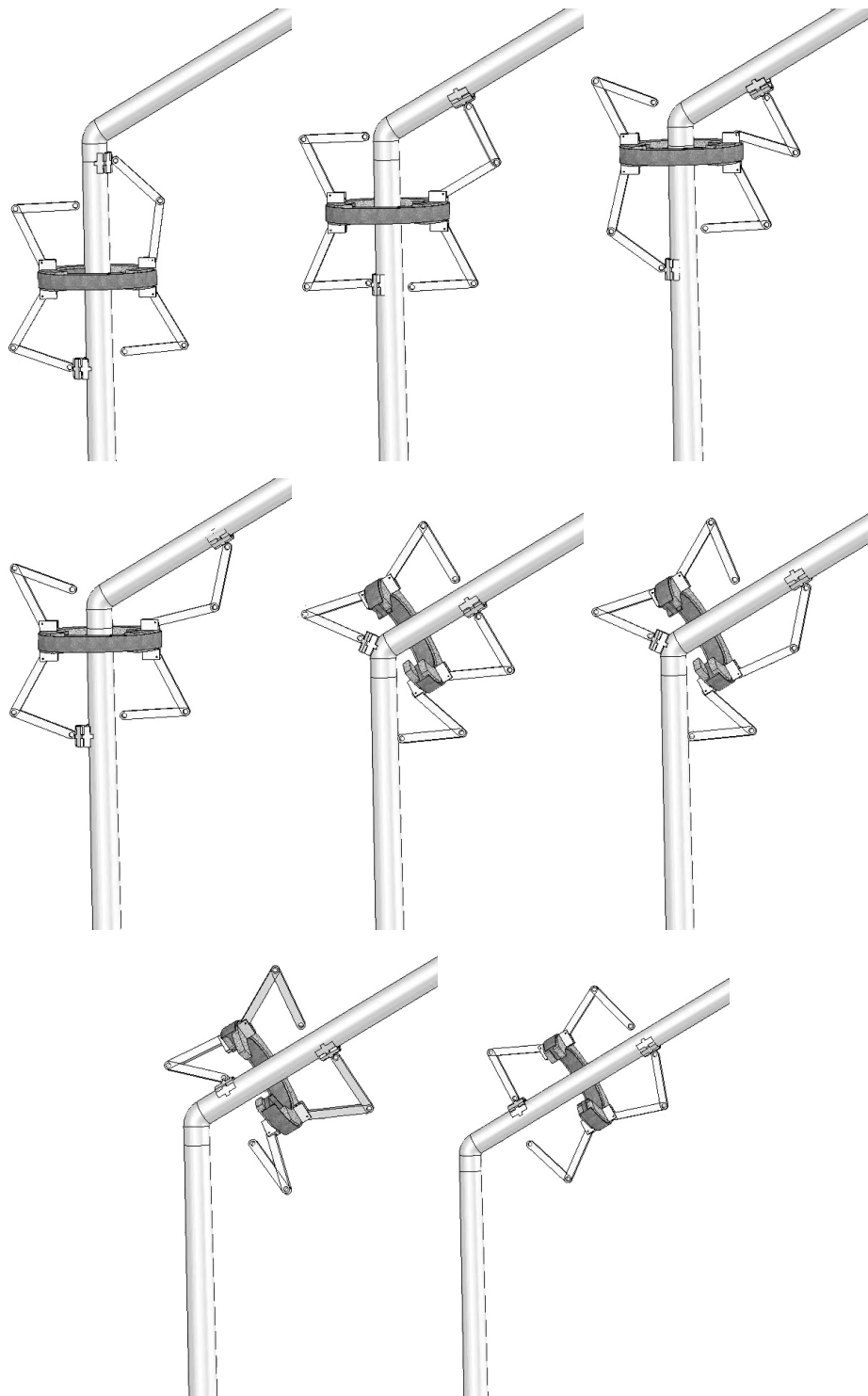
Figure 3.9: Biologically inspired climbing robot consisting of 4 articulated arms.
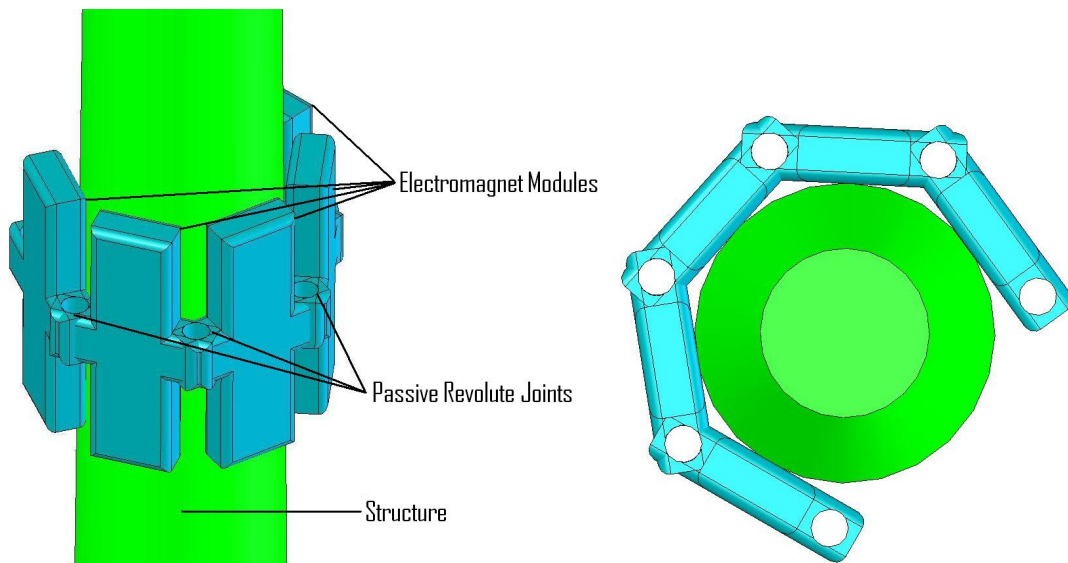
Figure 3.10: A gripper concept consisting of electromagnet modules.
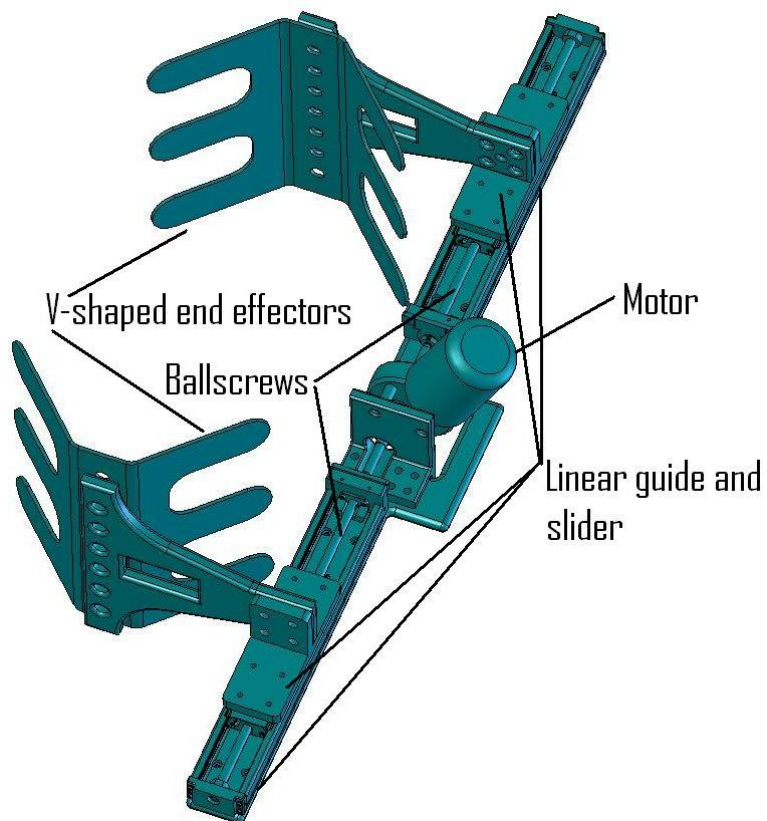
Figure 3.11: V shaped gripper concept.

promote a better perception of each category and its advantages and disadvantages. Therefore considering the previously developed PCRs and the proposed conceptual designs, PCRs can be categorized to 4 main design groups.

- Continuous motion PCRs.

- Noncontinuous PCRs with serial climbing structure.

- Noncontinuous PCRs with parallel climbing structure.

- Noncontinuous PCRs with hybrid climbing structure.

Each category will be described and its advantages and disadvantages will be discussed. These discussions are based on a comprehensive investigation on previously developed PCRs [SSA$^+$00, SSA$^+$06, ABG$^+$99, RJGB06, VBT$^+$04, HH01, YAH$^+$04] and personal experience of the author in design of PCRs [VBT$^+$04, ZVB$^+$04, ZTVB04, TZV$^+$04, TZVB05].

3.3.1 Continuous motion PCRs

Continuous motion PCRs use tires to move along poles and structures. Tires are used both for climbing and gripping. Bagheri et al. have developed a wheel based pole climbing robot which does not have the ability of passing bends and branches, but, like all the other robots in this category, it has a high climbing speed [YAH$^+$04, MNA06]. Hosokai et al. developed a robot with three modules [HH01]. Each module has three wheels and connected to its adjacent module with a revolute joint. Each module of the robot is able to climb a straight pole independently. The robot can adapt to different diameters of the pipeline by adjusting the length of arms of the robot. Tripod climbing concept and Belt-pushing continuous climbing concept which were introduced in the last section, are also continuous motion concepts. The main advantages of continuous motion PCRs include:

- High climbing speed: Because it takes advantage of continuous climbing along the pole using wheels.

- Simplicity of the design and implementation.

- Possibility of modular design: Similar simple wheeled modules can be connected to each other through active or passive joints.

The main disadvantages of these robots include:

- Difficulties in passing the bent section: This design group can pass the bent section of the structure, just if the robot contains a separate arm, or several climbing modules are connected together through active joints (See [YAH$^+$04] and [MNA06]).

- Inability of passing branches: Due to the closed structure of each module as it can be seen in [YAH$^+$04, MNA06, LXGL07, HH01] and also in the proposed conceptual designs, it can not pass the bent section on structures with branches.

- Low maneuverability: To perform some manipulation around the pole, they need an extra articulated arm.

3.3.2 Noncontinuous serial climbing structures

Noncontinuous motion PCRs don't use wheels for climbing. Their motion is based on step by step sequence. They always have separate gripping and climbing module which enable them to climb over poles on a step-by-step basis. Noncontinuous PCRs are divided into several groups, regarding their climbing structure i.e. serial, parallel, or hybrid (serial-parallel) structure. Serial structures are the most wide-spread structures in robotic applications. Most of the industrial robots are serial robots. But what make them so wide spread? The most important reason is their simplicity including simplicity of structure, kinematics and dynamics, and control. In comparison with parallel mechanisms they have some advantageous and disadvantages, which will be analyzed in the next section. Balaguer et al, have developed a serial structure PCR for inspection applications in 3D complex environments[BGP$^+$00a]. The main advantages of serial climbing structures include:

- Ability of passing bends and branches.

- Built-in manipulating arm: When one gripper grasps the pole, the other gripper can detach from the pole and manipulate over the pole. So in case of existence of an appropriate climbing mechanism which has enough degrees of freedom to act as an articulated arm, and also existence of an appropriate gripping mechanism which can withstand all forces and torques generated by the robot weight, there would be no need to an extra arm for manipulation and inspection applications.

- Safety and failure tolerance: Due to existence of separate climbing and gripping mechanisms, any failure in gripping mechanism is not also a failure in climbing mechanism and vice versa. For instance if the gripper is tolerant to power failure, the robot can maintain its last position on the structure in case of power failure.

- Simplicity: Simplicity of implementation, analysis, and control.

- Good workspace and Maneuverability.

The main drawbacks are:

- Low climbing speed.

- Heaviness (compared to parallel structures).

- low payload/weight ratio (compared to parallel structures).

3.3.3 Noncontinuous parallel climbing structures

The manipulating structures, now known as the parallel manipulators, have their origin in the tire testing machine designed by Gough and Whitehall [GW62], and the flight simulator platform devised by Stewart [Ste65]. It is well known that serial configurations demand a greater amount of torque at the joints than parallel configuration. Thus, application of serial configurations as climbing structure would call for larger and heavier actuators which results in smaller payload to weight ratio which is a critical factor in climbing robots. In contrast, using parallel platforms can result in decrease of the weight to power ratio, thus allowing for larger payloads.

On the other hand, parallel mechanisms have smaller workspace compared with serial mechanisms which reduce their maneuverability. Besides, they have a complex structure. Kinematics, dynamics, and singularity analysis of these structures are more complicated than those of serials. To the best of author's knowledge, the only PCR with fully parallel structure was developed at Miguel Hernandez University of Elche, Spain [ASS99]. The main advantages of parallel climbing structures include:

- Ability of passing bends and branches.

- Built-in manipulation arm.

- Safety and failure tolerance.

- High payload to weight ratio (compared with serial configurations).

The main drawbacks are:

- Low climbing speed.

- Complexity of mechanical implementation and control.

- Lower workspace and consequently lower maneuverability.

3.3.4   Noncontinuous hybrid climbing structures

Hybrid mechanisms, combination of serial and parallel structures, can take advantages of both parallel and serial structures namely good payload to weight ratio, good workspace, and good maneuverability. The most important design issue in hybrid structures is the appropriate design of the structure. It means usage of serial mechanism on joints which need more workspace and less force, and usage of parallel mechanisms on joints which may need high force (or torque) for running. The author developed Sharif PCR with a hybrid mechanism as the climbing module, in Sharif University of Technology in Iran [TZVB05, TZV$^+$04]. Using hybrid mechanisms has advantages of both serial and parallel mechanisms provided that the mechanism is well designed and optimized for achievement of desired missions. On the other hand, it may have some of the

disadvantages of both parallel and serial configurations. Therefore, the pros and cons of such mechanisms, depends on the specific design. However in any case it inherits complexity of implementation and control from parallel mechanisms.

3.4   Selection of the final design category

Four design categories for PCRs were introduced in the last section. One of these categories which fits better with the objectives of the 3DCLIMBER, should be selected. For this purpose the objectives of the project which were discussed in the last section should be considered.

1. The 3DCLIMBER, should be able to climb from the designed structure with bends and branches.

2. It should be able to scan the whole surface of the structure.

3. It should be tolerant to power failure according to the benchmark definition. In the other word, the robot should maintain its position on the pole in case of power failure.

4. It should be autonomous with a priori knowledge of the structure. It means that the structure geometry will be provided to the robot beforehand, and the robot should be able to reach to any location in the structure autonomously.

5. Modularity, simplicity, and weight optimization should be considered in design of the robot.

From the previous discussion and according to the objectives number 1, 3, and 5, continuous motion climbing robots can not fulfill the objectives of the project. As it is discussed they have difficulties to pass T-junctions. Furthermore, to pass the bent section they need a separate arm. As they do not have separate climbing and gripping modules, design of fault tolerant mechanisms would be more problematic. Finally, they have a very low maneuverability unless they are equipped with an articulated arm. The other three design groups can act similar in some of the objectives. For instance, due to availability of separate climbing and gripping modules, they

can be fault tolerant if an appropriate gripper design is applied and also they can manipulate over the structure without a need to an extra arm. Besides, if a robot is able to pass structures with bents, it can also pass bent section on structures with branches, provided that the gripper design is not a closed structure. But to pass the bent section, the workspace of the climbing mechanism should be sufficient. Therefore, decision making for selection of the most appropriate configuration depends mainly on 2 factors: Simplicity and Workspace of the robot. On the other hand, the main advantage of serial arms over parallel configurations is simplicity and better workspace. The previous experience of the author in development and optimization of hybrid configurations [TZV$^+$04] revealed that even though an optimized hybrid configuration has a reasonable workspace and payload to weight ratio, it inherits the complexity of the parallel robots. Furthermore, when the robot is passing the bent section, a large constant angle workspace is required, otherwise the robot either can not pass the bent section or should take too many steps to pass the bent section. Considering previous experiences on design of climbing robots, and many literatures about cons and pros of serial and parallel robots we concluded that a serial configuration fits better to the objectives of the project. The most important reason for choosing serial configuration as climbing mechanism is to increase workspace and manipulability which is a key factor for a multi purpose robot. The details of the analysis is published in [TMdA06b].

3.5   Minimum degrees of freedom

As PCRs should take their weight up during climbing; it is very important to design optimized and dedicated mechanisms to decrease the weight of the robot. Based on this fact, a designer should consider optimization in all steps of the design process to reduce the weight and the size of the robot as much as possible. The most significant optimization step takes place in the conceptual design step. Redundant DOF make the robot heavier without necessarily increasing the robot abilities for performing a given task.

Therefore we should address the problem of designing a mechanism with minimum degrees

of freedom which can climb over structures with bends and branches. Some of the previously developed PCRs [SAS$^+$99, ABG$^+$99] include 6 degrees of freedom, and thus can reach to any pose within their workspace. But is it necessary to employ a 6-DOF mechanism for climbing and manipulation over 3D Structures?

To design the climbing mechanism with minimum DOF a survey was performed in order to study the necessary degrees of freedom for climbing and manipulating over 3D structures. Figure 3.12 represents a step-by-step based PCR climbing along the straight part of a pole. As can be seen in figure 3.12, one DOF is sufficient to perform this task.

Figure 3.13 represents a PCR passing a bent section. It requires two additional degrees of freedom: One rotation in order to overcome the bend and another translation to move the upper gripper to the straight section after the bend.

But if the robot is not aligned with the desired XZ plane in poles containing T-junctions, then an additional rotation is necessary in order to align the robot with the desired straight segment (see figure 3.14).

The latterly mentioned DOF is also necessary for performing NDT tests as the robot's manipulator should be able to scan every point on the structure. The combination of the above 4 DOF provides the necessary manipulability not only to reach to every point on the structure, but also to perform necessary operations after reaching target point on pole. In figures 3.12, 3.13, and 3.14, "G" stands for gripper and "M" stands for Mechanism. Design of a serial arm which contains the mentioned DOF will be described in the next section.
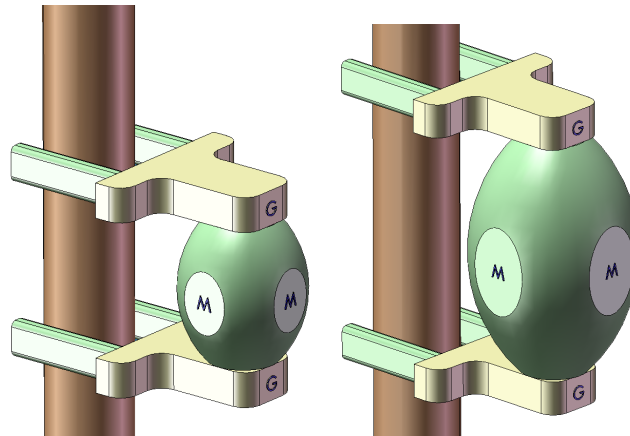
Figure 3.12: Climbing along a pole
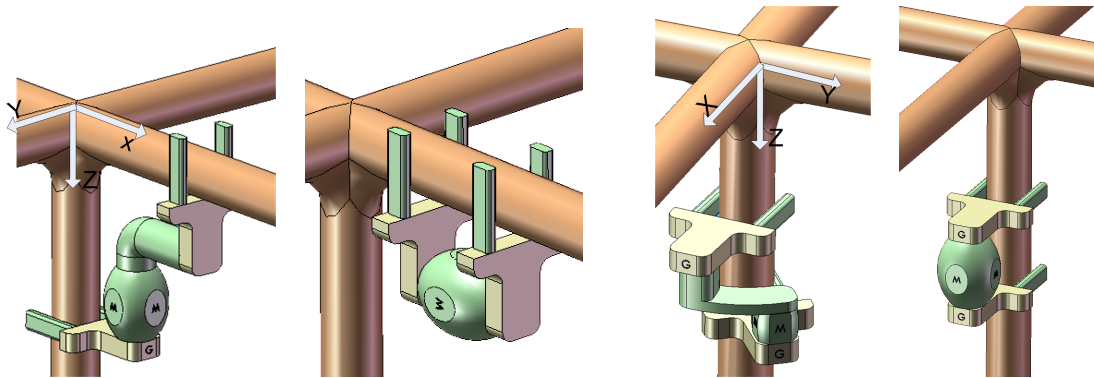
Figure 3.13: Overtaking the bent section

Figure 3.14: Rotating around pole

3.6 The final conceptual design

3.6.1 Climbing structure

A dedicated serial mechanism providing the required DOF, which was stated in the previous section, was designed. The designed climbing module consists of a 3-DOF planar serial arm and a Z axis rotating mechanism (see figure 3.15). Combining the 3-DOF arm with the rotating mechanism provides two rotations and two translations on the manipulator in relation with the base, which are necessary to achieve the design objectives as explained in the previous section. The 3-DOF planar serial arm consists of 3 arms connected together through three revolute joints. This arm can reach to any Pose in its workspace which is a part of a plane. Therefore it

provides 2 translations and 1 rotation which are Tz (Translation along Z), Tx (Translation along x), and Ry (Rotation around Y). An innovative rotating mechanism is designed in a different way from articulated arms. This mechanism can orient the robot for appropriate bent section and significantly increases the manipulability and workspace of the robot; the robot can rotate around the pole axis and scan the whole surface of the pole. An articulated 4-DOF serial arm without using the proposed rotating mechanism concept might also be designed, but as it can be seen in Figure 3.16, a 6-DOF arm can directly move from face A1 to A2, while a 4-DOF serial arm should transit from C1 and B1 to do so. A 4-DOF mechanism was applied by Balaguer et al. in ROMAII robot using a 4-DOF articulated serial arm[BGA02]. But this is not a desirable approach due to two reasons. First: Because if the robot is aimed to make NDT inspections, it should be able to rotate around the pole rapidly and scan the whole surface of the pole, which is not possible with articulated serial arm design. Second: Because the robot is not be able to traverse across all plane mates rapidly. The 3DCLIMBER rotating mechanism concept, solves these problems. It can rotate around the pole rapidly which allows a fast inspection of the whole surface. Also transition between different working planes is easier and faster.

Figure 3.15 shows a detailed design of the 4-DOF serial arm which is used as climbing module of the 3DCLIMBER.

3.6.2 Grippers

To design the gripper, we investigated advantages and disadvantages of the proposed conceptual designs. Flexible gripper concept that uses flexible belts for gripping action 3.4, has many advantages which were mentioned, namely simplicity, low weight, adaptation to different cross section shapes, and adaptability to a large range of sizes. On the other hand, due to its close mechanical structures, this gripper can not pass poles with branches, which is an important drawback which can not be neglected according to the project definition. Electromagnet gripper concept 3.10, also has several advantages which were mentioned, but after a survey and some researches, it was concluded that the force to weight ratio of the electromagnets is not enough for
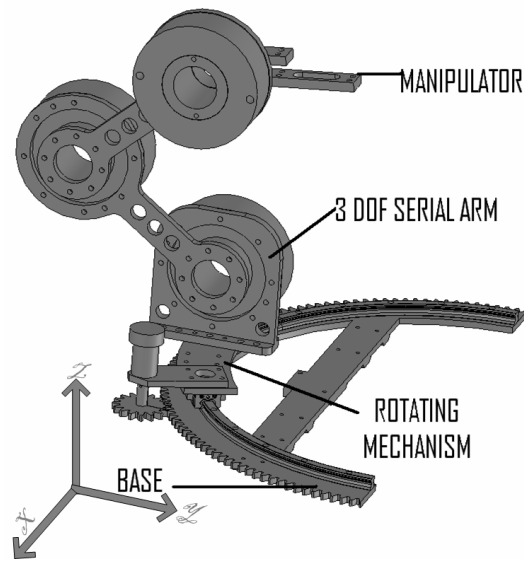
Figure 3.15: 3D model of the designed 4-DOF climbing structure
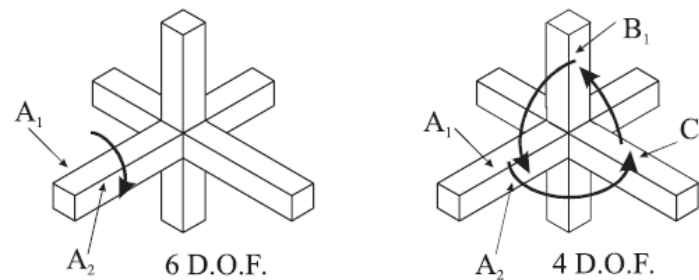
Figure 3.16: 6-DOF vs 4-DOF articulated serial arm motion.

the 3DCLIMBER application and, furthermore, they can not be used in non-metallic structures. We also investigated the possibility of using a vacuum gripper, but it was problematic due to the curvature of the pipes. This problem might be solved by a dedicated design of a curvy vacuum pads but then it will not be adaptable to different cross section sizes. Finally, we chose the V-shaped concept 3.11; as it can pass branches, it can adapt to a range of cross section sizes and it has the self centralizing characteristic. The main drawback of this concept is that for structures with a large cross section size, the gripper will be heavy and large.

3.7 Conclusion

The systematic approach for design and development of a mechanism was employed for the development of the 3DCLIMBER. In the first phase, the conceptual design of the robot was studied. Considering all proposed conceptual designs for the gripping and climbing mechanisms, the developed benchmark which took into account the objectives of the project, the optimal weight strategy and some other factors, the best gripping and climbing concepts for the defined objectives of the project were selected. Other proposed concepts in this chapter are a valuable source of design ideas which might have a contribution in similar projects.

Chapter 4

Kinematics, Dynamics, and Workspace Analyses
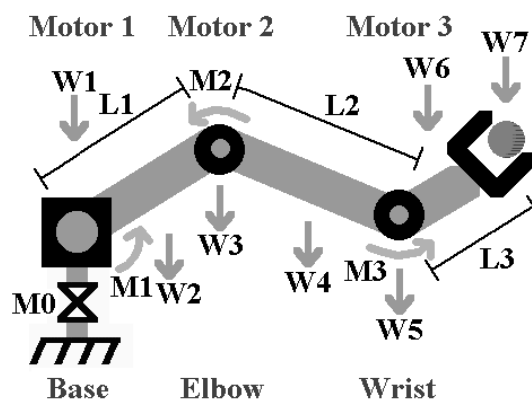
4.1   Introduction

To transit from the conceptual design phase to the detailed design phase, it is necessary to perform kinematics and workspace analyses in order to determine the optimum length of the links and dynamics analysis in order to calculate the required torque for actuators. Furthermore these analyses will be necessary for path planning and control of the robot.

49

4.2 Kinematics analysis

The study of manipulator kinematics is divided into two parts, inverse (or reverse) kinematics and forward (or direct) kinematics. The inverse kinematics problem involves mapping a known pose (position and orientation) of the moving platform of the manipulator to a set of input joint variables that will achieve that pose. The forward kinematics problem involves the mapping from a known set of input joint variables to a pose of the moving platform that results from those given inputs [Cra89]. To perform kinematics analysis, a simplified model of the robot is considered which is showed in figure 4.1 along with the original model. In this model the rotation mechanism is substituted by an arm, which has an equal length with the radius of the rotation guide. The reference coordinate system is placed in the center of the rotation mechanism.

Note the following common abbreviations in kinematic analysis:

s represents *sinus*.

c represents *cosinus*.

s_{12} represents $\sin(\theta 1 + \theta 2)$.

Figure 4.2 shows the Denavit-Hartenberg frame assignments. As it can be seen l_0, l_1, l_2, and l_3 are the lengths of the links 1 to 4. Relatively $\theta_0, \theta_1, \theta_2$, and θ_3 are the angles of the joints 0 to 3. Table 4.1 shows the Denavit-Hartenberg parameters.

1	$\alpha_{(i-1)}$	$a_{(i-1)}$	d_i	θ_i
0	0	0	0	θ_0
1	90	l_0	0	θ_1
2	90	l_1	0	θ_2
3	90	l_2	0	θ_3

Table 4.1: Denavit-Hartenberg parameters.
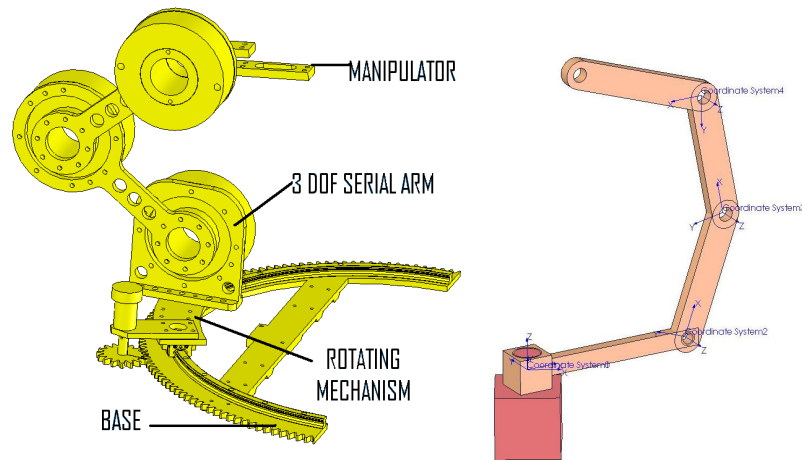
Figure 4.1: The 4-DOF climbing mechanism and the simplified model for the kinematics analysis
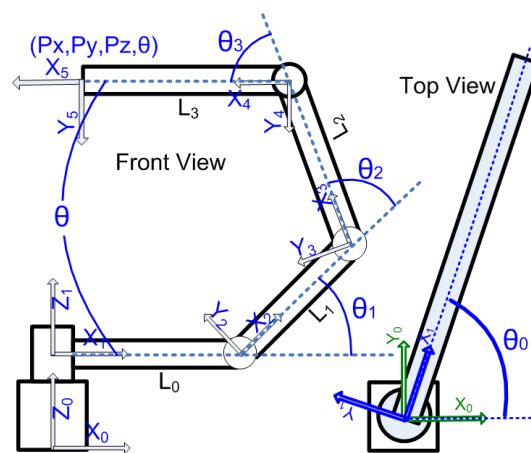
Figure 4.2: Kinematic configuration of the climbing module.

4.2.1 Direct kinematics problem

Using the Denavit-Hartenberg joint parameters listed above and according to the assigned coordinate axes in Fig. 4.2, transform matrices of joint coordinate systems are derived as follows:

$$
{}^0T_1 =
\begin{pmatrix}
\cos(\theta_0) & -\sin(\theta_0) & 0 & 0 \\
\sin(\theta_0) & \cos(\theta_0) & 0 & 0 \\
0 & 0 & 1 & 0 \\
0 & 0 & 0 & 1
\end{pmatrix}
\tag{4.1}
$$

$$
{}^1T_2 =
\begin{pmatrix}
\cos(\theta_1) & -\sin(\theta_1) & 0 & l_0 \\
0 & 0 & -1 & 0 \\
\sin(\theta_1) & \cos(\theta_1) & 0 & 0 \\
\\
0 & 0 & 0 & 1
\end{pmatrix}
\tag{4.2}
$$

$$
{}^2T_3 =
\begin{pmatrix}
\cos(\theta_2) & -\sin(\theta_2) & 0 & l_1 \\
\sin(\theta_2) & \cos(\theta_0) & 0 & 0 \\
0 & 0 & 1 & 0 \\
0 & 0 & 0 & 1
\end{pmatrix}
\tag{4.3}
$$

$$
{}^3T_4 =
\begin{pmatrix}
\cos(\theta_3) & -\sin(\theta_3) & 0 & l_2 \\
\sin(\theta_3) & \cos(\theta_3) & 0 & 0 \\
0 & 0 & 1 & 0 \\
0 & 0 & 0 & 1
\end{pmatrix}
\tag{4.4}
$$

Therefore, the overall transform matrix, ${}^4_0T$ can be written in the form:

${}^0T_4 = {}^0T_1 \times {}^1T_2 \times {}^2T_3 \times {}^3T_4.$

After multiplication and simplification:

$$
{}^0T_4 =
\begin{pmatrix}
0.5(\cos(v) + c_{0123}) & 0.5(\sin(v) - s_{0123}) & s_0 & P_x \\
0.5(\sin(v) - s_{0123}) & 0.5(-\cos(v) + c_{0123}) & c_0 & P_y \\
s_{123} & c_{123} & 0 & P_z \\
0 & 0 & 0 & 1
\end{pmatrix}
\tag{4.5}
$$

Where:

$$v = -\theta_3 - \theta_2 - \theta_1 + \theta_0$$

And:

$$P_x = 0.5 l_2 \cos(\theta_0 - \theta_1 - \theta_2) + 0.5 l_2 c_{012} + 0.5 l_1 \cos(\theta_0 - \theta_1) + 0.5 l_1 c_{01} + c_0 l_0$$

$$P_y = 0.5 l_2 \sin(-\theta_2 \theta_0 - \theta_1) + 0.5 l_2 s_{012} + 0.5 l_1 \sin(\theta_0 - \theta_1) + 0.5 l_1 s_{01} + s_0 l_0$$

$$P_z = s_{12} l_2 + s_1 l_1$$

$\theta_0, \theta_1, \theta_2, \theta_3$ are joint angles of the serial arm. $\{P_x, P_y, P_z\}$ shows the position of the manipulator coordinate system in relation with the base coordinate system. The above $^0T_4$ matrix represents the direct kinematics equation for the 4-DOF climbing mechanism. The position vector P(q) and the orientation Matrix R(q) of the tool frame (manipulator) relative to the base frame are:

$$P(q) = \begin{pmatrix} P_x \\ P_y \\ P_z \end{pmatrix}$$

$$R(q) = \begin{pmatrix} 0.5(\cos(v) + c_{0123}) & 0.5(\sin(v) - s_{0123}) & s_0 \\ 0.5(\sin(v) - s_{0123}) & 0.5(-\cos(v) + c_{0123}) & c_0 \\ s_{123} & c_{123} & 0 \end{pmatrix} \tag{4.6}$$

4.2.2   Inverse kinematics problem

For the inverse kinematics analysis, the position and orientation of the moving frame is considered known, thus the input joint variables that achieve that pose should be obtained.

$$^0T_4 = ^0T_1 \times ^1T_2 \times ^2T_3 \times ^3T_4 \tag{4.7}$$

And:

$$(^0T_1)^{-1} \times ^0T_4 = ^1T_4 \Longrightarrow ^1T_4 = ^1T_2 \times ^2T_3 \times ^3T_4 \tag{4.8}$$

From 4.7, and 4.8:

$$
\begin{pmatrix}
c_0 & s_0 & 0 & 0 \\
-s_0 & c_0 & 0 & 0 \\
0 & 0 & 0 & 1 \\
0 & 0 & 0 & 0
\end{pmatrix}
\begin{pmatrix}
R_{11} & R_{12} & R_{13} & P_x \\
R_{21} & R_{22} & R_{23} & P_y \\
R_{31} & R_{32} & R_{33} & P_z \\
0 & 0 & 0 & 1
\end{pmatrix}
=
\begin{pmatrix}
c_{123} & -s_{123} & 0 & l_2 c_{12} + l_1 c_1 + l_0 \\
0 & 0 & -1 & 0 \\
s_{123} & c_{123} & 0 & l_2 s_{12} + l_1 s_1 \\
0 & 0 & 0 & 1
\end{pmatrix}
$$

consequently:

$$c_0 P_x + s_0 P_y = l_2 c_{12} + l_1 c_1 + l_0 \tag{4.9}$$

$$-s_0 P_x + c_0 P_y = 0 \tag{4.10}$$

$$P_z = l_2 s_{12} + l_1 s_1 \tag{4.11}$$

From 4.10:

$$\theta_0 = \arctan 2 \frac{P_y}{P_x} \tag{4.12}$$

let us define Q as:

$$Q = \frac{P_x^2 + P_y^2 + P_z^2 - 2l_0 \sqrt{P_x^2 + P_y^2} + l_0^2 - l_1^2 - l_2^2}{2l_1 l_2}$$

squaring both sides of equations 4.9 and 4.11 and adding the sides:

$$c_2 = Q \quad \& \quad s_2 = \pm \sqrt{1 - Q^2}$$

consequently θ_2 can be obtained as:

$$\theta_{21}, \theta_{22} = \arctan 2(\pm \sqrt{1 - Q^2}, Q) \tag{4.13}$$

Therefore the inverse kinematics equation results in 2 answers for the θ_2. To obtain the inverse kinematics equation for θ_1, one can write the equations 4.9 and 4.11 in the following form:

$$c_0 P_x + s_0 P_y - l_0 = K_1 c_1 - K_2 s_1$$

$$P_z = K_1 s_1 + K_2 c_1$$

letting:

$$K_1 = l_1 + l_2 c_2$$

$$K_2 = l_2 s_2$$

considering:

$$r = +\sqrt{K_1^2 + k_2^2}$$

$$\gamma = \arctan 2(K_2, K_1)$$

consequently:

$$K_1 = r \cos \gamma$$

$$K_2 = r \sin \gamma \longrightarrow$$

$$\cos(\gamma + \theta_1) = \frac{x}{\gamma}$$

$$\sin(\gamma + \theta_1) = \frac{y}{\gamma} \longrightarrow$$

$$\theta_1 = \arctan 2(P_z, c_0 P_x + s_0 P_y - l_0) - \arctan 2(K_2, K_1) \tag{4.14}$$

As there are 2 values for θ_2 , relatively there are also 2 values for k1 and k2 and consequently 2 values for θ_1 which are called θ_{11} *and* θ12. Finally from the geometrical solutions one can

easily find:

$$\theta 31 = \theta - \theta 11 - \theta 21 \tag{4.15}$$

$$\theta 32 = \theta - \theta 12 - \theta 22 \tag{4.16}$$

Where θ is the angle between X_4 and X_1, around Z4. θ is a known parameter in the inverse kinematics problem of the 4-DOF climbing mechanism. Therefore, the inverse kinematics problem has two solutions:

$$\theta_0 = \arctan 2 \frac{P_y}{P_x} \tag{4.17}$$

$$\theta_{21} = \arctan 2 (+ \sqrt{1 - Q^2}, Q) \tag{4.18}$$

$$\theta_{22} = \arctan 2 (- \sqrt{1 - Q^2}, Q) \tag{4.19}$$

$$\theta_{11} = \arctan 2 (P_z, c_0 P_x + s_0 P_y - l_0) - \arctan 2 (K_{21}, K_{11}) \tag{4.20}$$

$$\theta_{12} = \arctan 2 (P_z, c_0 P_x + s_0 P_y - l_0) - \arctan 2 (K_{22}, K_{11}) \tag{4.21}$$

$$\theta_{31} = \theta - \theta_{11} - \theta_{21} \tag{4.22}$$

$$\theta_{32} = \theta - \theta_{12} - \theta_{22} \tag{4.23}$$

Where:

$$Q = \frac{P_x^2 + P_y^2 + P_z^2 - 2l_0 \sqrt{P_x^2 + P_y^2} + l_0^2 - l_1^2 - l_2^2}{2l_1 l_2} \tag{4.24}$$

$$K_{11} = l_1 + l_2 c_{21}, K_{21} = l_2 s_{21} \tag{4.25}$$

$$K_{12} = l_1 + l_2 c_{22}, K_{22} = l_2 s_{22} \tag{4.26}$$

4.3 Jacobian matrix and singularities

The Jacobian matrix is a first-order partial derivatives matrix. For robots, the Jacobian relates the end-effector velocity to the joint speeds. Jacobian matrix is a dynamic matrix which is a

function of joint space positions θ_0 to θ_4. Singularities are commonly used to indicate a position where a particular mathematical formulation fails. In robotics, singularity is a position in the robot's workspace where one or more joints no longer represent independent controlling variables. Singularities of serial arms are either boundary or Interior. Boundary singularities occur when the tool tip is on the surface of the robot's workspace. Interior singularities occur inside the work envelope when two or more of the axes of the robot form a straight line, i.e., collinear. To calculate the Jacobean matrix, the following formulation [Cra89] should be replaced by the 4-DOF mechanism formulas:

$$^{i+1}w_{i+1} = {}^{i+1}_i R \, {}^i w_i + \dot{\theta}_{i+1} \, {}^{i+1}Z_{i+1} \tag{4.27}$$

$$^{i+1}v_{i+1} = {}^{i+1}_i R({}^i v_i + {}^i w_i \times {}^i P_{i+1}) \tag{4.28}$$

Therefore:

$$^1w_1 = \begin{pmatrix} 0 \\ 0 \\ \dot{\theta}_0 \end{pmatrix} \quad \& \quad {}^1v_1 = \begin{pmatrix} 0 \\ 0 \\ 0 \end{pmatrix}$$

$$^2w_2 = \begin{pmatrix} c_1 & 0 & s_1 \\ -s_1 & 0 & c_1 \\ 0 & -1 & 0 \end{pmatrix} \begin{pmatrix} 0 \\ 0 \\ \dot{\theta}_0 \end{pmatrix} + \begin{pmatrix} 0 \\ 0 \\ \dot{\theta}_1 \end{pmatrix} = \begin{pmatrix} s_1\dot{\theta}_0 \\ c_1\dot{\theta}_0 \\ \dot{\theta}_1 \end{pmatrix}$$

$$^2v_2 = \begin{pmatrix} c_1 & 0 & s_1 \\ -s_1 & 0 & c_1 \\ 0 & -1 & 0 \end{pmatrix} \left(\begin{pmatrix} 0 \\ 0 \\ \dot{\theta}_0 \end{pmatrix} \times \begin{pmatrix} l_0 \\ 0 \\ 0 \end{pmatrix} \right) = \begin{pmatrix} 0 \\ 0 \\ -l_0\dot{\theta}_0 \end{pmatrix}$$

$$
{}^3w_3 = \begin{pmatrix} c_2 & s_2 & 0 \\ -s_2 & c_2 & 0 \\ 0 & 0 & 1 \end{pmatrix} \begin{pmatrix} s_1\dot{\theta}_0 \\ c_1\dot{\theta}_0 \\ \dot{\theta}_1 \end{pmatrix} + \begin{pmatrix} 0 \\ 0 \\ \dot{\theta}_2 \end{pmatrix} = \begin{pmatrix} s_{12}\dot{\theta}_0 \\ c_{12}\dot{\theta}_0 \\ \dot{\theta}_1 + \dot{\theta}_2 \end{pmatrix}
$$

$$
{}^3v_3 = \begin{pmatrix} c_2 & s_2 & 0 \\ -s_2 & c_2 & 0 \\ 0 & 0 & 1 \end{pmatrix} \left(\begin{pmatrix} 0 \\ 0 \\ -l_0\dot{\theta}_0 \end{pmatrix} + \begin{pmatrix} s_1\dot{\theta}_0 \\ c_1\dot{\theta}_0 \\ \dot{\theta}_1 \end{pmatrix} \times \begin{pmatrix} l_1 \\ 0 \\ 0 \end{pmatrix} \right)
$$

$$
= \begin{pmatrix} s_2 l_1\dot{\theta}_1 \\ c_2 l_1\dot{\theta}_1 \\ -c_1 l_1\dot{\theta}_0 - l_0\dot{\theta}_0 \end{pmatrix}
$$

$$
{}^4w_4 = \begin{pmatrix} c_3 & s_3 & 0 \\ -s_3 & c_3 & 0 \\ 0 & 0 & 1 \end{pmatrix} \begin{pmatrix} s_12\dot{\theta}_0 \\ c_12\dot{\theta}_0 \\ \dot{\theta}_1 + \dot{\theta}_2 \end{pmatrix} + \begin{pmatrix} 0 \\ 0 \\ \dot{\theta}_2 \end{pmatrix} = \begin{pmatrix} s_{123}\dot{\theta}_0 \\ c_{123}\dot{\theta}_0 \\ \dot{\theta}_1 + \dot{\theta}_2 + +\dot{\theta}_3 \end{pmatrix}
$$

$$
{}^4v_4 = \begin{pmatrix} c_3 & s_3 & 0 \\ -s_3 & c_3 & 0 \\ 0 & 0 & 1 \end{pmatrix} \left(\begin{pmatrix} s_2 l_1\dot{\theta}_1 \\ c_2 l_1\dot{\theta}_1 \\ -c_1 l_1\dot{\theta}_0 - l_0\dot{\theta}_0 \end{pmatrix} + \begin{pmatrix} s_{12}\dot{\theta}_0 \\ c_{12}\dot{\theta}_0 \\ \dot{\theta}_1 + \dot{\theta}_2 \end{pmatrix} \times \begin{pmatrix} l_1 \\ 0 \\ 0 \end{pmatrix} \right)
$$

$$
= \begin{pmatrix} s_{23} l_1\dot{\theta}_1 + l_2 s_3(\dot{\theta}_1 + \dot{\theta}_2) \\ c_{23} l_1\dot{\theta}_1 + l_2 c_3(\dot{\theta}_1 + \dot{\theta}_2) \\ \dot{\theta}_0(-l_2 c_{12} - l_1 c_1 2 - l_0) \end{pmatrix}
$$

$$
{}^5w_5 = {}^4w_4 = \begin{pmatrix} s_{123}\dot{\theta}_0 \\ c_{123}\dot{\theta}_0 \\ \dot{\theta}_1 + \dot{\theta}_2 + +\dot{\theta}_3 \end{pmatrix}
$$

$$^5v_5 = {}^4v_4 + {}^4w_4 \times \begin{pmatrix} l_3 \\ 0 \\ 0 \end{pmatrix} = \begin{pmatrix} s_{23}l_1\dot{\theta}_1 + l_2s_3(\dot{\theta}_1 + \dot{\theta}_2) \\ c_{23}l_1\dot{\theta}_1 + l_2c_3(\dot{\theta}_1 + \dot{\theta}_2) + l_3(\dot{\theta}_1 + \dot{\theta}_2 + \dot{\theta}_3) \\ \dot{\theta}_0(-l_2c_{12} - l_1c_12 - l_0 - l_3c_{123}) \end{pmatrix}$$

consequently considering the velocity matrix v as

$$v = \begin{pmatrix} v \\ \omega \end{pmatrix} \Longrightarrow$$

$$v = \begin{bmatrix} v_x & v_y & v_z & \omega_x & \omega_y & \omega_z \end{bmatrix}^T \tag{4.29}$$

We also know:

$$v = J(\theta).\dot{\theta} \tag{4.30}$$

$$\tag{4.31}$$

As the mechanism include 4 degrees of freedom, the right side of the equation 4.30 is a 4×1 matrix while the left side is a 6×1 matrix. Therefore, the Jacobean matrix is a 6×4 matrix which can be written in the following form:

$$^5J(\theta) = \begin{pmatrix} 0 & s_{23}l_1 + l_2s_3 & l_2s_3 & 0 \\ 0 & c_{23}l_1 + l_2c_3 + l_3 & l_2c_3 & l_3 \\ -(l_2c_{12} + l_1c_12 + l_0 + l_3c_{123}) & 0 & 0 & 0 \\ s_{123} & 0 & 0 & 0 \\ c_{123} & 0 & 0 & 0 \\ 1 & 0 & 0 & 0 \end{pmatrix}$$

$$^0 J(\theta) = \begin{pmatrix} {}_5^0 R & 0 \\ \\ 0 & {}_5^0 R \end{pmatrix} {}^{.5} J(\theta)$$

But the ν matrix on the equation 4.29 has six elements because all elements are not independent and in fact 2 of the variables are dependent to the others which are ν_y and ω_x. Eliminating them from the ν matrix, we will have: $\nu = \begin{pmatrix} \nu_x & \nu_z & \omega_y & \omega_z \end{pmatrix}^T$ and consequently:

$$^0\nu = \begin{pmatrix} {}^0\nu_x \\ {}^0\nu_z \\ {}^0\omega_y \\ {}^0\omega_z \end{pmatrix} = {}^0 J' \cdot \begin{pmatrix} \theta_0 \\ \theta_1 \\ \theta_2 \\ \theta_3 \end{pmatrix}$$

In which:

$$^0 J' = \begin{pmatrix} {}^0 J(1) \\ {}^0 J(2) \\ {}^0 J(3) \\ {}^0 J(4) \end{pmatrix}$$

Where $^0 J(n)$ is the nth row of the J matrix.

4.3.1 Singularities

A configuration where $|J| = 0$ is called a singularity of the robot. In this configuration the forces in the leg of the robot may go to infinity, causing a breakdown of the robot. Hence a very important issue is to be able to determine if there is a singularity within a given workspace $\mathcal{W}$ of the robot. $|J'| = 0$ equation leads to:

$$\sin(\theta_2 + 2\theta_0) + \sin(\theta2 - 2\theta_0) + 2\sin(\theta_2) = 0 \implies 2\sin(\theta_2)(1 + \cos(2\theta_0)) = 0$$

Consequently 2 conditions sating this equation are:

Case 1: $\theta_2 = 0$ or $\theta_2 = 180$

Case 2: $\theta_0 = \pm 90$

Both cases are well known singularity configurations for robotic arms which happen at the boarders of the workspace. Therefore, the 4-DOF climbing mechanism does not have singularities inside its workspace except on borders. This facilitates the trajectory generation algorithms as the need for singularity avoidance algorithms is abolished.

4.4   Optimization of the links length of the 3-DOF arm

The kinematics analysis was performed with parameters, because the numerical values of the links were not determined yet. The length of the links affects the workspace and the demanded torque of the serial mechanism. Lengthier links may construct a bigger workspace, but they also increase the demanded torque by the joints. The length of the links should be calculated with the objective of reaching a more efficient workspace and not necessarily a bigger workspace. A more efficient workspace can be obtained when the required workspace (The workspace which makes the arm able to pass bends up to $90°$) coincides with the robot's actual workspace. Analytical and geometrical analyses were performed to increase the workspace efficiency. These analyses led to two specific formulas between the design parameters which will be presented in this section.

Figure 4.3 shows the schematics of the 3DCLIMBER climbing mechanism when climbing a structure. l_1, l_2, and l_3 are the lengths of the climbing arm links, D is the diameter of the Z-axis rotating mechanism guide, and d is the diameter of the pole. The concentric circles show the constant workspace of the serial mechanism considering $\theta = 180^o$ (θ is the angle between the manipulator and the base of the robot as it can be seen in figure 4.2). The exterior radius of the circles is equal to $l_1 + l_2$ and the interior radius is equal to $|l_1 - l_2|$. If we neglect the third link in the workspace analysis, the center of these concentric circles would locate on "O" (see

figure 4.3). However the third link transfers the center from "O" to "C" equal to the length of the links (l_3).

To have the **the maximum straight step size**, or in the other word the maximum thrust on the pole in each step following issues should be observed:

1. "$l_1 + l_2$" is the diameter of the exterior workspace circle and determines the maximum thrust of the robot and thus should be as big as possible.

2. For the maximum thrust, the difference between the minimum and maximum distances of the manipulator and the base should be maximized. This means that the minimum distance (S_{min} in figure 4.4) should be as small as possible and the maximum distance (S_{max} in figure 4.4) should be as big as possible.

While the first condition is to enlarge the workspace of the robot, the second condition tries to make the workspace as efficient as possible. Enlarging the workspace as suggested by the first condition increases other costs like the weight, required torque, and size. To maximize S_{min}, the vertical diameter of the concentric circles of the workspace should coincide with the axis of the pole. In this way, the maximum thrust would be possible. To do this the $l_3 = \frac{D}{2}$ condition should be fulfilled (figure 4.4).

The minimum and maximum distance between the base and the manipulator are also shown in figure 4.4. To minimize S_{min}, should be minimized. To do this, the radius of the internal circle of the workspace should be zero. This leads to the condition $l_1 = l_2$ which is shown in figure 4.5.

To **maximize the thrust on the X direction** which is necessary for passing the 90° bend sections in minimum number of steps, the vertical distance S_v (see figure 4.6) should be minimum. As it can be seen in figure 4.6, the maximum possible X thrust happens at the horizontal diameter of the workspace circle. Thus, by minimizing the S_v, workspace circles shift toward the Z axis direction and consequently the thrust on the X direction increases. To minimize S_v, S_{min} should be minimized, which is indeed the same condition which has been discussed previously ($l_1 = l_2$).
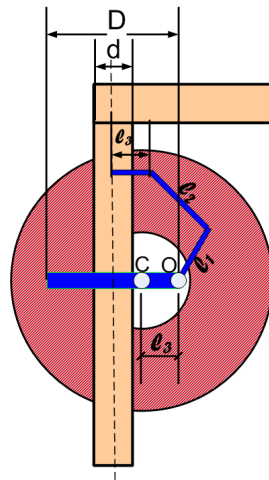
Figure 4.3: The constant workspace of the articulated 3-DOF arm.
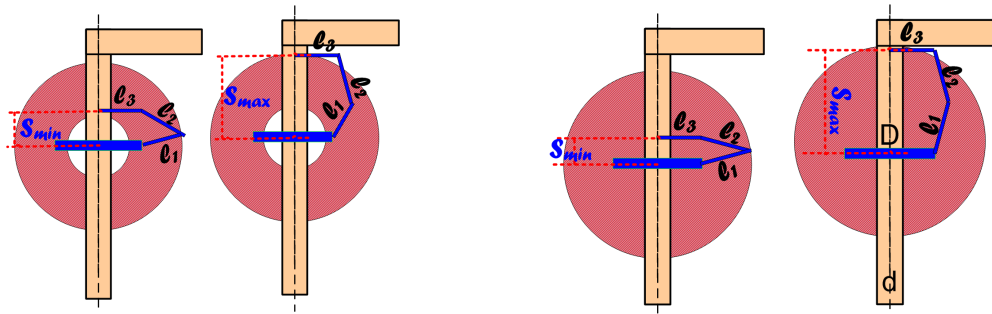
Figure 4.4: If $l_3 = D/2$, the vertical diameter of the concentric circles coincides with the axis of the pole.

Figure 4.5: The condition $l_1 = l_2$ increases the thrust of the articulated arm.
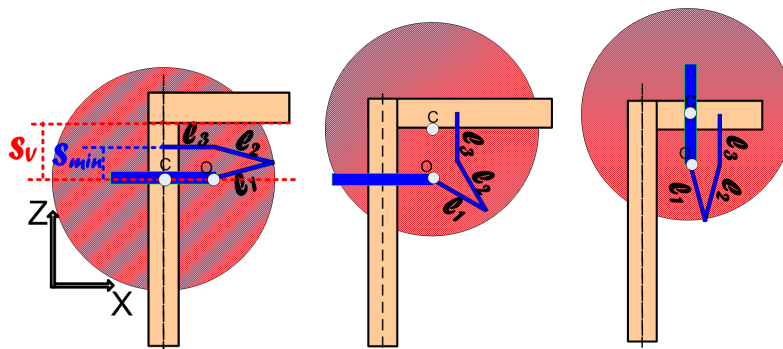
Figure 4.6: The condition $l_1 = l_2$ minimizes the S_v, which indeed maximizes the arm thrust in X (bent section) direction. In the middle and the right figure, the constant workspace for $\theta = 90^o$ is demonstrated. The center of the workspace shifts in Z direction equal to l_3.

Therefore in order to maximize the thrust, the following three conditions were considered in the detailed design phase.

1. $l_1 + l_2$ should be maximized within the limits of the robot's weight and the joint required torques.

2. $|l_3 - \frac{D}{2}|$ should be minimized or in the optimal condition should be zero.

3. $|l_1 - l_2|$ should be minimized or in the optimal condition should be zero.

Considering the above conditions and some other affective parameters, the numerical values for the length of the links were obtained as $[l_0, l_1, l_2, l_3] = [300, 220, 220, 350]$ (all in *mm*). The other affecting parameters and the method that was used to calculate these values are related to the detailed design of the robot and will be described in the next chapter.

4.5   Constant orientation workspace analysis

The constant orientation workspace is defined as the region that can be reached, by the reference point on the moving platform, when the orientation of the moving platform is kept constant.

When the 3DCLIMBER climbs over 3D structures, most of the time it has a constant θ angle. θ is the angle between manipulator and base of the robot 4.2. For climbing across the straight pole the angle is always $\theta = 180°$ and for passing bends, θ is equal to the bent angle (for a bent angle of $90°$, $\theta = 90°$). A MATLAB script was developed for constant workspace analysis of the mechanism considering physical limitations of the joints. The results of the constant workspace analysis for $\theta = 180°$ and $\theta = 90°$ is shown in figures 4.7 and 4.8.

4.6   Dynamic analysis

Dynamic analysis of the robot is required for several reasons:

- To calculate the required torque for the joints and to select the appropriate actuator.
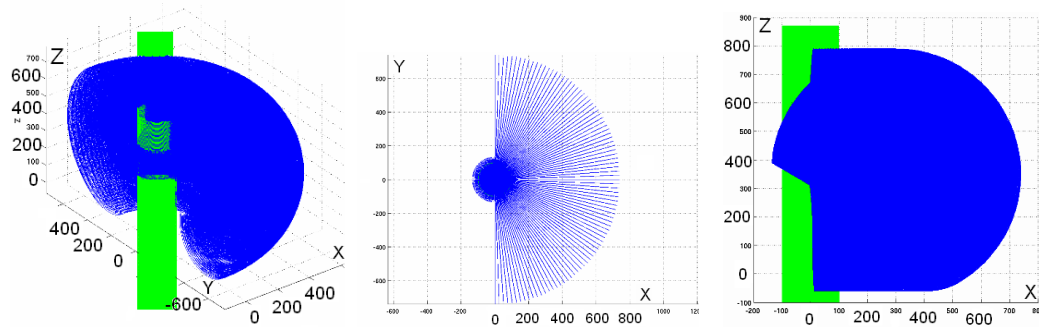
Figure 4.7: Different views of the workspace for θ = 90°, dimensions in *mm*.
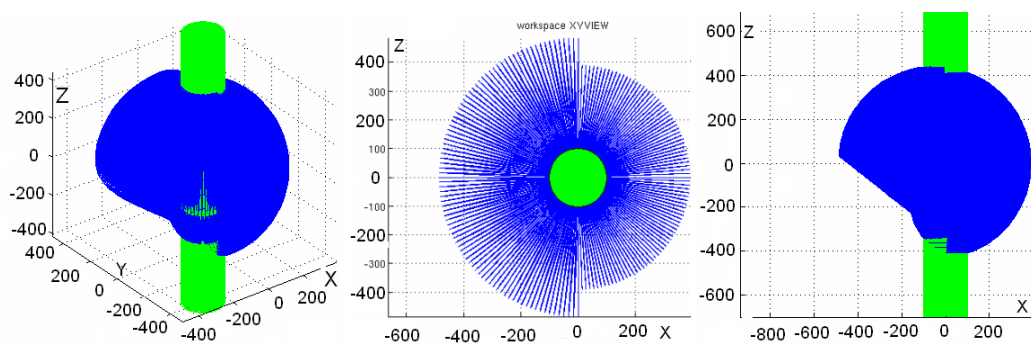
Figure 4.8: Different views of the workspace for θ = 180°, dimensions in *mm*.

• To reduce the controller effort and thus controlling the robot joints precisely.

• For applications which may need precise control of the applied force by the manipulator.

Yet, in the current status of the project we have only used the dynamic analysis for calculating the required torque for the joints. The 4-DOF mechanism consists of the 3-DOF serial arm and the Z axis rotation mechanism. The rotation only changes the working plane of 3-DOF arm around the Z axis. Once the 3-DOF arm reached the desired φ angle, the Z axis rotation mechanism maintains its position, and manipulation is performed by the planar serial arm. Therefore, the Z axis rotation mechanism is neglected in the dynamic analysis in order to avoid unnecessary complication. Figure 4.9 shows the schematic draw of the 3-DOF arm along with the links parameters. The recursive Newton-Euler algorithm was applied to obtain dynamic equations. Recursive Newton-Euler algorithm was firstly proposed by Luh et al. in 1980 [LWP80]. Recur-

sive algorithms are desirable from the viewpoint of simplicity and uniformity of computation. On the other hand, in this phase, the detailed design of the parts and actuators is not achieved. Therefore numerical values for many parameters namely: moment of inertia of links, moment of inertia of actuators, weights, frictions, etc. is not known yet. Consequently the closed form of the inverse dynamics equations of the robot arm were obtained by parametric variables. Application of recursive Newton-Euler algorithm to obtain parametric equations of the 3-DOF arm resulted in complicated and long equations. To simplify and shorten those equations and make them in the standard format, symbolic computation toolboxes of Maple and MATLAB were employed. Further Simplifications were performed manually. As probably it is not necessary to present all of the detailed calculations and simplifications, here the final inverse dynamic equations are presented:

$$
\begin{aligned}
\tau_3 \quad = \quad & (\alpha_1 + \alpha_2 + \alpha_3)(I_{zz3} + P_{xc3}^2 m_3) + P_{xc3} m_3 (L_2 s_3 (\omega_1 + \omega_2) \\
+ \quad & L_2 c_3 (\alpha_1 + \alpha_2) + c_{123} g + s_{23} \omega_1^2 L_1 + c_{23} \alpha_1 L_1) + L_3 f_y \qquad (4.32)
\end{aligned}
$$

$$
\begin{aligned}
\tau_2 \quad = \quad & (\alpha_1 + \alpha_2 + \alpha_3)(I_{zz3} + P_{xc3}^2 m_3 + P_{xc3} m_3 c_3 L_2) \\
+ \quad & (\alpha_1 + \alpha_2)(I_{zz2} + P_{xc3} m_3 c_3 L_2 + P_{xc2}^2 m_2 + L_2^2 m_3) \\
+ \quad & \alpha_1 (c_2 3 L_1 P_{xc3} m_3 + c_2 L_1 P_{xc2} m_2 + c_2 L_1 L_2 m_3) \\
- \quad & (\omega_1 + \omega_2 + \omega_3)^2 P_{xc3} m_3 s_3 L_2 + (\omega_1 + \omega_2)^2 P_{xc3} m_3 L_2 s_3 \\
+ \quad & \omega_1^2 (P_{xc3} m_3 s_{23} L_1 + s_2 L_1 P_{xc2} m_2 + s_2 L_1 m_3 L_2) \\
+ \quad & P_{xc3} m_3 c_{123} g + L_3 f_y + m_2 P_{xc2} c_{12} g + L_2 s_3 f_x + L_2 c_3 f_y + L_2 m_3 c_{12} g \qquad (4.33)
\end{aligned}
$$

$$
\begin{aligned}
\tau_1 \quad = \quad & (\alpha_1 + \alpha_2 + \alpha_3)(I_{zz3} + P_{xc3}^2 m_3 + P_{xc3} m_3 c_3 L_2 + C_{23} L_1 P_{xc3} m_3) \\[4pt]
+ \quad & (\alpha_1 + \alpha_2)(I_{zz2} + P_{xc3} m_3 c_3 L_2 + P_{xc2}^2 m_2 + L_2^2 m_3 + L_1(L_2 m_3 m_2 P_{xc2} c_2)) \\[4pt]
+ \quad & \alpha_1(I_{zz1} + c_{23} L_1 P_{xc3} m_3 + c_2 L_1 P_{xc2} m_2 + c_2 L_1 L_2 m_3 + P_{xc1}^2 m_1 + L_1^2(m_2 + m_3)) \\[4pt]
- \quad & (\omega_1 + \omega_2 + \omega_3)^2(-P_{xc3} m_3 s_3 L_2 - P_{xc3} m_3 s_{23} L_1) \\[4pt]
- \quad & (\omega_1 + \omega_2)^2(P_{xc3} m_3 L_2 s_3 + L_1 s_2(-L_2 m_3 - m_2 P_{xc2})) \\[4pt]
+ \quad & \omega_1^2(P_{xc3} m_3 s_{23} L_1 + s_2 L_1 P_{xc2} m_2 + s_2 L_1 m_3 L_2) \\[4pt]
+ \quad & g(P_{xc3} m_3 c_{123} + P_{xc2} m_2 c_{12} + P_{xc1} m_1 c_1 + L_2 m_3 c_{12} + L_1(m_3 + m_2)c_1) \\[4pt]
+ \quad & f_y(L_3 + L_2 c_3 + L_1 c_{23}) + f_x(L_2 s_3 + L_1 s_{23}) \tag{4.34}
\end{aligned}
$$

In which:

τ_n is the required torque for the nth joint.

θ_n is the angle of the nth joint.

ω_n is the angular velocity of the nth joint.

α_n is the angular acceleration of the nth joint.

I_n is the moment of inertia of the nth link.

m_n is the weight of the nth link.

4.7 3D modeling and validation of equations

4.7.1 3D modelling in SolidWorks

SolidWorks were used as the modeling software from the early stages of conceptual design. COSMOSMotion, a plug-in software for SolidWorks was used to simulate the motion of the 3D model in SolidWorks. COSMOSWorks, also a plug-in software for SolidWorks, was used for structural analysis of the mechanical parts.
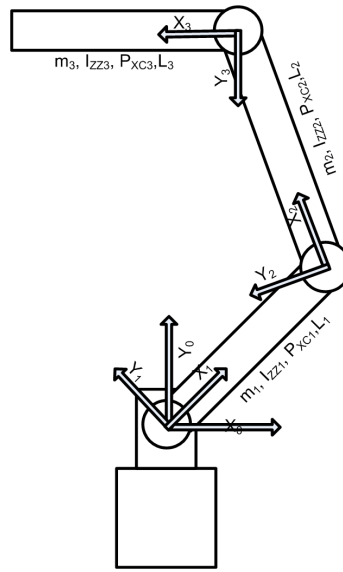
Figure 4.9: Schematic draw of the 3-DOF arm along with the links parameters.

4.7.2   Validation of developed codes

As stated earlier, a routine for direct kinematics and a routine for inverse kinematics of the 4-DOF mechanism were developed in MATLAB. These routines will be used in all further steps like workspace analysis, path planning, and optimization. The validity of kinematics equations and also MATLAB codes was verified through some numerical examples. Numerical examples were solved by the MATLAB functions and then were demonstrated by the 3D model in SolidWorks and their results were compared. For example, considering a mechanism with the following parameters for the links: $[L_0, L_1, L_2, L_3] = [300, 220, 220, 350]$ (all in *mm*) and the following values for the angles of the joints: $\theta_0 = 10°$, $\theta_1 = 30°$, $\theta_2 = 60°$, $\theta_3 = 60°$, the output of the direct kinematics routine is the pose vector of the 3rd joint coordinate system relative to the base coordinate system. The pose vector from the MATLAB routine was obtained as:

$$P = (X\ Y\ Z\ \theta)^T = (\ 483.07 \quad 85.18 \quad 330.00 \quad 150.00\ )$$
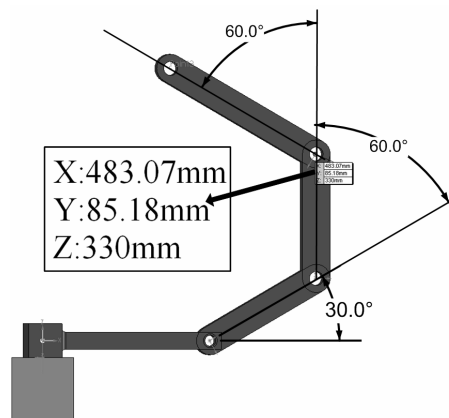
Figure 4.10: Validation of the direct kinematics equations and related MATLAB routines.

The validity of this result is checked by the Solidworks model as it can be seen in figure 4.10. The inputs of the Inverse kinematics routine are numerical values of the link lengths of the 4-DOF mechanisms, and the pose vector of the tool coordinate system relative to the base coordinate system. For the 4-DOF mechanism pose vector is shown as $P = (X\ Y\ Z\ \theta)^T$. The output of the routine is the vector of the joint angles, which is indeed $[\theta_0, \theta_1, \theta_2, \theta_3]$ which leads to the desired Pose. As the inverse kinematics of the mechanism have 2 answers, 2 vectors will be obtained.

The pose vector example is considered as: $P = [483.07, 85.18, 330.0000, 180]$

Matlab function:

$[solution1, solution2] = invkin(\ L_0\quad L_1\quad L_2\quad L_3\quad X\quad Y\quad Z\quad \theta\ )$

$[solution1, solution2] = invkin(\ 300\quad 220\quad 220\quad 350\quad 483.07\quad 85.18\quad 330.0000\quad 180\ ) \longrightarrow$

$[solution1] = (\ 10.0002\quad 30.0000\quad 60.0008\quad 89.9992\ )$

$[solution2] = (\ 10.0002\quad 90.0008\quad -60.0008\quad 150.0000\ )$

Both solutions were given as inputs for the joint values and the Pose vector was obtained. As it can be seen in figure 4.11, both solutions lead to the same pose which is $P = [483.07, 85.18, 330.0000, 180]$.

Considering link length of $[L_0, L_1, L_2, L_3] = [300, 220, 220, 350]$ (all in *mm*).
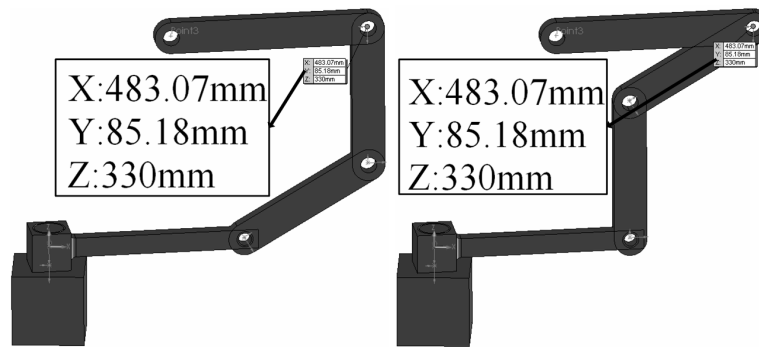
Figure 4.11: Validation of Inverse kinematics equations and related routines.

4.8 Conclusion

The kinematics, Jacobian matrix, singularities, and dynamics of the climbing mechanism were studied and the related equations were obtained and simplified. The accuracy of the kinematics equations were validated through a numerical example and the simulation softwares.

Chapter 5

Detailed Mechanical Design, Manufacturing, and Assembly

"The primary function of the design engineer is to make things difficult for the fabricator and impossible for the serviceman."

citation related to Murphy's Law.

5.1   Introduction

The detailed design of the 3DCLIMBER is described in this chapter. In the conceptual design phase, the 4-DOF structure was introduced as the climbing mechanism of the 3DCLIMBER. Further theoretical analyses including kinematics and dynamics analysis of the structure were achieved parametrically as the length of the links were not obtained yet. Obtaining the length of the links as well as selection of the appropriate actuator for the joints are interrelating issues which will be described in the next section.

Afterwards, the detailed design of the robot will be comprehensively described. Some of the robot's parts are commercially available while others are custom design and should be manufactured. In selection process of the standard parts and design process of the custom made parts, minimum weight concept was considered as a critical factor. Therefore, COSMOSWorks, a finite element analysis software was used for optimum structural design of non standard parts. After finalizing the detailed design of the robot and development of a trajectory generation routine, the system was simulated and validated. The 3D model of the parts were developed in SolidWorks and using the trajectory generating routine, the robot's ability to climb from the structure and to pass bent sections was examined through simulation in COSMOSMotion.

5.2   Link lengths and actuators

Long links have the advantage of increasing the workspace of the serial climbing mechanism resulting in longer climbing steps and consequently higher climbing speeds. But application of longer links increases the required torque for driving each joint. Therefore, application of heavier actuators would be necessary which results in a heavier robot. The lengths of the links should be calculated so that a reasonable balance between the robot's speed and it's weight to be established. Also the following conditions which were obtained through analytical optimization of the links lengths through workspace analysis (demonstrated in the previous chapter) should be considered:

1. $l_1 + l_2$ should be maximized within the limits of the required torques on the joints.

2. $|l_3 - \frac{D}{2}|$ should be minimized.

3. $|l_1 - l_2|$ should be minimized.

The method that was applied to obtain numerical values of the links lengths is partially demonstrated in figure 5.1 as a flowchart and can be described as the following steps:

1. The length of the first link (l_0 in figure 4.2), depends on the diameter of the structure which the robot should climb from, and the detailed design of the rotation mechanism.

Considering the diameter of the structure (219 *mm*-figure 2.2), and other design restrictions, the Z-axis rotation guide was chosen from the commercially available guides with a diameter of $\phi = 600$ *mm*. Therefore $l_0 = 300$ *mm* was obtained.

2. The 2nd and the 3rd conditions are considered for calculation of the length of the other links. Considering that the $|l_3 - \frac{D}{2}|$ should be minimized, one can calculate $l_3 = 300$ *mm*. However as the value of the l_3 is dependent to the design of the upper gripper and some structural analysis, the minimum value that we could obtain was $l_3 = 350$ *mm*.

3. Considering the value obtained for l_0 and l_3, and the fact that the length of the links should allow the robot to pass a bent section of 90°, the minimum possible length for l_1 and l_2 were calculated. The third condition i.e. $l_1 = l_2$ was respected.

4. Considering the preliminary lengths, an actuator was selected from available options and then the length of the links (l_1 and l_2) were increased within the limits of the actuators torque and considering a factor of safety.

When choosing high-tech actuators (e.g. Harmonic Drive actuators), designer should opt from what is available in market as ordering an actuator with custom torque and speed is costly (for normal gears, one may design and manufacture a gearbox with a custom ratio and obtain the exact torque and speed combination at a low price). As the serial arm joints demand for high torques, then high ratio gearboxes should be used. After a comprehensive survey about available commercial high ratio gearboxes we concluded that Harmonic Drive technology is the lightest and the most efficient technology for high ratio gearboxes (figure A.7 presented in annex A). Therefore actuators were selected from the Harmonic Drive catalogue. Using the dynamics analysis formulas, the required torques for driving the joints for the primarily considered link lengths were estimated. Also, these values were estimated by COSMOSMotion through simulating the model of the robot passing the bent section. Figure 5.2 shows the results of a simulation achieved through COSMOSMotion software. Due to problems on modeling of the "contacts" in the simulation software, the demonstrated curves in figure 5.2 could not be trusted. However the
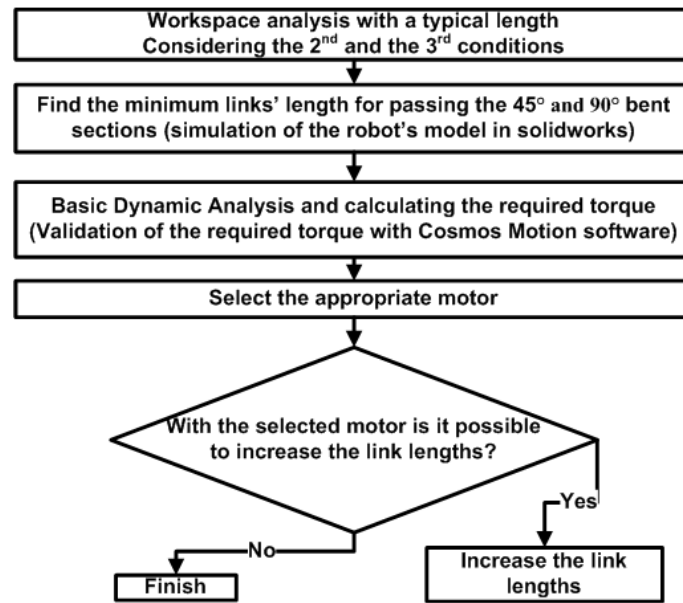
Figure 5.1: The method which was used for calculation of the length of the links

Gear Ratio		160:1.
Max Torque	N.m	260.
Continuous stall torque	N.m	102.
Max Output Speed	rpm	28.
Weight without brake	Kg	4.3.

Table 5.1: Characteristics of the FHA-25C-160H Harmonic Drive actuator [LLC08].

simulations helped us to estimate the required torque with less complicated models, e.g. fixing the gripper to the "simulation ground" rather than modeling the contacts.

The Harmonic Drive FHA-25C-160H actuator (figure A.7), which was opted for all three joints, is composed of a $600\,W$ AC motor coupled with a 160:1 Harmonic Drive gearbox. It can deliver torques up to $261\,N.m.$ and a continuous torque of $102\,N.m.$ Figure 5.3 shows the performance graph of the actuator and table 5.1 summarizes its characteristics. The length of the links were recalculated so that the torque which can be delivered by the actuator be at least 2.5 times bigger than the required torque by the joints(FOS=2.5) . As a result, following values for the link lengths were obtained: $[L_1, L_2, L_3] = [220, 220, 350]$ (all in mm).
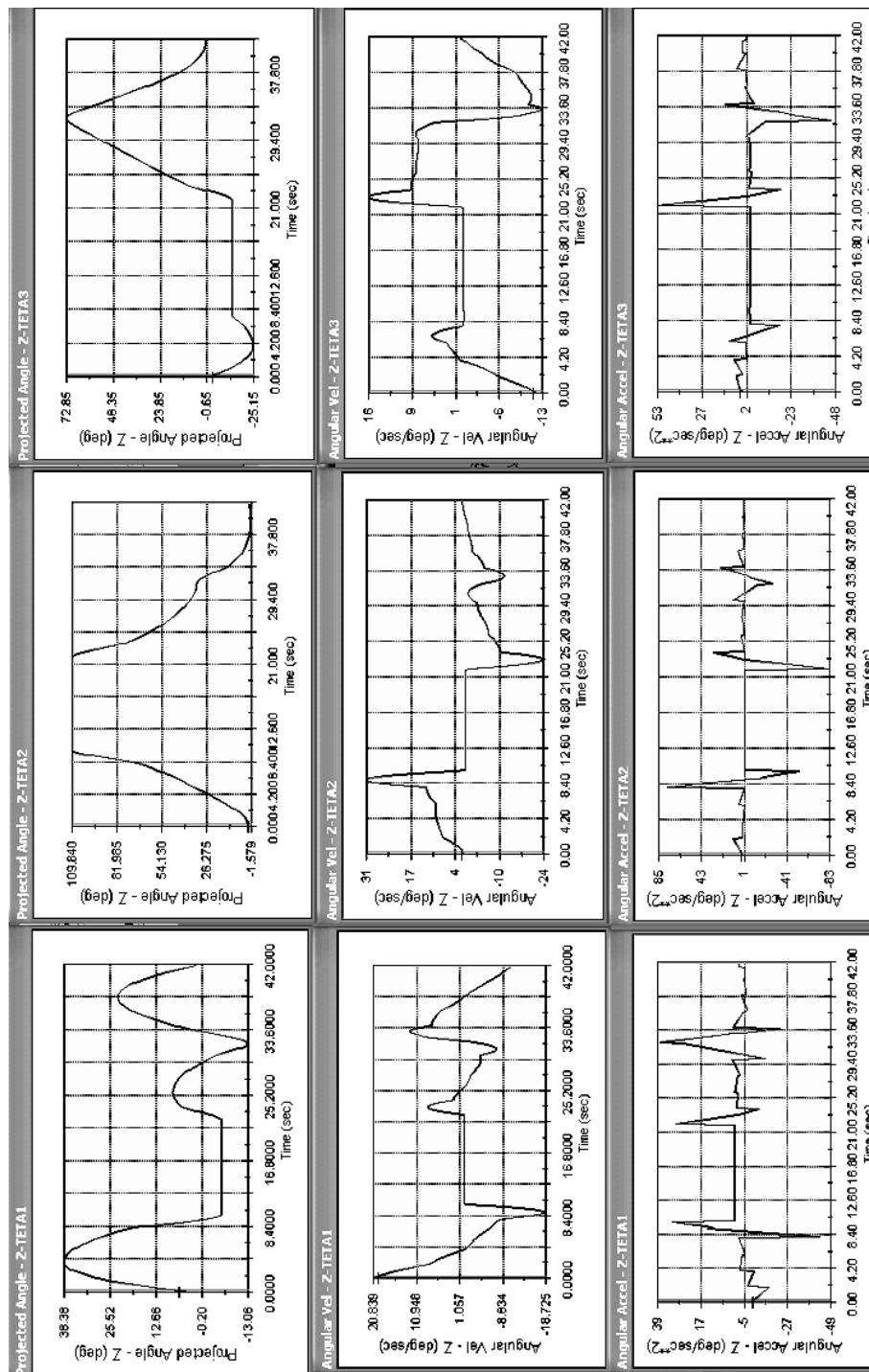
Figure 5.2: Position, velocity, and angular acceleration of all joints, when the robot is passing a 90° bent section. The trajectory of each joint (position and time) was introduced to the software as input. The occasional abrupt changes in curves are due to problems associated with the modeling of the contact between the grippers and the structure.
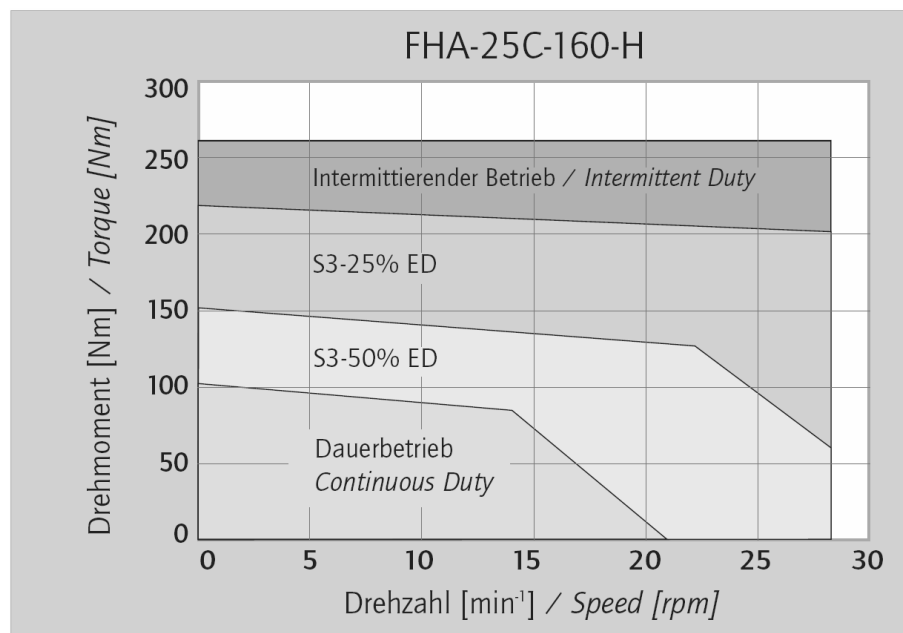
Figure 5.3: Performance graph of the FHA-25C-160H Harmonic Drive actuator [LLC08].

5.2.1   Payload

A minimum FOS(Factor of Safety) of 2.5 was considered for the actuators of the climbing mechanism in the worst case. The value of FOS for all of the parts, mechanisms and actuators was bigger then 2. Therefore, one can say that theoretically the robot can carry a payload equal to its own weight, reducing the FOS to 1. As many NDT devices are lighter than the weight of the robot itself, the current robot can carry those devices. For instance video inspection of pipes only needs a light camera. The eddy current NDT probes are also light and small. GemX-160 [S.A08] is a portable X-ray NDT device which can be mentioned as an example of a heavier NDT device and weights 15 kg. All of these devices can be carried by the robot, slightly reducing the FOS of the system.

5.3   Detailed design of the robot

Figure 5.4 shows the detailed design of the robot. The proposed design consists of two main parts: the 4-DOF climbing module and two similar gripping modules. One of the grippers is
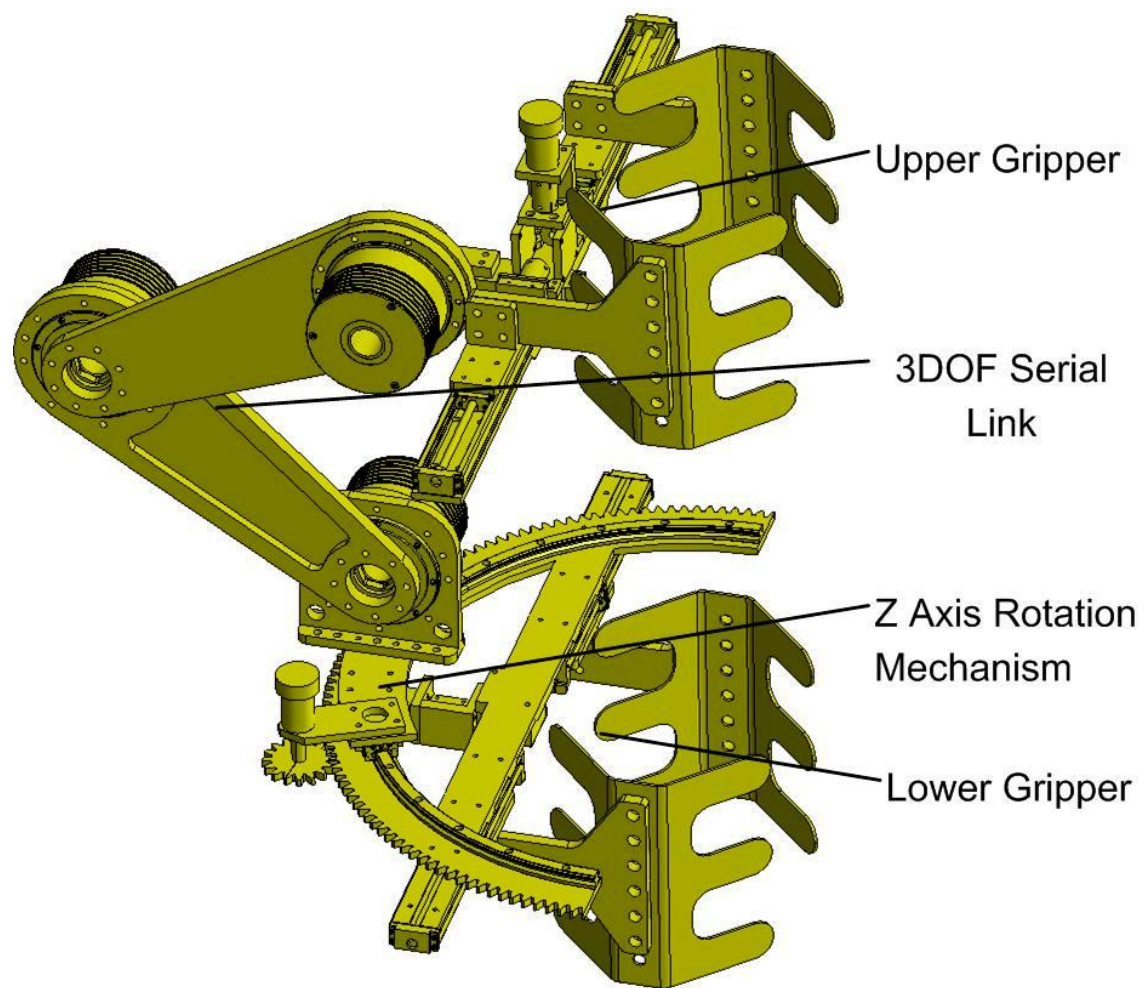
Figure 5.4: The detailed design of the 3DCLIMBER.

attached to a manipulator, and the other one is attached to the base of the rotating platform. This configuration provides four DOF between grippers, allowing the movement along poles with different cross sections and geometric configurations. The proposed design takes advantage of novelties in the design of both climbing and gripping modules.

5.3.1 Climbing structure

Figure 5.5 shows the detailed design of the 4-DOF climbing structure. The climbing structure previously described was implemented with the following elements:
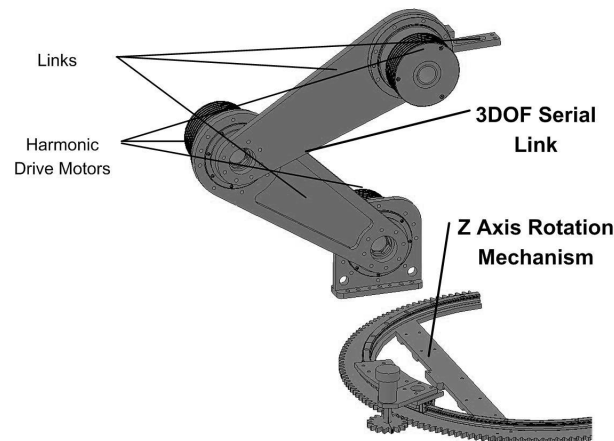
Figure 5.5: 4-DOF climbing structure.

- The 3-DOF serial link.

- The rotation mechanism around the axis of the structure.

The 3-DOF serial link

The 3-DOF serial link consists of 3 Harmonic Drive AC brushless motors coupled with 160 to 1 Harmonic Drive gearbox, capable of generating torques upto $260\,N.m$. Links are custom design and therefore were designed and simulated against the reacting forces and torques. The structural design of custom made parts will be described in the next section.

The Z axis rotation mechanism

One of the novelties in design of the 3DCLIMBER is the Z axis rotation mechanism. The Z axis rotation mechanism provides a fast manipulation around the structure axis, which is necessary for performing most of the inspection tasks like inspection of welding. Using traditional serial mechanisms as in [BGP⁺00a], makes the inspection operations time consuming and inefficient. Using the Z axis rotation mechanism, a fast transition between working planes of the 3-DOF arm is obtainable. The Z axis rotation mechanism is also necessary for placing the manipulator below one of the bent sections of a T-junction. Figure 5.6 shows the detailed design and parts of
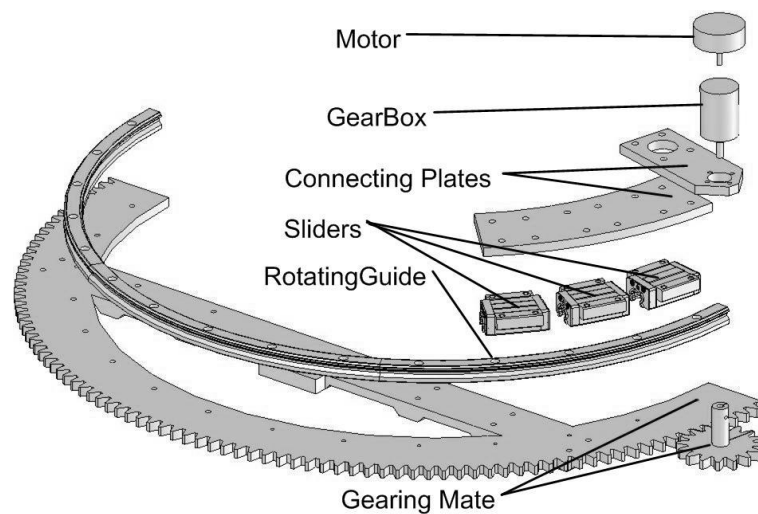
Figure 5.6: The Detailed design of the Z axis rotation mechanism.

the Z axis rotation mechanism. The motor is MAXON EC-45 brushless motor. It is a 50 *watt* motor capable of generating a nominal torque of $84\,mNm$ and a stall torque of $822\,mNm$. The gearbox is Maxon Planetary Gearhead GP-32C, with a 111:1 gearbox ratio. Coupling the motor and gearbox and considering the 70% efficiency of the gearbox, a nominal torque of 5 N.m at 60 rpm is reachable. More information can be found from MAXON motor website [mot08]. The circular sliding mechanism consists of three THK rotation guides (each of them making a 60°arc), three sliders and a gearing mate. Figure 5.7 shows the detailed construction of the guide and structures. Balls roll in four rows of precision-ground raceways on the rail and the slider. The end plate attached to the slider causes the trains of balls to circulate. Integrated balls increase the efficiency by decreasing the friction. Therefore, it is possible to drive the mechanism with a small torque and thus a light actuator. It should be considered that sliders should withstand the reaction moments generated by the actuators of the 3-DOF arm and the moments generated by the weight of the robot (figure A.2 presented in annex A). They should also withstand the normal and lateral forces (figure A.3 presented in annex A). Taking into consideration all of such forces and torques in all directions and a safety factor of 3, we concluded that 3 sliders should be mounted on the guide in order to withstand all torques and forces.
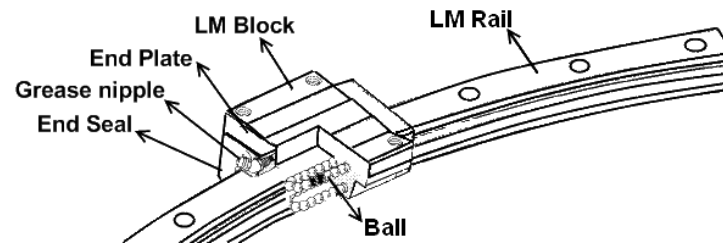
Figure 5.7: Construction of the HCR guide and slider.

5.3.2 Grippers

Grippers have an important role in the performance of the climbing robots, including:

- The safety of the robot during the normal operation and during the power failure depends on the grippers.

- Positioning precision of the 3-DOF serial arm manipulator depends on the stability of its basement, which indeed is one of the grippers at each time. Therefore quality of grasping the pole affects the precision of the manipulator.

Figure 5.8 shows the detailed design of the grippers. Each gripper consists of:

- Two unique multi-fingered V-shaped bodies.

- A brushless motor and planetary gearbox.

- One right-hand and one left-hand ball screws integrated in linear guides.

- Base and adapting plates.

V-shaped grippers

Grippers take advantage of a novel design which have mechanical self centering properties due to their "V" shape. Such design significantly reduces the necessity for integration of sensors and control algorithms for precise control and positioning of the gripper. In industrial applications,

ITEM NO.	PART NUMBER	QTY.
1	kr2602 Linear Guide	2
2	Slider Blocks	4
3	Plate	2
4	Link	2
5	V shape gripper	2
6	Bevel Gear	1
7	Plate	1
8	Maxon Gear	1
9	MaxonMotor	1
10	Couplings	3
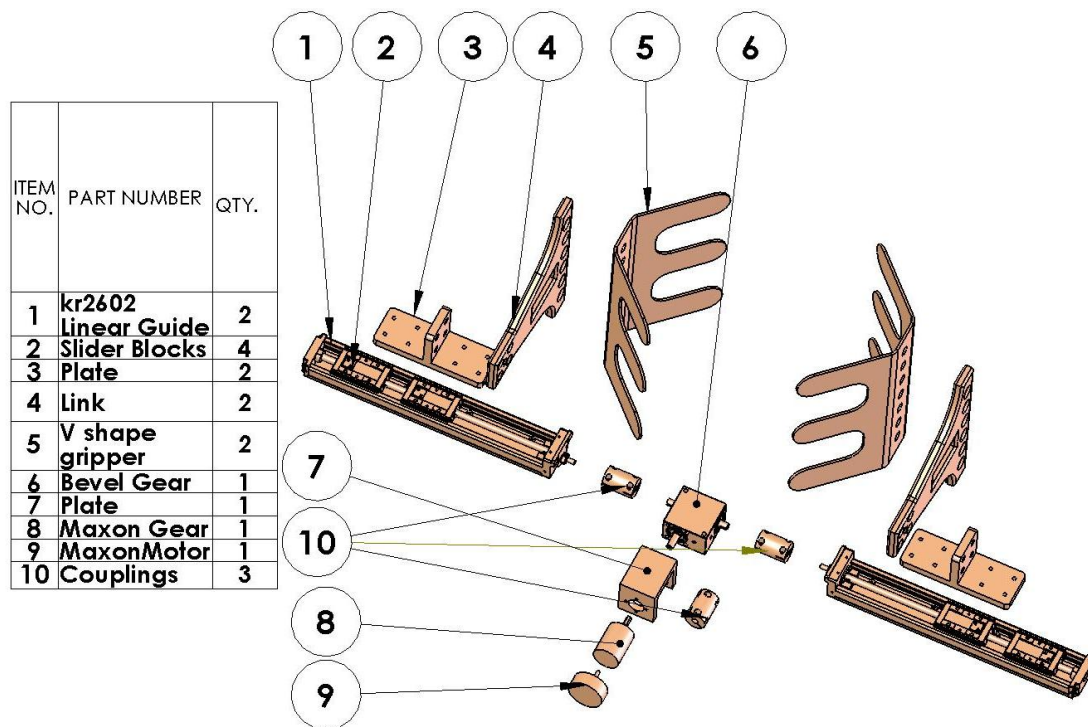
Figure 5.8: The detailed design and parts of each gripper.

"V" shaped gauges are used as jigs and fixtures for positioning of the circular profiles.

Another main factor which increases significantly the efficiency of the robot is that the grippers are designed in a way that each gripper can withstand the total torque that is generated by the robot weight and by the motors reaction torques. Therefore, when one of the grippers is attached to the pole the other gripper can freely manipulate over the pole and perform some tests on the structure. This eliminates the need for an extra manipulating arm and increases the maneuverability of the robot. To do so, all parts of the gripper should be able to withstand high forces and moments. Consequently the V-shaped part is designed long enough ($250\,mm$) to withstand such moments.

Grippers' Actuator

The grippers' actuators are same as the actuator for the Z axis rotation mechanism and can provide a nominal torque of 5 N.m at 60 rpm.

Ball screws and linear guide

Ball screws are used for efficient transformation of rotary motion to linear motion. Using One right-hand and one left-hand ball screws, makes it possible to drive the grippers with one motor. For selection of appropriate ball screw and linear guide, following issues were considered:

1. To increase safety, the gearbox ratio and ball screw's pitch are calculated in a way that the robot can stay attached to the pole by only one of the grippers.

2. In case of power failure, the robot should stay attached to the pole without slippage on the structure. For this purpose, when the gripper is closed, the total force required to open the gripper (or to make it slip on the structure), i.e. inertia of the gripper, should be higher than forces exerted to it by weight of the robot. The inertia of the gripper depends on several factors, namely the inertia of the motor's rotor, the ratio of the gearbox, and the pitch of the ballscrew.

3. The linear guide should be able to withstand all existing forces and moments.

4. Gripper should be able to grasp a range of pole diameters. First, because in industrial applications there exist pipes and poles with different diameters and second, because there are flange couplings (see figure 1.3 for instance) which should be overtaken by the robot. Therefore the gripper was designed to operate on structures with diamater range of $200\,mm$ to $350\,mm$.

Considering all of these measures, an integrated linear guide and ballscrew was selected. THK kr2602 linear guide consists of a linear guide, a slider block, and a built-in ballscrew. Figure A.4 (presented in annex A) shows the construction of the kr2602 linear guide. Load-bearing ball trains are arranged with two trains on each side, thus constituting a double-row angular contact

design. The slider with such design can bear an equal rated load in all four directions (upward, downward, right side, and left side) (see figure A.5 presented in annex A) [Co.08]. All forces and torques which are applied to the gripper during climbing a straight pole or when passing a bent section were calculated. Based on this calculation, two slider blocks with a center distance of $90\,mm$ should be installed on each THK linear guide to be able to withstand all torques and forces.

On the other hand, the pitch of the ball screw determines the travel speed and force of the gripper. Using lower pitches results in higher forces but lower travel speeds. Also, lower pitches increase the total inertia of the system which increases the safety during power failure. As the travel distance for the grippers is short, high travel speed is not required. Therefore, the pitch of the ballscrews was considered $2\,mm$. We calculated that the force applied by the gripper to the structure can reach to $1250\,N$ and the travel speed of the gripper can reach $120\,mm/min$. This might seem slow, but during each step of the operation, normally the gripper should open just about $2\,cm$ ($2\,cm$ each side) which takes about 5 seconds. For obtaining a higher velocity, the gripper's motor can be replaced.

Couplings and Bevel gearbox

Figure A.6 (Presented in annex A) shows the bevel gear and the coupling which have been used. The bevel gearbox is used in order to transform the rotation axis of the motor by $90°$ and also to transform the rotation to both ballscrews. Therefor, it includes a bevel gear set and double-side shaft. To couple these shafts to ballscrews, couplings with a small degree of radial and angular flexibility were selected. This flexibility allows the system working even with existence of small misalignments due to imprecise assembly of parts.

5.3.3 Custom design links and base plates

As it can be seen in figure 5.8, each gripper consists of custom design links and a base plate. Therefore, similar to other parts, optimum structural design was achieved and will be described

in the next section.

5.4   Optimum structural design

Many parts of the 3DCLIMBER are custom design and should be manufactured. For the structural analysis of the parts, the first step is to estimate forces and torques that the part should withstand and then consider a safety factor. Designing the parts with the determined safety factor guarantees the safe operation of the part without failure. When a part is under load, the stress is not distributed equally in all volume of the part. Computer aided structural analysis helps to demonstrate stress and strain analysis and safety factor distribution of a part subject to loads and moments. Using such tools, one can redesign a part several times until it reaches the nearly minimum weight. To achieve a minimum-weight design, the variance of the safety factor distribution should be decreased. For instance if the minimum FOS is 3, the least-weight structure is a structure which has a FOS equal to 3 (and not more) everywhere in the part. But this might not be possible due to some other constraints i.e. geometrical and manufacturing restrictions as well as manufacturing costs. Many optimization techniques might be used for selecting the best element from some set of available alternatives. But these methods are not easily applicable to the least-weight structural design problem. This is due to difficulties associated with modeling and formulation of manufacturing costs and limitations. But using finite element structural analysis software, one can redesign a part several times until it reaches the near optimal structure, while considering the manufacturing limitations and costs. This method was applied in design of all non-standard and non-commercial parts of the 3DCLIMBER. COSMOSMotion engine which is a plug-in for SolidWorks was used as the finite elements analysis tool. Figure 5.10 shows the safety factor distribution in structural analysis of one of the grippers' arm. The minimum safety factor is 3, but the variance in the distribution of the safety factor is decreased as much as the geometrical design parameters and also manufacturing limitations allowed. While the distribution of FOS is the most important factor related to the design optimization, other factors should also be verified. Figure 5.9 shows the definition of the torques, forces, and fixed points. The
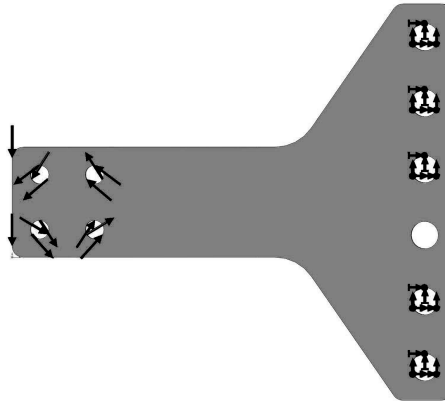
Figure 5.9: For the structural analysis of the gripper arm, the holes on the right side of the link are set as fixed. On the left a torque and a force are applied.

holes on the right side of the link will be fixed by bolts, and therefore in this analysis they are set as fixed. On the left a torque and a force are applied. The amount of the forces and the torques applied to each part were calculated based on the worst cases. Then for a reliable design many parameters were checked. For instance, the deflection on each part should be less than a certain value which is the maximum permissible deflection value. This value depends on many factors including the material being used and the permissible geometrical deflection of the part due to restrictions related to the whole mechanism design. Here the maximum permissible deflection of the gripper arm was considered $0.2\,mm$. Figure 5.12 shows the deflection which is the result of the applied force and torque in an exaggerated scale of about 500 times. As it can be seen the maximum deflection is about $0.05\,mm$. Figure 5.11 shows relatively the strain distribution on the gripper's arm.

Such analysis was performed for all custom design parts of the 3DCLIMBER, in order to reduce the weight of the robot as much as possible. Figure 5.13 shows the analysis of the final design of some parts.
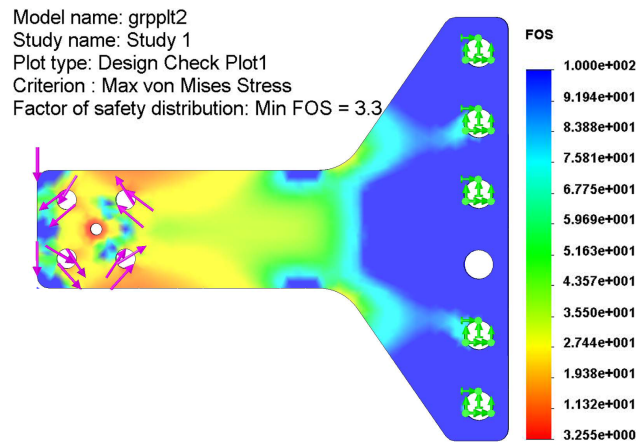
Figure 5.10: The safety factor distribution in structural analysis of one of the grippers' arm.
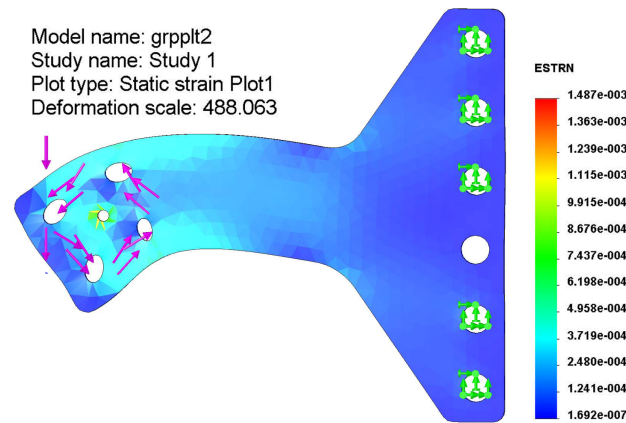
Figure 5.11: The strain distribution in structural analysis of the grippers' arm.
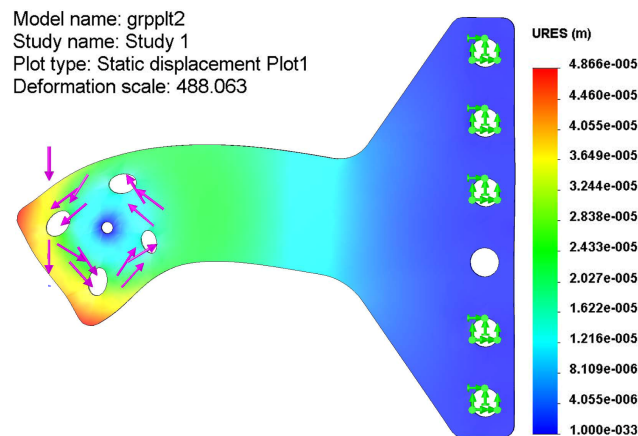
Figure 5.12: The deflection which is the result of the applied force and torque in an exaggerated scale of about 488 times.
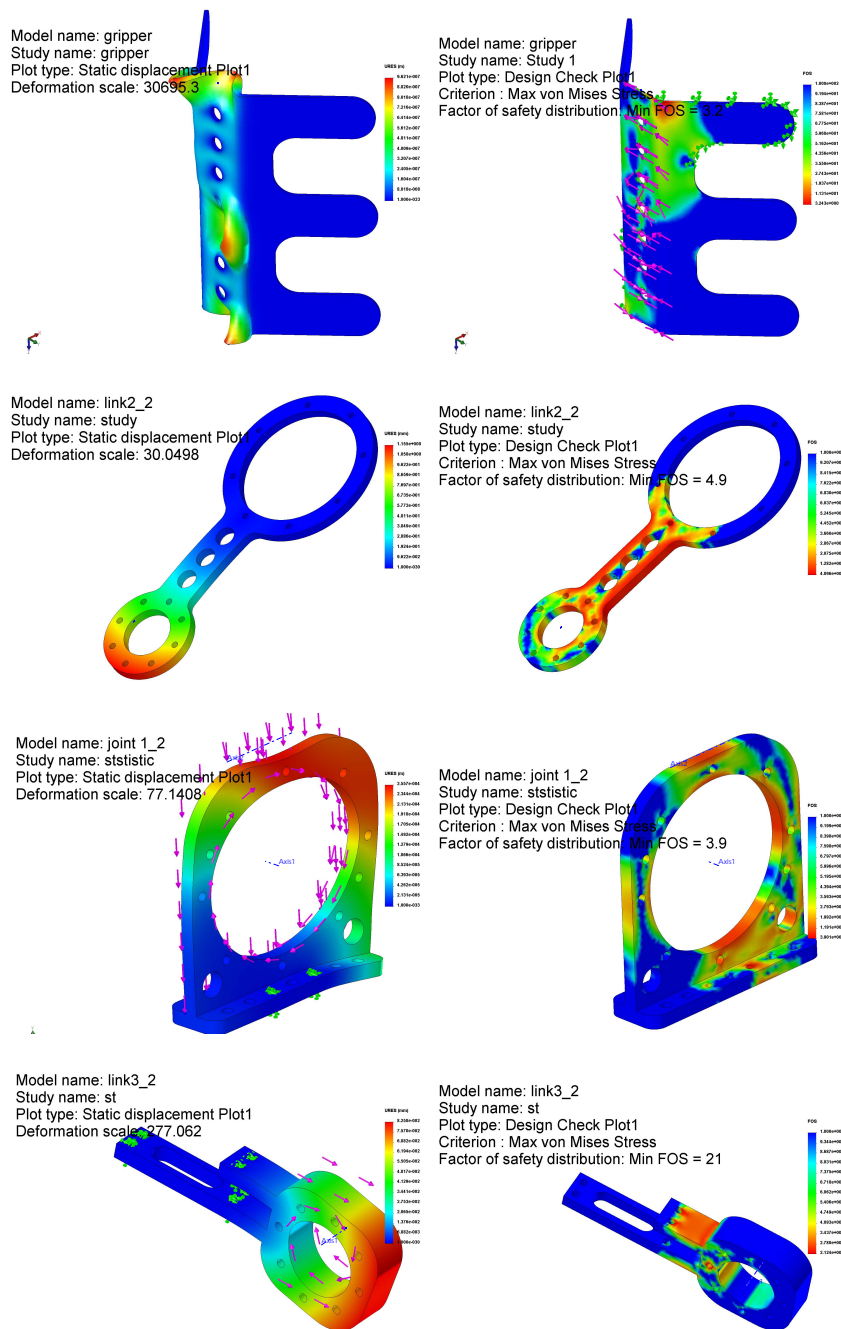
Figure 5.13: The structural analysis was performed for most of the parts with the objective of minimizing the weight of the parts and thus to minimize the over all weight of the robot.

5.5   Motion simulation and validation of the design

After completion of the detailed design of the robot, the model of the robot in Solidworks was simulated in COSMOSMotion in order to validate the detailed design of the robot. The motion simulation of the model has several advantages:

- To detect the possible collisions between the parts of the robot during operation.

- To check undesired collision between the parts of the robot and the structure.

- To determine the boundaries of each joint.

- To determine more precisely the required torques for deriving the joints of the climbing structure and gripping mechanism and to verify if the selected actuators can provide it.

To simulate the motion of the robot, the motion input should be provided to all actuators in the robot model. As the geometry of the structure is defined in the Cartesian space, the robot motion should be planned in the Cartesian space as well. Some routines were developed to turn a specified Cartesian-space trajectory (P_e) into appropriate joint position reference values. The routine has two steps:

1. Convert the trajectory in Cartesian space, to a series of intermediate manipulator poses.

2. Use inverse kinematics of a robot manipulator arm to find joint values for any particular location of (P_e).

And the output would be a series of joint position/velocity reference values to be sent to the controller (in this case is the simulation engine). The path planning of the robot and detailed trajectory generation will be extensively described in chapter 7. Therefore, in this section the details of the trajectory generating algorithms are not described, but results from these algorithms are used for the simulation purpose. The proposed tasks of the robot are climbing and manipulating over the structure. All of these tasks are performable with composition of 3 more basic tasks:

1. Climbing over the straight part of the structure.

2. Rotating around the axis of the structure.

3. Passing the bent section of the pole.

Since the second item is rather simple, the simulation results of the first and the third items are presented.

5.5.1 Climbing over the straight path

Supposing the upper gripper is open and the lower gripper is closed in the beginning, a straight climbing step includes moving up the manipulator, closing of the top gripper, opening of the bottom gripper, moving up the base, and closing of the bottom gripper. A routine was developed in MATLAB which receives the values of the manipulator's coordinate system relative to the base coordinate system and angle of the manipulator relative to the base (θ), at the start and end points (P_s and P_e) of each step and the total time for implementation of the step. The output includes vectors of joint position versus time for 4 joints of the 4-DOF climbing structure, and torque versus time for the actuators of the grippers. Considering inputs as (all dimensions in *mm*):

$$P_s = \begin{bmatrix} X_s & Y_s & Z_s & \theta_s \end{bmatrix}$$

$$= \begin{bmatrix} 0 & 0 & 310 & 180 \end{bmatrix}$$

$$P_e = \begin{bmatrix} X_e & Y_e & Z_e & \theta_e \end{bmatrix}$$

$$= \begin{bmatrix} 0 & 0 & 470 & 180 \end{bmatrix}$$

$$T_t = 22 \; sec$$

In which X_s is the X value of the manipulators coordinate system relative to the base coordinate system in *mm* at the start point. The output of the routine is showed in the figure 5.14, which
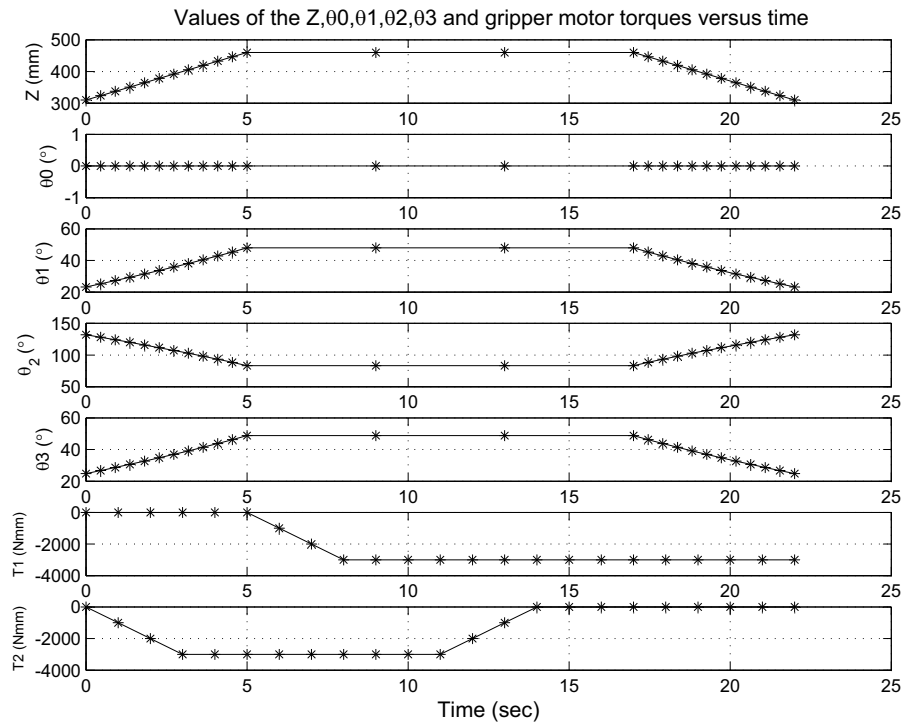
Figure 5.14: Trajectory of the joints and torque of the electrical actuators for a straight climbing step.

shows the trajectory of the joints in degrees and the torque which should be applied by the gripper's actuators in *Nmm*.

These trajectories were transfered to the simulation engine. Figure 5.15 shows sample shots from the simulation.

5.5.2 Passing the bent section

Similar to climbing over a straight pole, a routine was developed in MATLAB for passing the bent section of the structure. Figure 5.17 shows trajectory of the joints and torque of the electrical actuators for passing a 90° bent section in which θ_{rel} shows the travel angle of each joint relative to its initial position and θ_{abs} shows the absolute value of the joint. These trajectories were transfered to the simulation engine. Figure 5.16 shows sample shots from the simulation. In fact the result of the simulations was a proof of the concept, and also validated the detailed
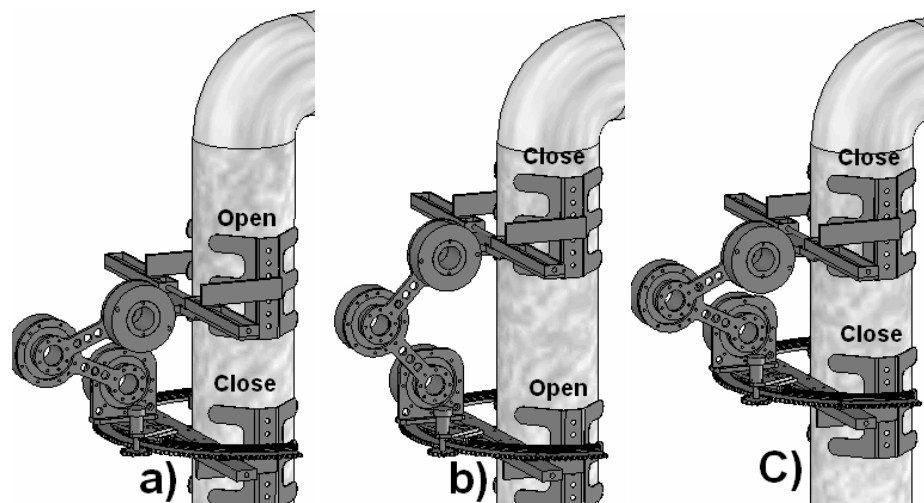
Figure 5.15: Sample shots of simulated motion of the robot model over a straight pole.

design of the robot. The simulation was based on position control. In the position control mode, the simulation engine can generate the chart of the deriving torques for all joints. Based on those graphs we were assured that the joints can be derived by the selected actuators.

5.6 Manufacturing, assembly, and mechanical characteristics

After the detailed design of the robot was completed and validated by simulations, the standard parts were ordered and the custom design parts were manufactured and assembled.

It should be highlighted that after the assembly of the robot, the first test of the 3DCLIMBER on the structure was successful and did not show any failure in the concept, the detailed design, structural analysis, kinematics analysis etc.

Figure 5.18 shows all custom designed and manufactured parts. As it is the first prototype it was tried to design the parts in several pieces so that in case of any change on the design, one can easily redesign and change only one part rather than the whole system. Easy access to all parts were considered in the design of each subassembly. All non-standard parts were designed
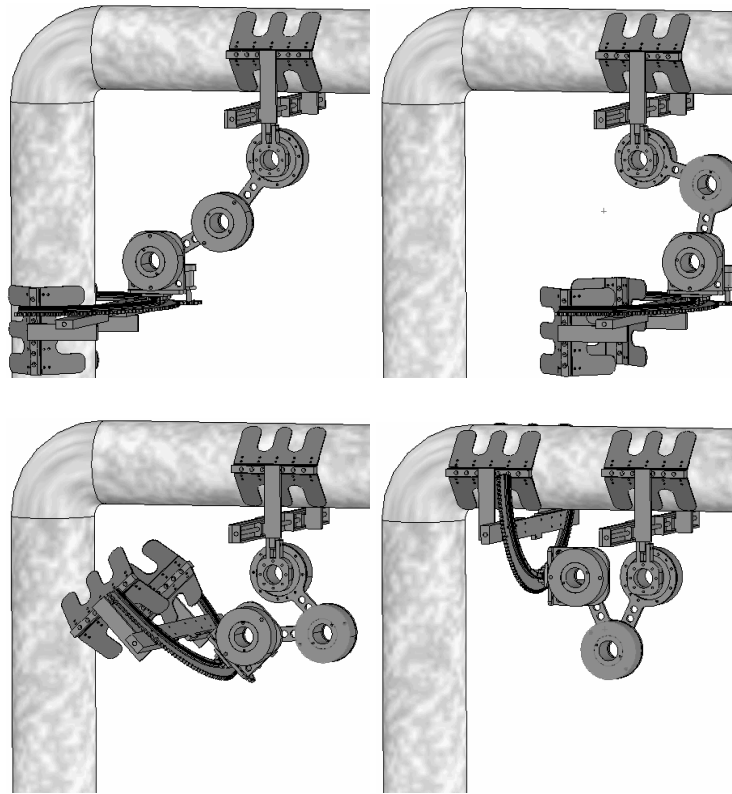
Figure 5.16: Sample shots of simulated motion of the robot model passing a bent section of $90^o deg$.

and manufactured with 7075-T6 aluminum. This type of aluminum is heavily alloyed with zinc making it very tough and strong. It has an ultimate tensile strength of $510 - 538 MPa$ (better than steel 1018) and thus has a very good strength to weight property [Rob08].

5.6.1   Grippers

Each gripper consists of two unique multi-fingered V-shaped bodies, a brushless motor, one right-hand and one left-hand ball screws, and 2 linear guides. Figure 5.19 shows one of the grippers. When one of the grippers is attached to the pole the other gripper can manipulate over the pole and perform some tests on the structure. This eliminates the need for an extra manipulating arm and therefore significantly increases the maneuverability of the robot. The contacting part of the gripper is covered with rubber in order to increase the friction between the
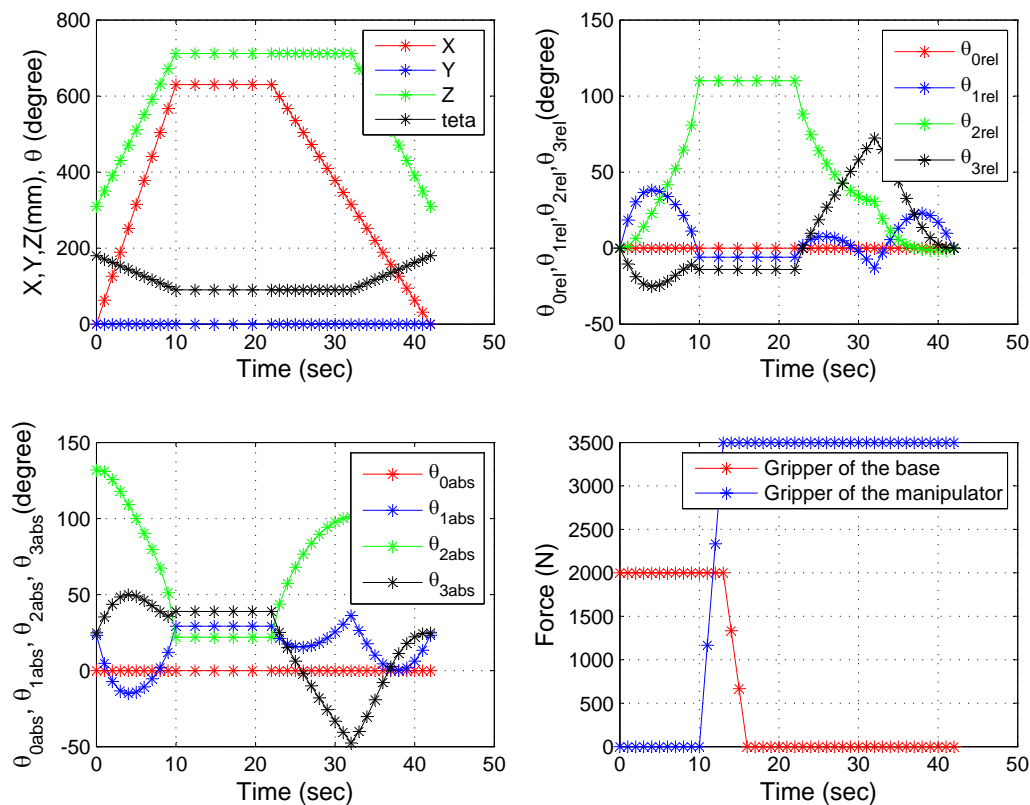
Figure 5.17: Trajectory of the joints and torque of the electrical actuators for passing a 90° bent section.

pole and the gripper. Each gripper is actuated by a $50\,Watt$ Maxon brushless DC motor coupled with a planetary gearbox which can apply $5\,N.m$ torque. Coupled by THK ballscrew with $2\,mm$ pitch, the gripper can exert forces up to $1250\,N$. To increase the safety, the gearbox ratio and ball screw pitch are calculated in a way that after that one gripper grasps the structure, the robot can stay attached to the pole by one gripper even if there is a power failure. This was successfully tested. But during the robot operation, after the gripper grasps the structure, the motor will still remain powered and apply torque to increase safety.

5.6.2 Climbing structure

The climbing structure was implemented with the following elements:

Table 5.2: Main Robot Characteristics

Degrees of Freedom	4
Quantity of Motors	6
Climbing Procedure	Step by Step
Weight (kg)	42
Material of the Parts	Aluminium 7075-T6
Robot Size (m)	$0.5 \times 0.6 \times 0.5$
Extended Robot Size (m)	$0.5 \times 0.6 \times 0.85$
Climbing Speed (m/min)	0.8
Minimum diameter of the pole that gripper is able to grasp	$200\,mm$
Maximum diameter of the pole that gripper is able to grasp	$350\,mm$

- The 3-DOF serial link includes 3 Harmonic Drives AC brushless motors coupled with 160 to 1 Harmonic Drive gearbox, capable of generating torques up to 260 N.m. Harmonicdrive gearboxes are lighter, more precise, and more efficient than many other types of gearboxes. Figure 5.20 shows the 3-DOF serial link while the trajectory generation routines and motion control algorithms were being tested.

- The rotation mechanism consists of three THK rotation guides and three sliders, one gearing mate, and one Maxon brushless DC motor. Figure 5.21 shows the Z axis rotation mechanism. This mechanism provides a fast manipulation around the structure axis, which is necessary for performing most of the inspection tasks like inspection of welding. Figure 5.22 shows the 3DCLIMBER robot. Table 5.2 shows the main characteristics of the robot.

5.7   Conclusion

The detailed design of the robot includes analysis and calculations of different but interrelating aspects of the mechanisms. The length of the links is determined by the required workspace of the robot while the required workspace depends on the project's objectives (e.g. to pass bent section up to 90°). Also, the length of the links has an effect on the driving torque of the joints
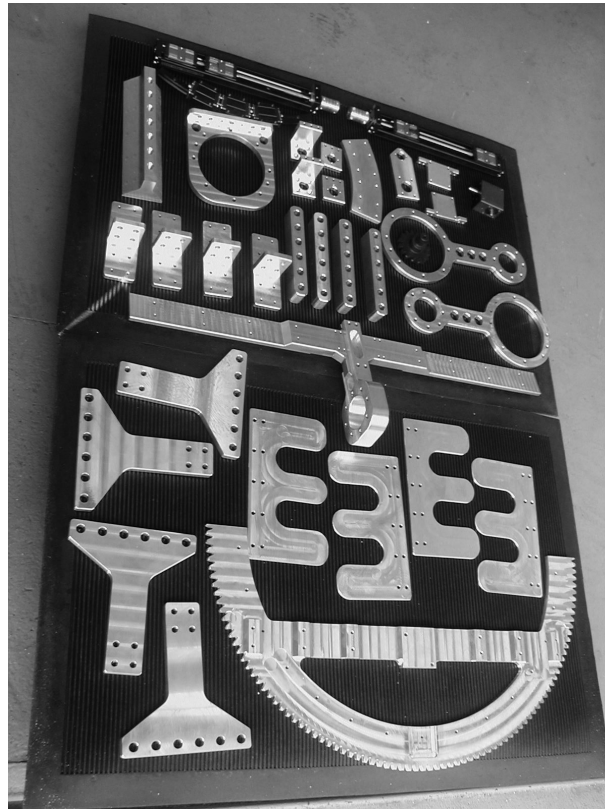
Figure 5.18: Custom designed and manufactured parts of the robot.

and thus on the actuator which should be selected. Furthermore the weight of the standard parts of the robot and the custom design parts influences the driving torque of the joints. One of the objective of the project was to minimize the weight of the standard and manufactured parts. Since all these parameters interact with each other, there could not be a determined single formulation for addressing all issues. Thus some of the parameters were fixed in each analysis step, and the others were analyzed by different tools. Structural analysis of the parts was achieved by structural analysis softwares in order to reduce the weight of the robot as much as possible. The standard parts were selected from the lightest possible technologies and the custom designed parts were manufactured from the 70 series aluminum which has a good yield stress to density ratio. Then a straight-climbing-step and also a bent-section-passing-step were successfully simulated using a path planning routine developed in MATLAB and a
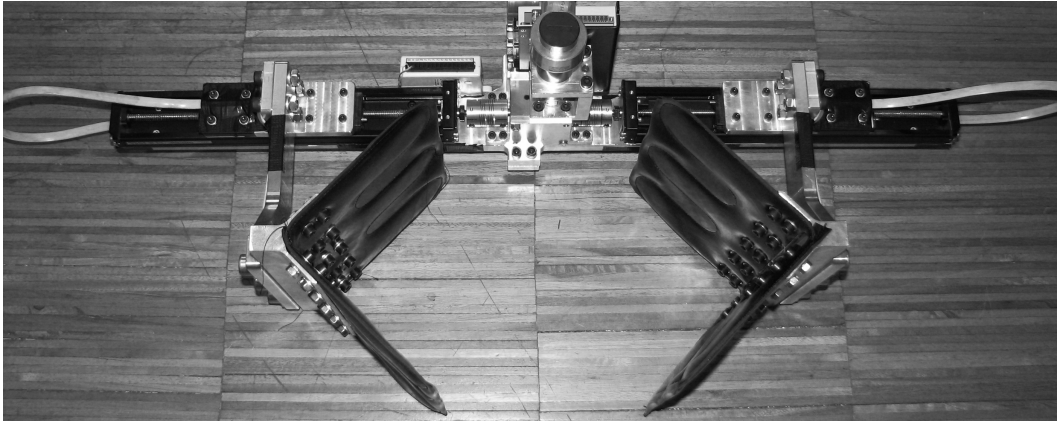
Figure 5.19: Gripper of the 3DCLIMBER.

motion simulating software. The robot was assembled and tested on the structure in order to examine the "proof of the concept" and also to validate the detailed design of the parts. The mechanical design of the system was completely validated after this test. During the test no problem was detected regarding the mechanical design. The tests and experiments of the robot will be described more extensively in chapter 8.
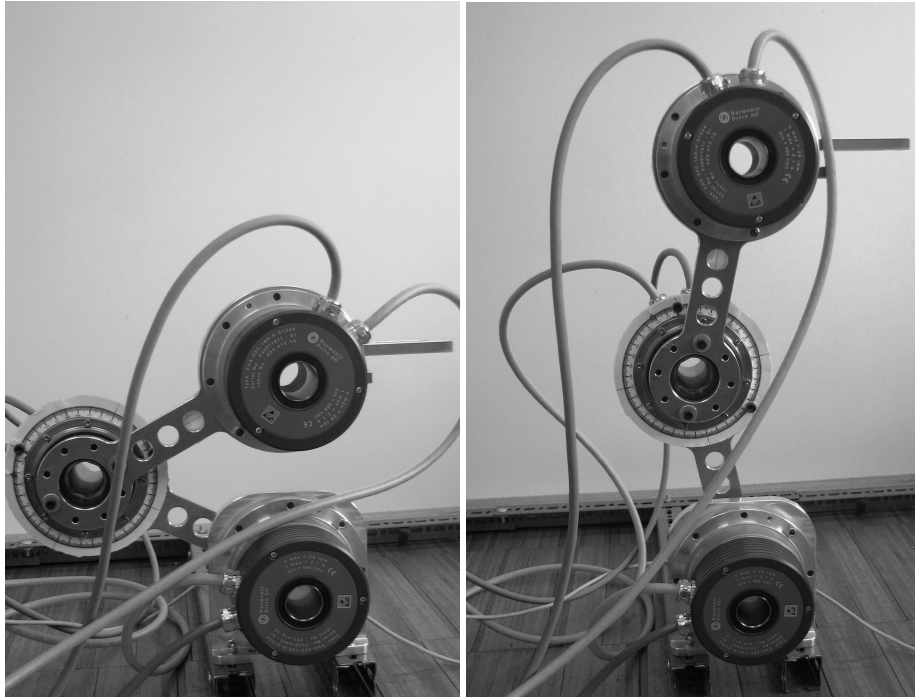
Figure 5.20: The 3-DOF serial link.

Figure 5.21: The Z axis rotation mechanism.
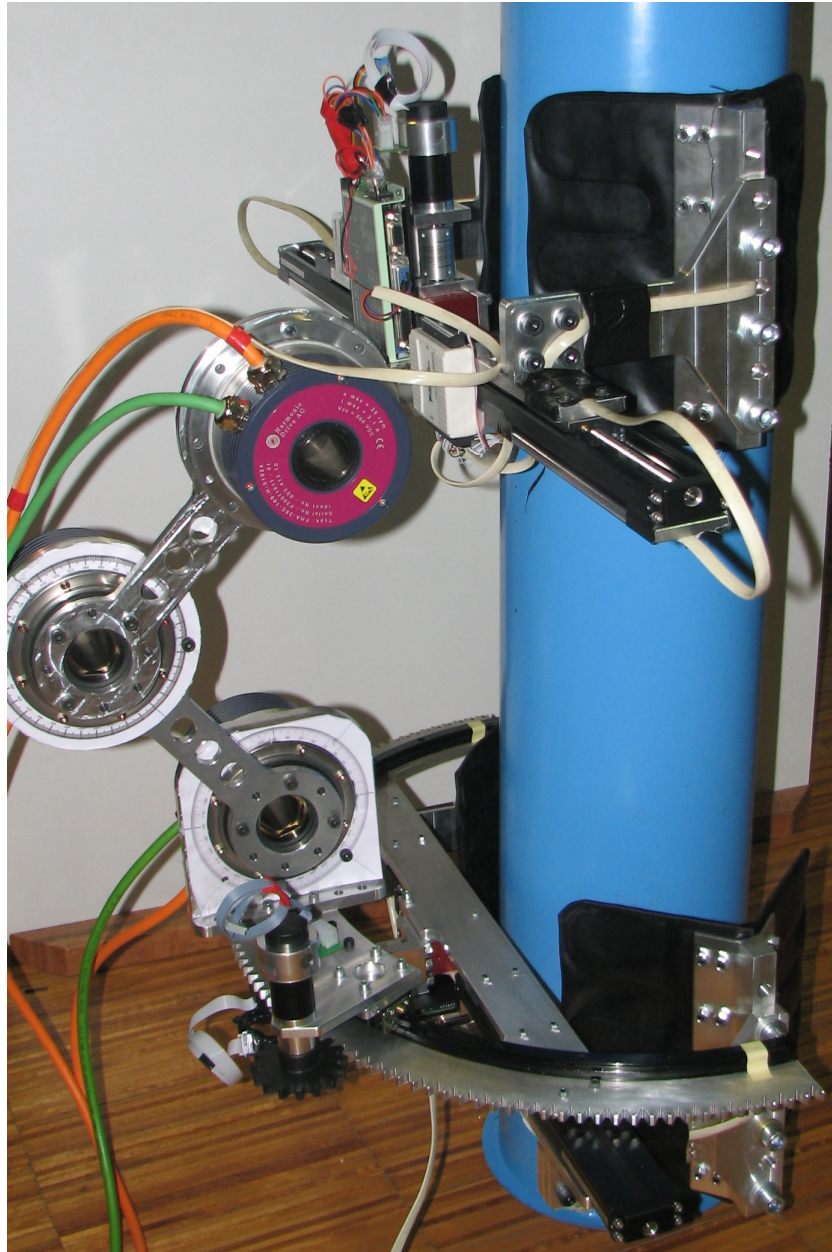
Figure 5.22: The 3DCLIMBER robot.

Chapter 6

Sensors and Electrical Architecture

6.1 Introduction

This chapter describes the sensors and the electrical architecture of the 3DCLIMBER. The necessity of application of some of the sensors which are described in the current chapter will be clarified more in the next chapter, where path planning algorithms of the 3DCLIMBER will be described. After describing the sensors, drivers of the actuators are described and then a schematics of the overall electrical architecture is presented. It should be mentioned that in general more emphasis in this thesis is given to the mechanical design of the robot due to the author's background in mechanical engineering.

6.2 Sensors

Sensors used in a system can be categorized to proprioceptive and exteroceptive. Proprioceptive sensors report internal state of a system part relative to an internal frame of reference. In the other word proprioception is sensing one's own internal status. Examples are encoders, gyros, and accelerometers. Exteroceptive sensors report current state of the working environment. Examples are light sensors, touch sensors, and range sensors. Both categories are used in 3DCLIMBER. But we only preferred not using external reference systems which use triangula-

tion or trilateration to a fixed reference system. Because in this case, a reference base station is required which should be calibrated before starting the robots operation. This is not a practical solution for outdoor industrial applications sometimes, as the installation and calibration of the observer is a time consuming task and requires an expert. 3DCLIMBER possess sensors on both gripping and climbing mechanisms.

6.2.1 Sensors of the gripping mechanism

The control aspects of the gripper will be discussed later, but in order to proceed with the description of sensors, it is necessary to mention that the gripper is controlled in positional control mode when it is opening and in torque control mode when it is closing. Therefore both position (openness) and contact forces should be measured. Furthermore for a precise gripping, it is important to know the position and orientation of the gripper relative to the structure before grasping.

Force Sensitive Resistors

As the name suggests, Force Sensitive Resistors (FSR) are sensors that change their electrical resistance as a function of the force exerted over their surface. A total of 16 FSRs were attached to the grippers in order to measure force on different locations of the gripper. Figure 6.1 shows 4 FSR sensors attached to one side of the gripper. The data from these sensors are used along with the amount of current of the motors to estimate the amount of force exerted by grippers and to serve as feedback for the torque control algorithm of the grippers' motors. They also provide more information about how grippers are connected to the structure. If during the operation of the robot, the 3-DOF link has some performance errors, or if the angle on the bend section of the robot is not exactly the one expected, it means that the gripper is not precisely oriented perpendicular to the pole. In this case different FSR sensors of the gripper report different values which means incorrect orientation of the gripper. Should this error be bigger than an specific adjustable amount, an error will be reported to the operator for further decision. In this
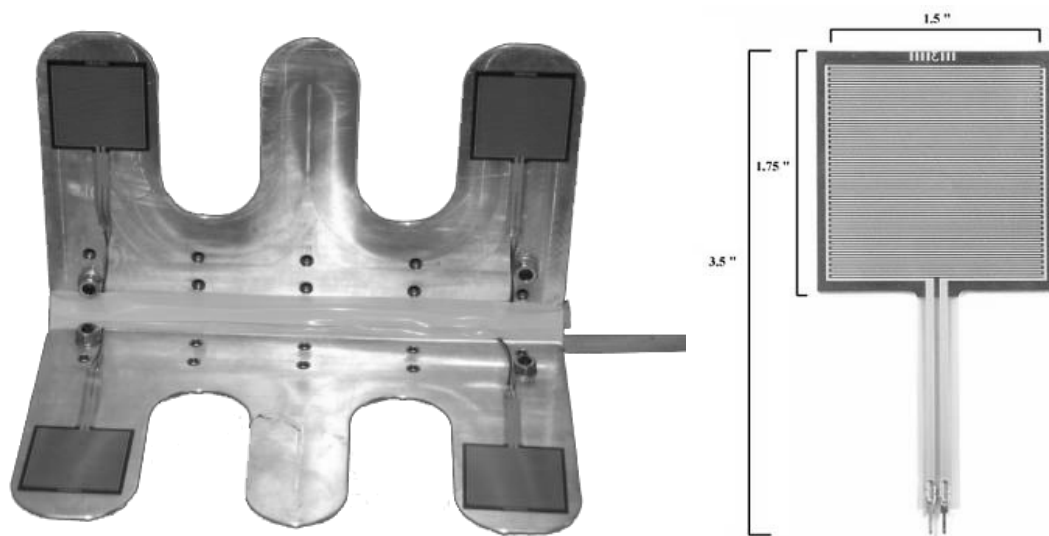
Figure 6.1: FSR sensors attached to a gripper.

case the operator may stop the operation and calibrate the system. It will be shown in the next chapter that after integration of a self calibration system, orientation of the grippers are corrected automatically before grasping, and FSR sensors will only report errors occurred after grasping. Another advantage of using FSR sensors are during the assembly and calibration of the grippers. As both links of each gripper should be installed completely symmetric to the center, measured values from the FSRs help us to precisely install and calibrate the grippers.

Encoders

Each gripper is actuated by a motor, whose encoder provides feedback to the position control mode. The encoder is an incremental encoder with 500 counts per revolution. Considering 111:1 gearbox ratio and 2 *mm* pitch of the ball screw, it provides a resolution of 40 η*m*. Obviously, the precision of the system is much less than the resolution due to mechanical system tolerance and clearances.
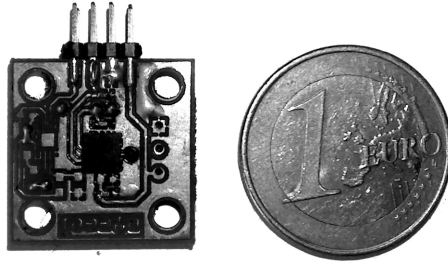
Figure 6.2: The inclinometer board developed at ISR.

6.2.2   Positioning sensors of the climbing mechanism

The sensors described in this section are internal encoders required for positioning control of the climbing mechanism manipulator and other sensors for calibration of the mechanism and compensation of the positioning errors. The application of these sensors on the 3DCLIMBER will be described in the next section along with the path planning algorithms.

Climbing mechanism encoders

HarmonicDrive motors used as actuators of the serial planar 3-DOF mechanism are equipped with an encoder with 1024 sin/cosine periods per count and HIPERFACE interface [Co.09] (figure A.8 in Annex A).

External reference sensors

External reference sensors are necessary for the robot autonomous calibration in the startup process of the robot. For all 4 DOF of the climbing mechanism, home made photocells based on opto-transistors were used. Consequently at the robot startup, an autonomous calibration step is defined in which all links move until aligning with a zero reference point.

Inclinometers

Inclinometers are necessary for estimation of absolute angle* of grippers as well as links of the climbing mechanism. They also serve for compensation of some other errors which will be

---

*Inclination angle relative to the horizon
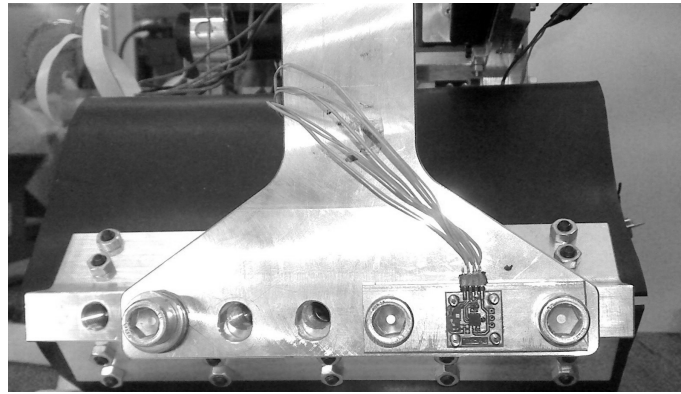
Figure 6.3: One of the inclinometer boards which is installed on the gripper.

described later. This inclinometers are based on STMicroelectronics ultra compact LIS244AL two-axis analogue accelerometer chips which are integrated in a board shown in figure 6.2 and figure 6.3. The board is fixed on a link vertical plane. This sensor has two analogue outputs for X and Y axes. Any change in the angle of each link, causes a change in the effect of the gravity acceleration on each axis and thus changes the output voltage of the accelerometers. The output voltage is read through a National Instrument data acquisition. The value is then compared with a pre-filled data table, in which "X" and "Y" axes voltages are assigned to each angle in range of $0° - 180°$ with $0.3°$ steps. Four accelerometers are necessary for absolute inclination measurement of all links including base and manipulator of the robot. Measuring absolute inclination of all links and using the direct kinematics formulation, the current task space position of the manipulator relative to the base can be calculated in every moment. Moreover, by installing an inclinometer on the base, the deviation of the robot's base angle from the desired angle can be measured. The absolute inclination of links acts as external positioning feedbacks. Encoders of actuators cannot report the deflection of the links and positioning errors initiated from the coupling errors and system backlash and/or tolerances of the system. Additionally, as the robot should climb from bent sections, inclinometers can provide useful data about the current angle of the manipulator for grasping a $45°$ or $90°$ bent section.
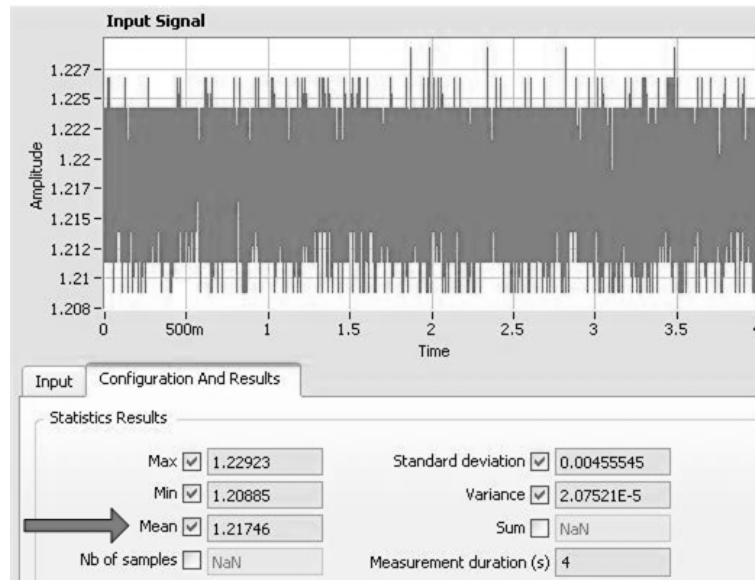
Figure 6.4: Y axis values of the accelerometer at $40°$.

Sensitivity of inclinometers $(\frac{\partial V_o}{\partial \theta})$ The sensitivity of accelerometers on each axis varies between $0.2\,mV$ to $6\,mV$ per degree. However, each axis is more sensitive in a specific range of values and less sensitive in other ranges (as the effect of the gravity is multiplied by the sine of the angle). For instance, sensitivity of Y axis in range of $45° - 135°$ degrees varies between $3\,mV$ to $6\,mV$ per degree. Consequently, using each axis on its more sensitive domain, a sensitivity of $3\,mV$ to $6\,mV$ per degree is possible. It should be noted that the angle which should be measured is always around the same axis, and application of the two-axis analog accelerometer was only in order to keep the adequate sensitivity in a range of $0° - 180°$. Figure 6.4 shows the measurement of signal on Y axis in 4 seconds, while the angle of the link relative to the horizon is 40 degrees.   The signal ranges from $1.209\,mV$ to $1.226\,mV$ which has a range of $17\,mV$. Considering the $4\,mV$ per degree the error on angle estimation based on a single sample might be up to $4°$.

Fault tolerance and filtering of mechanical vibrations   For an effective calibration of the system, a precision of about $0.5°$ is desired. This value is calculated based on the maximum
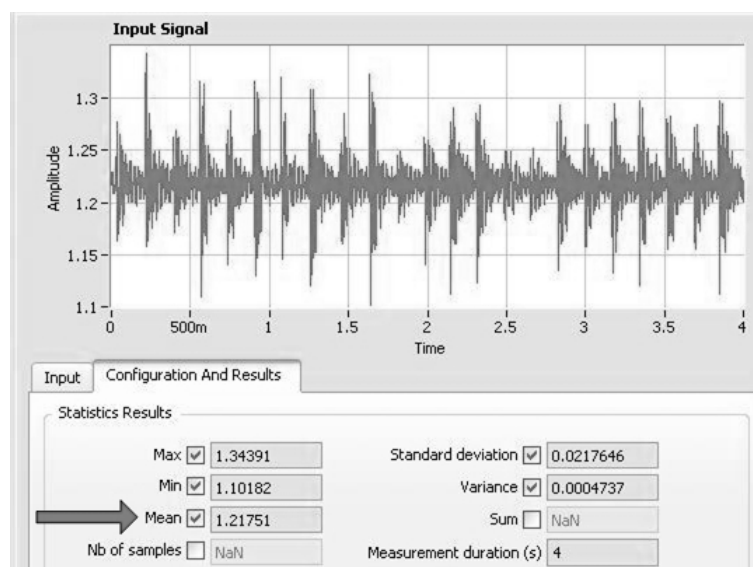
Figure 6.5: Y axis values of the accelerometer at $40°$ with a $6\,Hz$ normal amplitude vibration.

permissible error on the manipulator's pose in each step. It should be mentioned that in practice the 3DCLIMBER robot always has vibrations due to spring characteristics of the links. Vibrations change the angle of the base and manipulator of the robot. It also adds some acceleration to the links which affects the output value of the accelerometers. Therefore we should estimate the absolute angle of the links after filtering the vibration component. A positive aspect is that the mechanical vibrations are of low frequency and mostly under $10\,Hz$. Therefore, a method which averages sufficient samples acquired at high frequency was applied. If the sampling frequency is adequately greater than the mechanical vibration frequency and if a large enough number of samples gets acquired and averaged, the low frequency vibrations will be eliminated. With some experiments, we found the average value of 200 to 400 samples in a total time of 2-4 seconds, acquired at the rate of $100\,Hz$ (10 times larger than the mechanical vibrations frequency of the links) is very reliable. This method has good repeatability and can filter the effect of the mechanical vibrations. It showed a repeatability precision of $0.07°$ ($4'$). To test the repeatability against the mechanical vibrations effect, the accelerometer board was installed on a link and the link was manually vibrated with different frequencies and amplitudes similar to the frequency
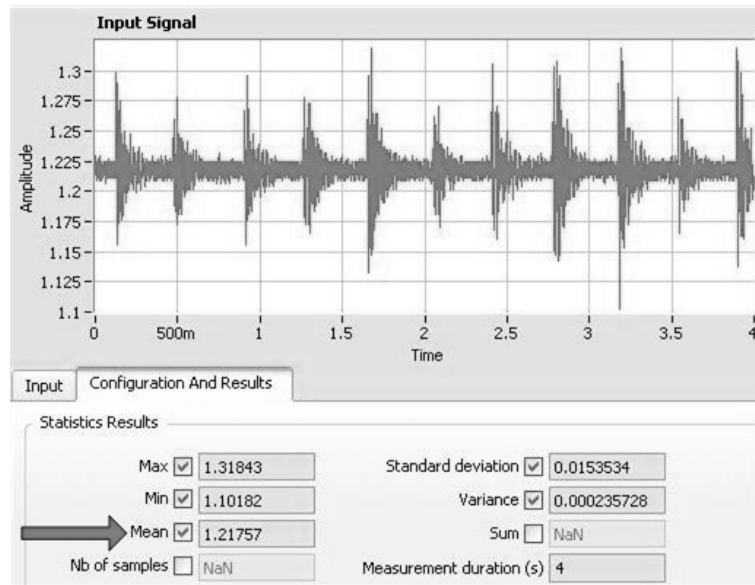
Figure 6.6: Y axis values of the accelerometer at 40° with a 3 Hz normal amplitude vibration.

and amplitude of vibrations which is happening in the 3DCLIMBER. This is shown in figure 6.5 and 6.6. In both cases the average value did not change more than 0.1 mV even with existence of vibrations with 6 Hz frequency.

The average value in a relatively high amplitude vibration (figure 6.7) has only changed about 1 mV. This provides us with a precision better than 0.3° (20′) even with existence of relatively high amplitude vibrations. The characteristics of the developed inclinometers are summarized in Table 6.1.

6.2.3   Range finders

The distance between the pole and the structure is measured using Sharp GP2Y0A21 optical triangulation sensors (figure 6.8). These sensors can measure distances in the range of 10 cm to 80 cm (figure 6.9) being used to estimate the distance between the manipulator and the structure. These sensors are based on geometrical principles, being highly independent of the optical properties of the target surface (figure 6.10). As it can be seen in figure 6.8, the pole surface is not flat and therefore the output voltage could be different from the flat surface. This was tested
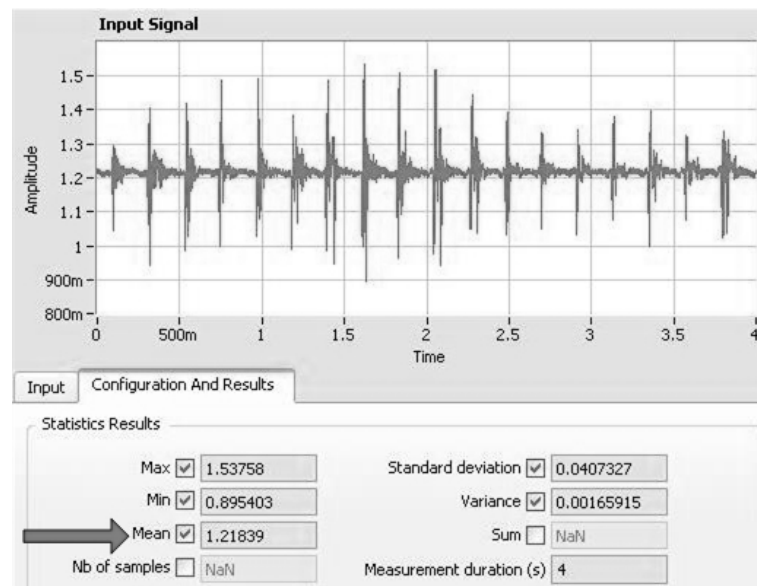
Figure 6.7: Y axis values of the accelerometer at $40°$ with a 5 Hz wide amplitude vibration.

as it can be seen in figure 6.11. This error depends on the radius of the circular profile but the amount of offset value is fixed for all distances for a specific radius (figure 6.11). Consequently, a compensation function was developed which receives the radius of the profile as an input and corrects the distance according to that. Finally, as can be seen in the figure 6.10, the sensor is more sensitive in the closer ranges. To increase the resolution, the range finder was placed as near as possible to the structure (in the distance of $60\,mm$ from the structure, when the gripper is closed). As an example, our experiments showed that in the distance of $200\,mm$ the sensitivity
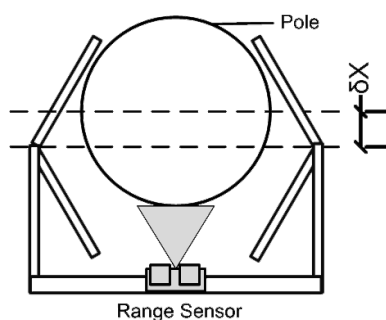
Figure 6.8: A range sensor faces the structure and measures the relative distance.
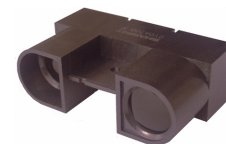
Figure 6.9: Sharp range finder used for distance measurement.

Type	STMicroelectronics ultra compact LIS244AL two-axis analogue accelerometer
Sensitivity	$3mV/\circ$ to $6mV/\circ$
Repeatability based on one sample	$4°$
Repeatability based on average of 400 samples at $100\,Hz$	$0.07°$
Repeatability based on average of 400 samples at $100\,Hz$ and existence of $5\,Hz$ mechanical vibrations	$0.3°$

Table 6.1: Characteristics of the inclinometer sensors.

of the sensor is $8\,mV/mm$. Using a 12 bit data acquisition and considering a $1\,mV$ resolution of voltage acquisition, a resolution of better than $0.2\,mm$ can be obtained. However, the accuracy of measurement is mainly limited by the accuracy of the calibration method for the specific color and radius. It is worth mentioning that the SHARP range sensors currently being used are very inexpensive (10-20 Euros) and with reasonable accuracy. An industrial grade triangulation sensor would be more accurate, but it would cost at least 500 Euros.

6.3   Motor drivers

There are tow types of actuators and consequently two types of drivers: DC drivers for MAXON DC motors (used in the grippers and the Z axis rotation mechanism) and SEW drivers for AC motors of the climbing mechanism.

6.3.1   DC drivers

DC motor drivers are IBL2403 from TECHNOSOFT (figure A.9 in Annex A) [Tec09]. It is an intelligent drive combining motion controller, driver, and PLC functionality in a single compact unit. The IBL2403 drive is a compact driver for distributed and coordinated control of brushless,
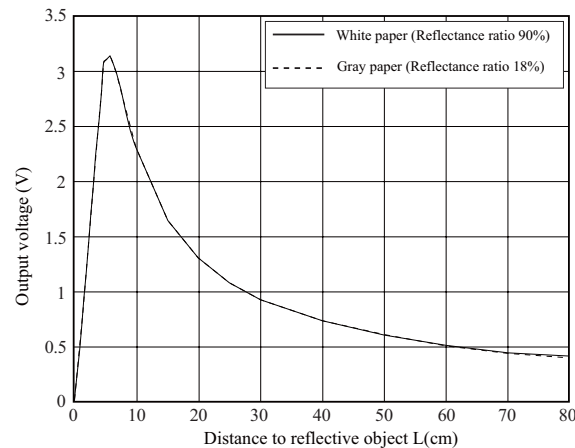
Figure 6.10: The output "voltage" of the Sharp sensor against the distance to a gray & a white paper.

DC or step motors of powers up to 75 W, and voltages up to 24 V. It functions in a CAN network and has various control modes, namely: Torque, speed, or position control. A high level graphical environment from TECHNOSOFT called "EasyMotion Studio", supports the configuration, parameterization and programming of the driver. Therefore in the first step the driver should be configured according to the motor characteristics through a set up process. Some of the motor parameters e.g. number of the poles, maximum current, etc. should be provided to the driver while some others e.g. the rotor inertia may be provided or can be detected automatically by the driver. EasyMotion Studio also has a programming environment in which high level routines
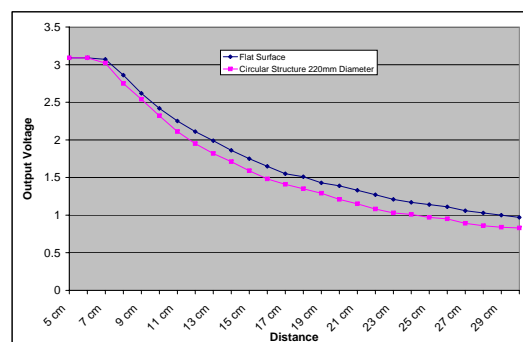
Figure 6.11: The output voltage of the range sensors for a flat surface and a circular pole with the diameter of 219 *mm*.

can be programmed using a specific programming language called Technosoft Programming Language (TML). Two TML programs (one for the gripping mechanism motors and one for the rotating mechanism motor) were developed and loaded to the drivers of the DC motors. Using this program, the driver receives motion trajectories as well as high level commands from the CAN network and transfers the low level commands to drive the motors. The trajectory generation algorithms will be described in the next chapter.

6.3.2   AC drivers

AC motor drivers are SEW MOVIDRIVE MDX61B 3-phase 1.4 *kW* drivers (figure A.11 in Annex A) [SE09]. These drivers are equipped with a CAN/CANopen interface card of DFC11B The MotionStudio program package allows start up, set parameters, and run diagnostics for MOVIDRIVE MDX60/61B drive inverters. MotionStudio also has a programming environment called IPOS positioning and sequence control system. IPOS includes four main control means which are user programs, PLC functions, positioning functions and monitoring. Currently we only use the high level programming environment. In a very similar manner to the DC drivers a routine was developed in AC drivers programming language which is loaded to all drivers. Motion trajectories are transfered from the upper level controller(here a PC) to the drivers through the CAN network. The higher level trajectory generation algorithms are executed on a PC and will be described in the next chapter. A protocol was defined for communication between the computer with the motor drivers that are all connected to each other via CAN bus interface. The high level trajectory generation routine (running on a PC) converts the position and velocity trajectories to a CAN command based on this protocol. The same protocol was used in the IPOS routine which converts the commands received from the CAN network to low level motion patterns of the driver.

6.4 Electronics architecture

6.4.1 Electronics architecture

As illustrated in figure 6.12, three AC brushless motor controllers, three DC brushless motor controllers, and National Instrument data acquisition modules are used. Controllers can control motors in position, velocity, and torque modes. The AC motors of the 3-DOF serial arm are controlled in velocity control mode. The Z axis rotation mechanism has a DC motor which is also controlled in velocity mode. Other 2 DC motors which are used in the grippers are controlled in position mode while opening and torque control mode while closing and gripping. All of the drivers are communicating by CAN bus through CANopen protocol. A CAN to USB module is used to connect the CANbus to a PC. Data acquisition modules are NI USB-6009 from National Instruments (figure A.10 in Annex A) [Ins09]. Each module provides connection to 8 analog inputs (14 bits, 48 kS/s), 2 analog outputs (12-bit, 15 kS/s) and 12 digital I/O. These modules are connected to a PC through USB.

A user interface and an upper level communicating software have been developed in Visual $C\sharp$.NET and will be described in the next chapter.

6.5 Conclusion

The sensors of the gripping and climbing mechanisms were described in this chapter. Their resolution and accuracy against the required accuracy were discussed. The motor drivers as well as their applications on the robot were delineated. Finally a global view of the electronics architecture was presented.
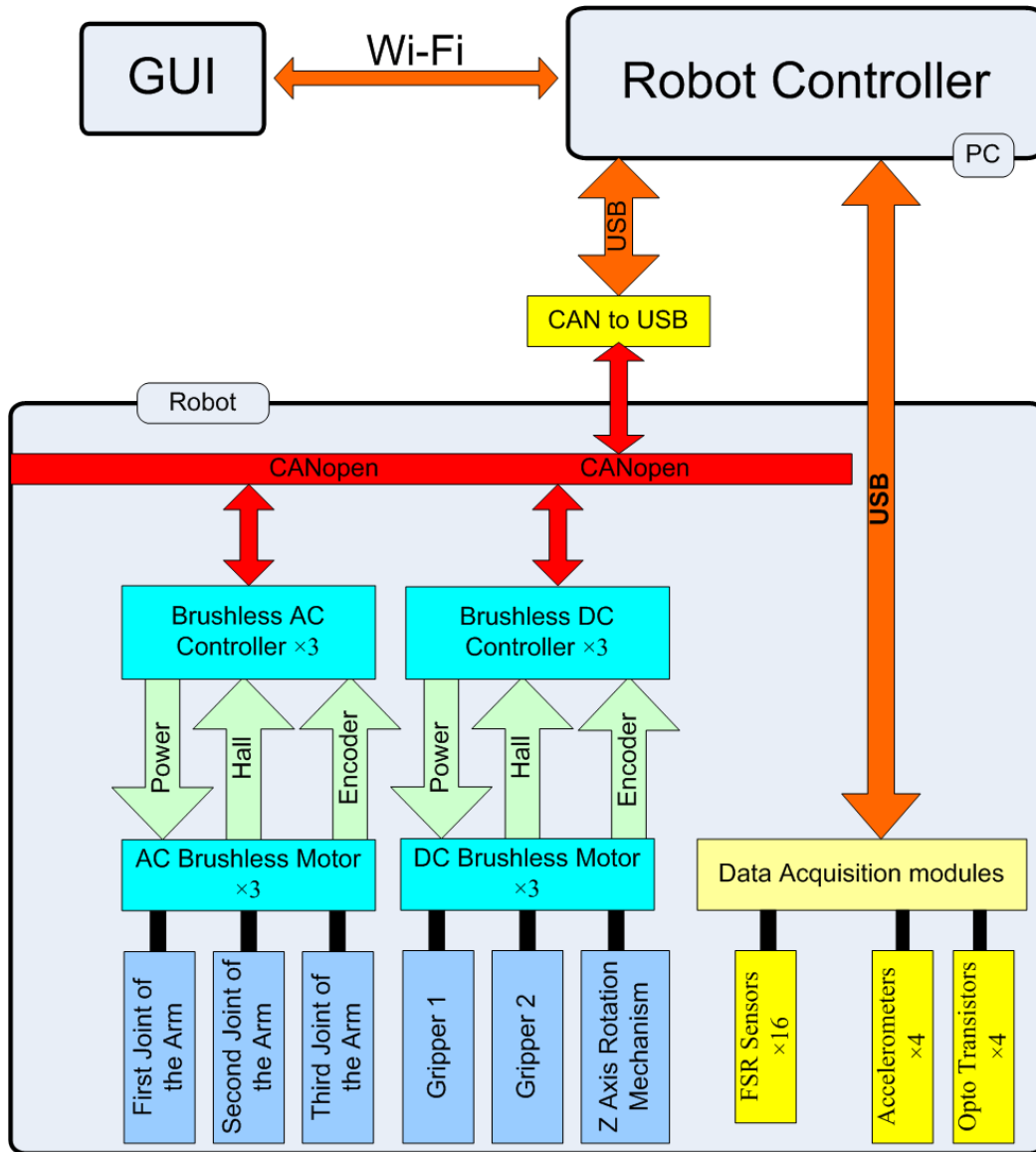
Figure 6.12: Electronics architecture of the 3DCLIMBER robot.

Chapter 7

Path Planning and User Interface

7.1 Introduction

This chapter describes the path planning, autonomy and control of the 3DCLIMBER. First the required level of autonomy for the 3DCLIMBER is discussed and then the path planing and control algorithms which have been applied in order to fulfill the required autonomy level will be discussed.

7.2 Autonomy level

In order to develop the path planning and control algorithms, and user interface of the 3DCLIMBER, it is important to first define the required level of autonomy. High level path planning algorithms highly depends on the required level of autonomy. In robotics applications, path planning can be done online or off-line (figure 7.1). This depends on several factors including existence of obstacles, predictability level of obstacle locations, and the amount of knowledge available from the robot working area before start of the robot operation [FGL87]. If some knowledge of the environment is available, the path can be planned before the execution. Planning paths before execution allows efforts to get shorter paths, more efficient dynamics, and absolute collision avoidance. A priori knowledge may not be used for unpredictable or random motion as

Collision
Avoidance

Yes   No

Path
Constraints

Yes   *Off-Line collision free*   *Off-Line path planning*
               path planning plus,   *plus, online path*
               online path tracking.   *tracking.*

               Positional control plus,
No   *online obstacle detection*   *Positional control.*
               and avoidance.
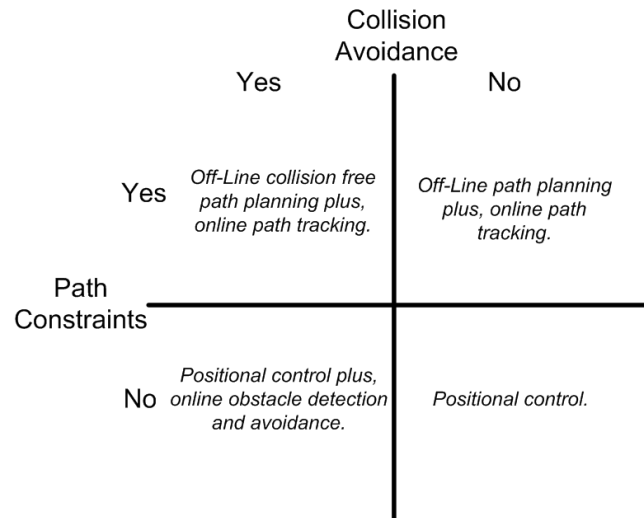
Figure 7.1: Path planning and path tracking in robotic applications

there is no detection method allowed by its definition. For the 3DCLIMBER application we should choose between a Priori path planner or a Postieri path planner, or combination of them. As stated earlier the working area of the 3DCLIMBER robot is human made 3D structures. Structures used in plants for piping purpose, are based on available maps and are not unknown environments. Consequently, equipments and algorithms for mapping, detection of obstacles, and world modeling are not necessary. The missions for the 3DCLIMBER might be defined as scanning a specific part of a structure. In order to do that, the robot should be able to reach any point and configuration on the structure. Therefore, autonomous approach to any specific point on the structure is desired. This means that the geometry and map of the structure will be given to the 3DCLIMBER as input. Then a specific point on the structure will be given as an input of the mission. The mission of the robot is to autonomously reach to the desired point. Therefore here the problem is defined as:

"Giving a known structure and a starting pose, how to reach a given point in the structure within a specified accuracy."

A more complex mission, such as scanning a specific area can be defined as a set of continuous

points that the 3DCLIMBER should reach to.

7.3 Path planning

The Path planning algorithm is composed of three hierarchy levels. The lower level trajectory generation algorithm, the mid-level straight line and bent section passing planners, and the high level autonomous path planner. Before describing the algorithms, the concept of one step and half steps should be described. Suppose that the lower gripper of the robot is closed and the upper gripper of the robot is in position P_c (stands for current position) relative to the base of the robot which is indeed the lower gripper. Also suppose that the upper gripper is closed and the manipulator (connected to the upper gripper) should move from its current position $P_c : \{X_c, Y_c, Z_c, \theta_c\}$ to a desired position $P_d : \{X_c, Y_c, Z_c, \theta_c\}$. If the desired point P_d falls within the workspace of the robot, then it is possible to perform the movement in a single step. Then the terms **"half step" and "one step"** are defined as:

- **Half step**:

  The upper gripper opens, then the manipulator (connected to the upper gripper) moves from P_c to P_d and finally the upper gripper closes and grasps the structure (figure 7.2 a and b).

- **One step**:

  One step is composed of a "half step", then the lower gripper opens, afterwards it moves from its current position to a new position in which the position of the manipulator relative to the base becomes again P_c and finally the lower gripper closes (figure 7.2 a,b and c).

7.3.1 Low level trajectory generation

The lowest level part of the path planner is the straight line trajectory generating algorithm. This algorithm generates appropriate data to control the motors of the 4-DOF mechanism and grippers so that the robot travels along a straight path. A routine was developed in MATLAB
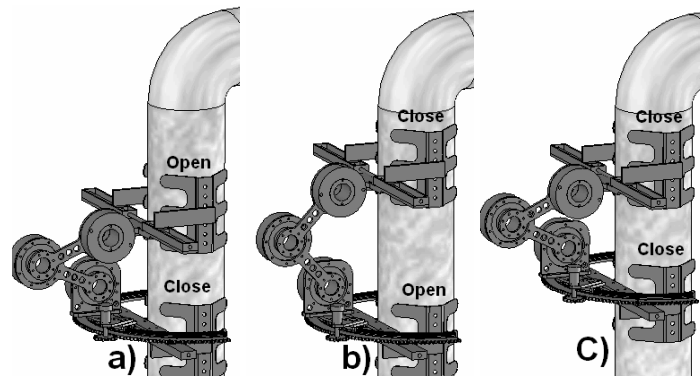
Figure 7.2: Half step and one step concepts (The opening and closing of grippers not shown).

to simulate the robot model in Cosmos motion* and after the successful experiment, a similar routine was developed in $C\sharp$ for the physical robot. The algorithm receives the start point $P_c : \{X_c, Y_c, Z_c, \theta_c\}$ and the end point $P_f : \{X_f, Y_f, Z_f, \theta_f\}$ of one climbing step in the Cartesian order. The desired travel time and desired "path following" precision are also the inputs of the algorithm. The output of the algorithm is the matrix of the position versus time for the 4-DOF mechanism motors, the applied algorithm estimates "n" points on the straight path and by applying inverse kinematics, it generates appropriate data for all motors for every time deviation. Clearly increasing the number of intermediate points "n" will result in better precision, but the calculation cost increases. Figure 7.3 shows the generated trajectory for making one step up. This is indeed the result of the mid-level straight line routine developed in Matlab, which uses the trajectory generation algorithm. In figure 7.3, the following values were considered as initial and final points of one straight line climbing step: $P_c = [0\ 0\ 200\ 180]$ and $P_d = [0\ 0\ 400\ 180]$. Figure 7.4 shows the generated trajectory for passing a bent section of 90°, where $P_c = [0\ 0\ 200\ 180]$ and $P_d = [600\ 0\ 400\ 90]$. After moving each step up or passing the bent section, the manipulator of the robot goes back to its previous location before making the step. Therefore, in all graphs the initial position of each joint is equal to its final position.

---

*http://www.cosmosm.com/
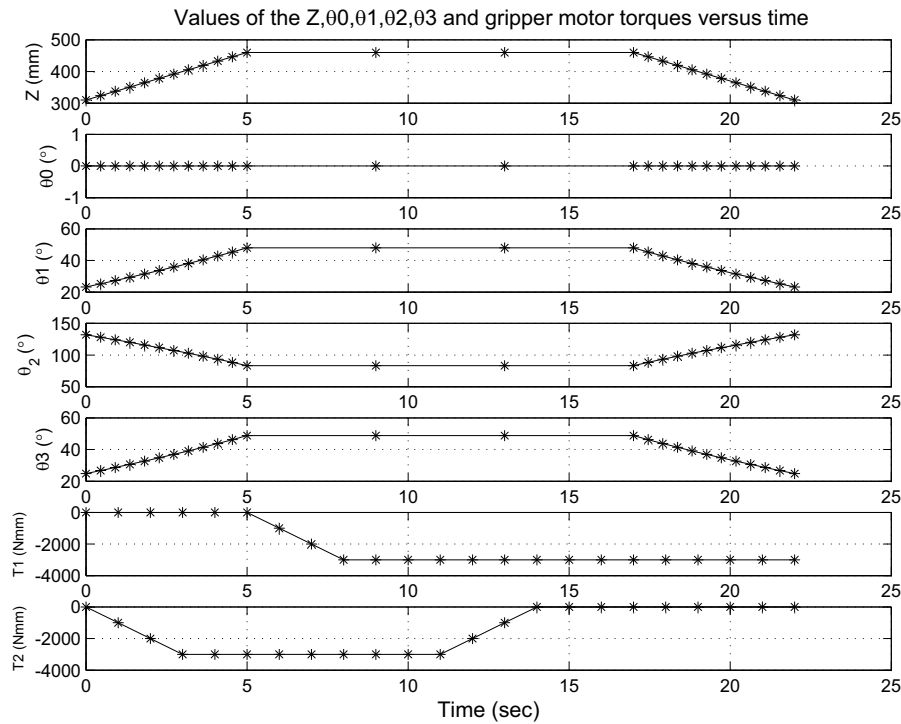
Figure 7.3: Generated trajectory for climbing mechanism motors for making one step up, including opening and closing of grippers.

Estimation of minimum number of necessary intermediate points

The inputs of the trajectory generation algorithm are the current and desired poses of the manipulator relative to the base of the robot and the desired "path following" precision. The "path following" precision is important, because it has a direct effect on the overall speed of the 3DCLIMBER. Since opening and closing of grippers are time consuming, the grippers should not open or close to their final possible stroke in each step. Instead, as long as the complete detachment of the gripper from the structure is not necessary (it might be necessary in some NDT applications and when the robot is passing the bent section), it is preferred that the gripper just takes the minimum stroke for opening and closing. On the other hand, a precise and accurate path tracking algorithm is necessary because if the manipulator can not precisely follow a straight line, the gripper should open more in order to avoid any collision with the structure. On the other side, if the precision is more than required, it means that there is an additional
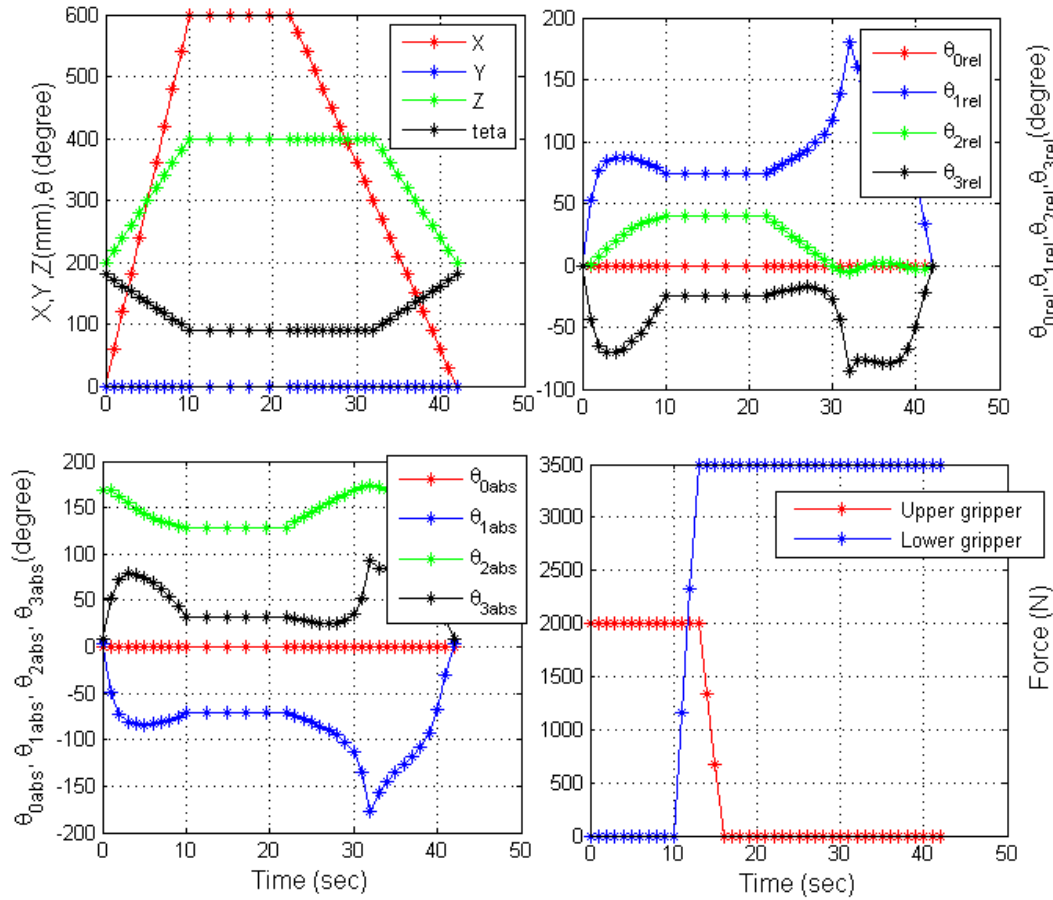
Figure 7.4: Generated trajectory for climbing mechanism motors while passing a bent section. In the figures, the term "rel" stands for the position relative to the initial position and "abs" stands for the absolute position.

unnecessary calculation cost and intermediate points are more than enough. This also reduces the calculation and path tracking speed. Taylor straight line planning method [Tay79] was used in order to calculate the minimum number of intermediate points between the poses which guarantees the required precision. Algorithm 1 shows the trajectory generation and execution algorithm based on this method.

7.3.2 Mid level straight line and bent section passing algorithms

The mid-level planners are:

Algorithm 1: Trajectory generation algorithm

Read$\theta_1, \theta_2, \theta_3$ from inclinometers
$P_c \leftarrow$ Calculate current Pose using direct kinematics
$P_d \leftarrow$ Read the desired Pose from inputs
$\delta_{max} \leftarrow$ Read the maximum possible deviation from the path
$n \leftarrow 0, \delta \leftarrow C$ (Constant big enough value) **while** $\delta > \delta_{max}$ **do**
$\quad | \quad n = n + 1;$
$\quad | \quad$ Calculate "n" points between P_c and P_d
$\quad | \quad \delta \leftarrow$ Calculate the error on the path based on "n" points
$\quad$ Calculate the trajectory based on "n" points using inverse kinematics
$\quad$ Execute the trajectory
End of algorithm

- One step straight line planner

- One maximum step planner

- ϕ angle planner (Rotation around the pole axis)

- Bent section passing algorithms

- Calibration algorithms

These algorithms also use the low level trajectory planners and are described below.

One step straight line planner

The one step straight line planner, receives the current and desired position of the manipulator P_c and P_d and the required precision. These information can be entered by the user in the user interface, or will be provided by an upper level algorithm. Then the low level trajectory generating algorithm is applied in which the number of intermediate points is calculated. Finally, upper gripper reaches to the desired destination P_d and closes and then lower gripper opens and goes to its target position. In all algorithms at least a gripper should always be closed and apply a specific amount of force to the structure. Yet another important function is used in the one step planner, which is called "angle compensation algorithm". This algorithm will be described later in this chapter. Figure 7.5 demonstrates the GRAFCET representation of the "one step forward" straight line planner algorithm.
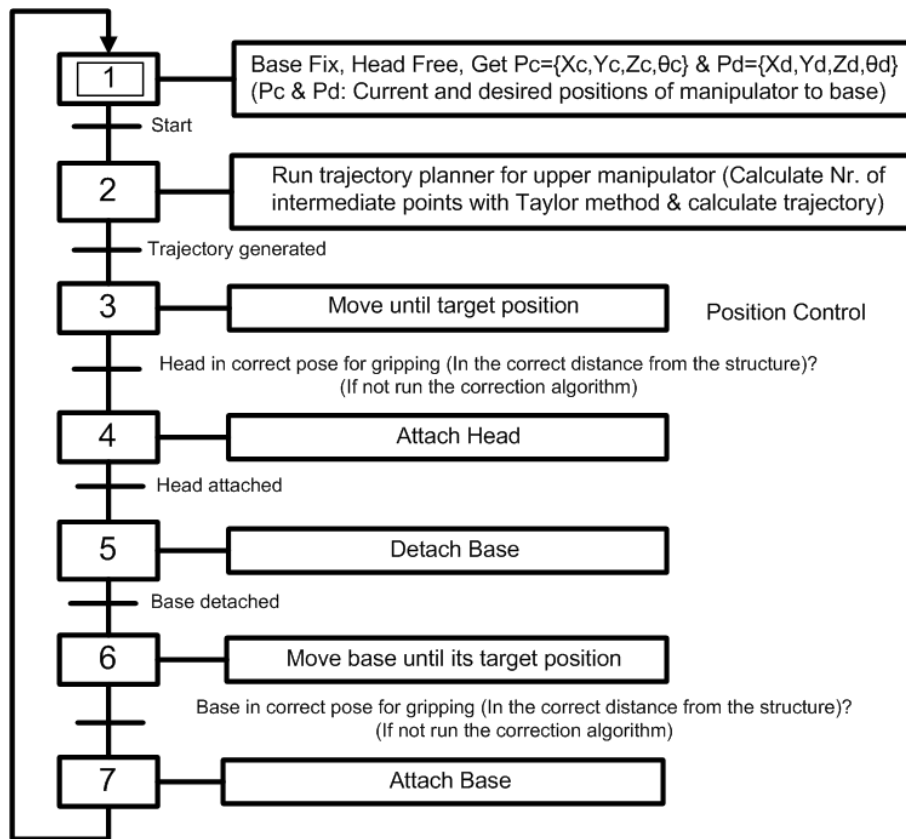
Figure 7.5: The GRAFCET representation of the "one step forward" straight line planner algorithm.

Maximum stroke step and maximum Z axis step

Some routines were designed according to the requirements of higher level planners and based on the straight line planner. The "maximum stroke algorithm" acts very similar to the "one step straight line planner". The difference is that the P_c and P_d are inserted automatically equal to the position of the climbing mechanism at minimum ($[0\ 0\ Z_{min}\ 180]$) and at maximum ($[0\ 0\ Z_{max}\ 180]$).

On the other hand, the "maximum Z step algorithm" is also a similar algorithm in which the manipulator moves from its current position to the maximum possible Z stroke and thus replaces P_c and P_d of the straight line planner as $P_c = [0\ 0\ Z_{current}\ 180]$ and $P_d = [0\ 0\ Z_{max}\ 180]$.

Bent section passing algorithms

To pass bent sections with any arbitrary angle the straight line trajectory generation algorithm should be applied in several consecutive steps. In the other word, while the final target pose is located on the structure after the bent section, some intermediate points which are not located on the structure should be defined so that the robot manipulator passes through these points to reach to the final target pose in some consecutive steps.

As some specific bend angles like 45° and specially 90° are very common in industrial pipings and 3D structures, specific routines for passing the bent section with these angles were developed.

The approach used for doing this, was to previously simulate passing a bent section with the robot model in Solidworks and determine the initial and final Positions of the manipulator on the structure for passing the bent section, as well as the number of necessary steps and the necessary intermediate points. Here the initial position means the position of a point on the structure where the high level planner changes from straight line passing routine to the bent section passing routine. In the other word, when the manipulator reaches to a specific distance from the bent section, then it can start to pass the bent section. Then a pre-planned trajectory for the climbing and gripping mechanisms which have been previously recorded based on the simulations will be executed. The GRAFCET representation of the algorithm is shown in figure 7.6.

ϕ angle planner

ϕ is the rotation angle around the pole axis. Before passing the bent section, the robot should be placed precisely below the bent section which means the X-Z plane of the robot and the X-Z plane of the structure should coincide (figure 7.7). The ϕ angle planner, uses a sharp range finder in order to estimate the minimum distance between the gripper and the bent section. In fact, when the mentioned planes coincide, the range finder will show a minimum distance value (figure 6.8). In this way the ϕ angle planner can find the appropriate place and compensate the
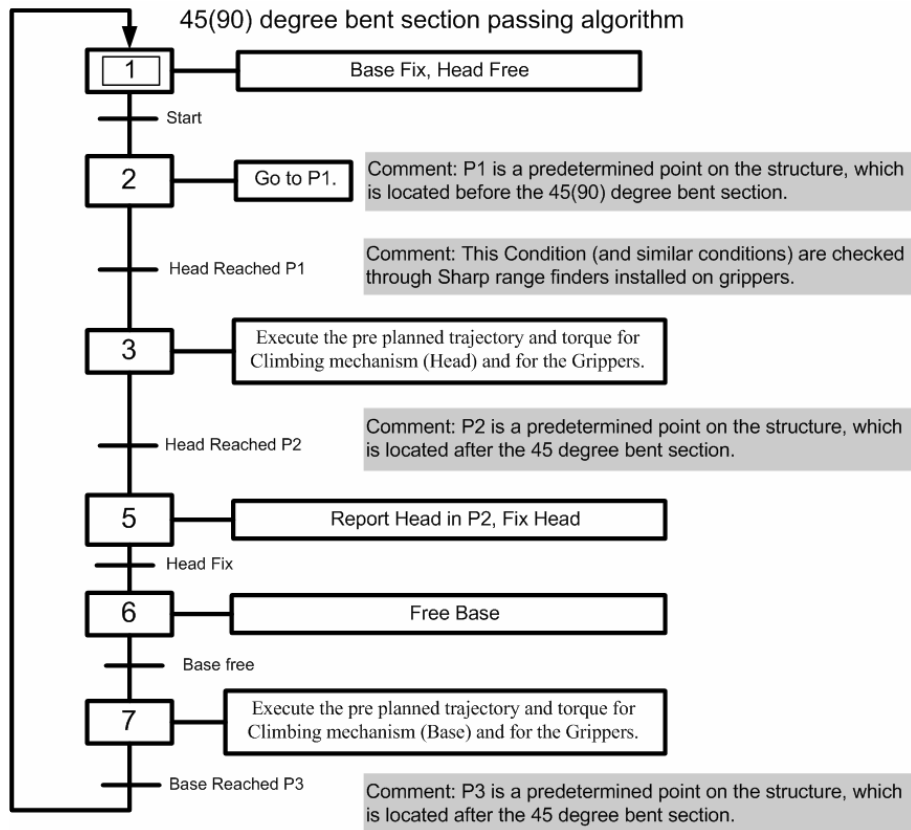
Figure 7.6: The GRAFCET representation of the 45° and 90° bent section passing algorithm.

related errors. Figure 7.8 shows the φ angle planner algorithm.

Start up calibration

When the operator starts the robot and place it on the structure, the startup algorithm should get the zero references of the climbing mechanism and also should calibrate the robot. For the robot initiation, the operator connects the upper gripper of the robot to the structure and the lower gripper is open. In this case, before powering actuators of the climbing mechanism and due to the inertia of the robot, the links move to the minimum energy state. As the mechanical characteristics of the robot does not change, the minimum energy state always locates on a fix pose. In this pose, the start up algorithm turns on all motors and send the command so that they move in a previously determined direction until finding the reference point. This direction is
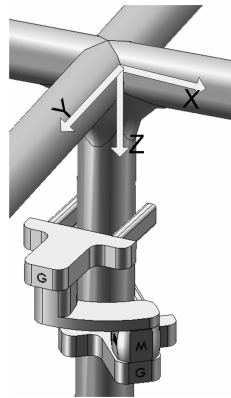
Figure 7.7: Z axis rotating mechanism is designed to place the X-Z plane of the robot coinciding with the X-Z plane of the structure.

determined previously and is a fixed direction, because the minimum energy position and also position of the zero point reference sensors (opto-transistors) are both fix. The start up flowchart is shown in figure 7.9. After finding the zero reference points of all actuators, the climbing mechanism will try to place the lower gripper at the correct distance from the structure and also perpendicular to it (using the accelerometers and sharp range finders). In this way, the lower gripper grasps the structure. Then the upper gripper opens and moves to the $\begin{bmatrix} 0 & 0 & Z_{min} & 180 \end{bmatrix}$ position. But before gripping, the position, the angle, and the distance of the upper gripper relative to the structure is checked using the range finder and inclinometers. Consequently any error will be compensated before the upper gripper grasps the structure. Now the robot is calibrated and can start its operation.

7.3.3 Multi step straight line path planner

The high level autonomous path planner should receive an absolute position on the structure and control the robot to reach to the desired position autonomously. However this is not totally implemented on the 3DCLIMBER. To perform this objective precisely, integration of additional localizing sensors (i.e. localization with triangulation methods by ultrasonic transceivers) and laser range finders or camera are necessary. The problem is mainly detection and overcoming a bent section autonomously and also absolute localization of the robot on the structure. With the
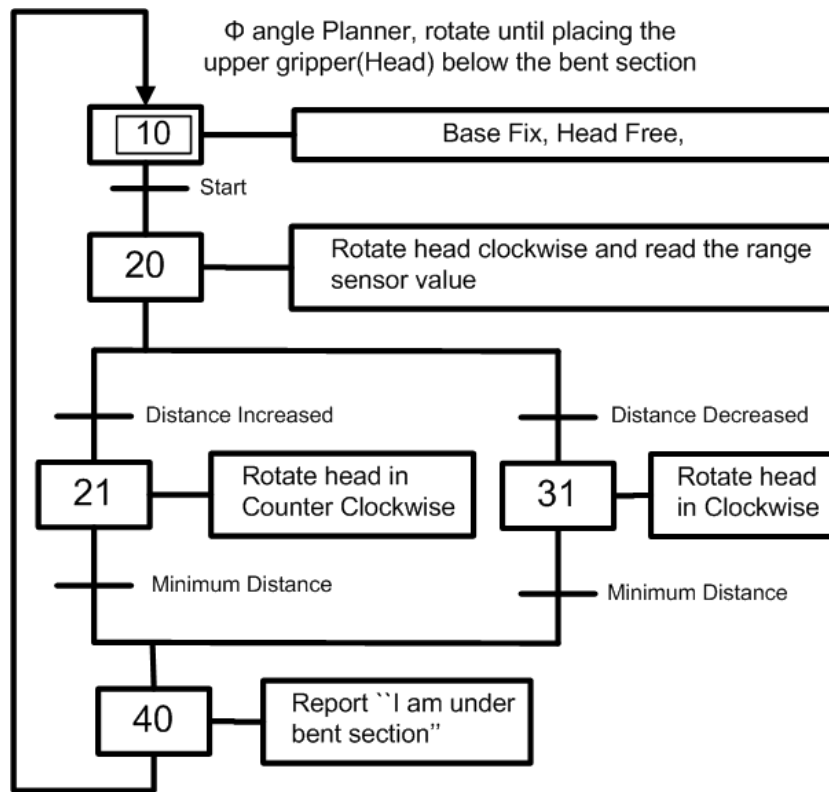
Figure 7.8: The GRAFCET representation of the φ angle planner algorithm.

current sensors, a multi step straight path planner is developed which calls the "one step straight line" algorithm and also "one maximum step" routine several times to pave a desired straight stroke which is not possible to pave or climb in a single step. The number of times that it calls the "one maximum step", and also the initial and final steps are also calculated by the "Multi step straight line path planner" algorithm. Figure 7.10 shows the algorithm for doing that.
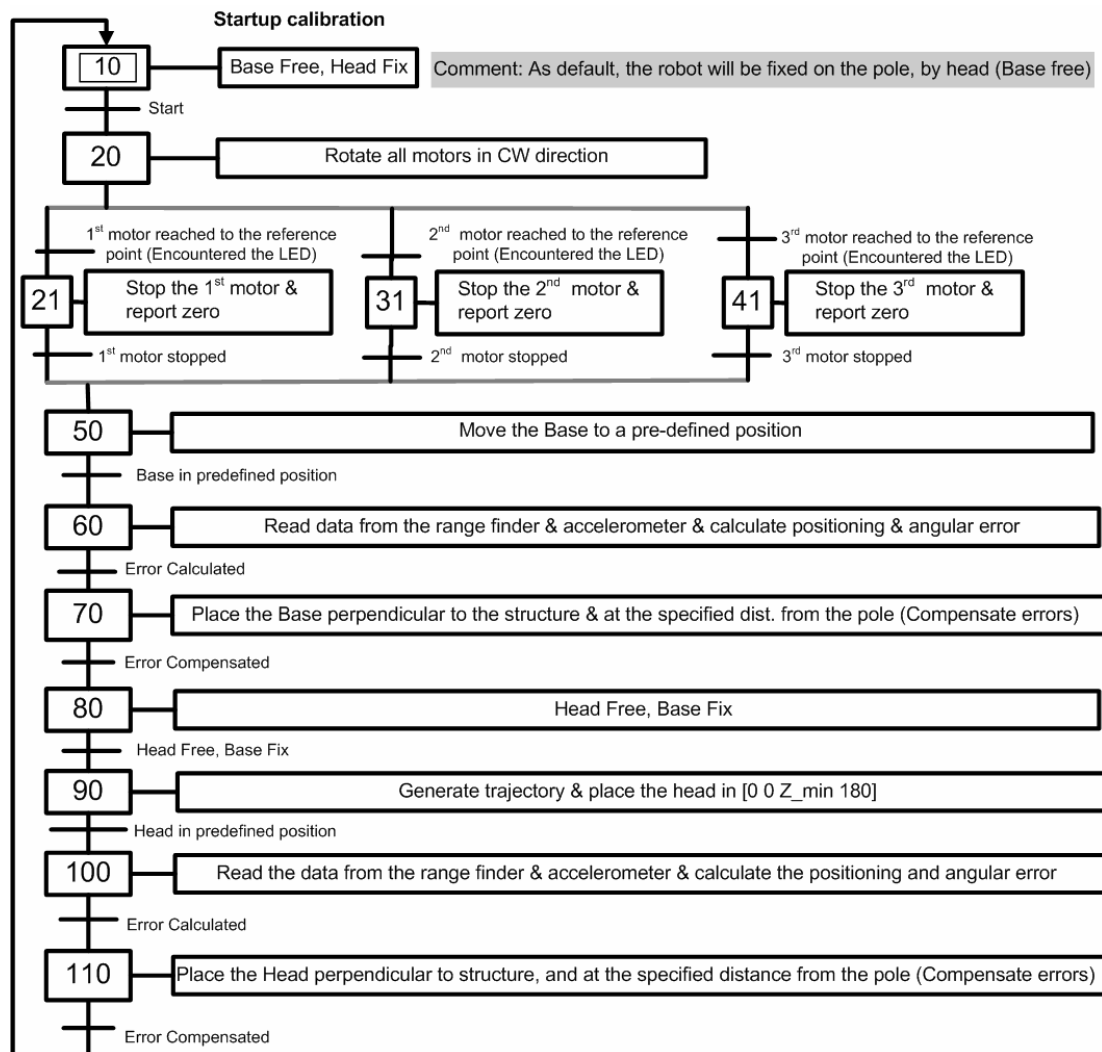
Figure 7.9: The GRAFCET representation of the start up calibration algorithm.
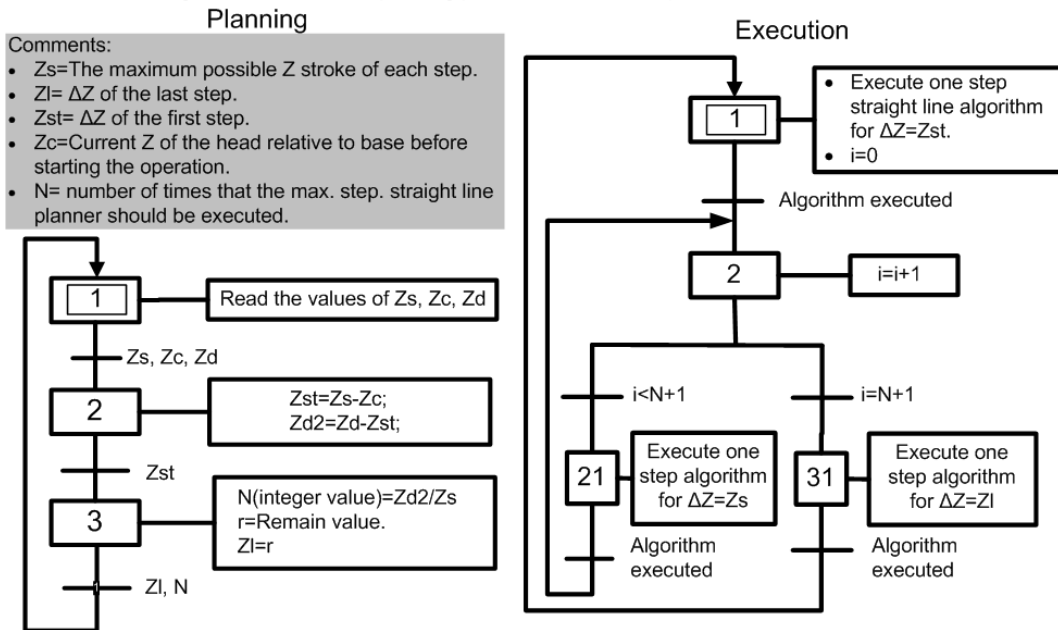
Figure 7.10: The GRAFCET representation of the multi step straight line planner.

7.4 Angular deviation compensation and calibration algorithms for fine manipulation

The error compensation and calibration algorithms were added to the robot control system after the first tests of the robot. During those tests some problems were revealed which were persuasive for integration of additional sensors and algorithms. The experiments and tests of the robot will be described in the next section, but for understanding the necessity of the algorithms and the functionality of algorithms, it is necessary to describe some of the revealed problems during the first test of the robot. Our preliminary experiments showed that shortly after a gripper grasps the pole, it tends changing its tilt angle. This is due to the torques resulted by the weight of the robot. Therefore, the closed gripper does not stay perpendicular to the pole until the end of the step (figure 7.11b). Consequently as the other gripper maintains 180° with the first gripper, it

will not be perpendicular to the pole. Therefore, a perfect gripping action can not be established. It should be noted that it is usually a small error, but it accumulates in each step and will result in an over defined system as the gripper tries to grasp the structure while it is not well positioned. Thus, even if the gripper succeeds in grasping, the actuators of the climbing mechanism will try to compensate the error, pulling maximum current, and consequently overheating. Therefore, precise positioning and gripping are necessary and such errors must be compensated in each step. Adding to all the aforementioned problems, this error is accumulative and the total deviation from the desired position and angle becomes increasingly larger after each step, making it impossible to grasp the structure and continue the movement after a couple of steps. Therefore, the operator has to stop the operation, manually calibrate the robot and then resume the operation.

Furthermore, an important advantage of step-by-step based climbing robots over the wheel based climbing robots is their better maneuverability due to the existence of a robotic manipulator and such advantage becomes more outstanding if the manipulator can perform fine manipulation. Fine manipulation is necessary for some maintenance applications (e.g. the light bulb changing operation) and if the manipulator can perform fine manipulation, the necessity of integrating a separate arm can be abolished. However, as it will be described later, fine manipulation with large manipulators can not be done only with internal motor encoders and requires external feedbacks to compensate positioning errors. In this section we suggest an algorithm for compensation of such errors.

7.4.1 Error sources

Error sources which are the cause of the mentioned problems can be divided into two main groups:

A. **General error sources of industrial robotic arms**: High accuracy is generally difficult to obtain in large manipulators capable of producing high forces because of the system elas-

tic and geometric distortions [MDM04]. Due to some sources of errors, namely tolerance on gears, coupling errors, deflection of the links, etc, positioning errors are unavoidable in manipulators. This is a general problem of the robotic arms which has been discussed in the literature. For instance, the control problem of flexible link robotic manipulators has been studied in the last two decades [CJS84, ESL06]. Some control strategies (e.g. fuzzy and adaptive control) have been proposed [LL03]. To measure the amount of the deflection, two strain gauges are usually stuck onto the arm [LL03]. The 3DCLIMBER consists of a relatively large robotic arm and consequently contains the same mentioned problems. It should be noticed that the robot is not designed with flexible links concept and its links are rigid considering the applied forces. But the high torques on joints (up to $200\,N.m$) cause small unavoidable deflections on the aluminum links. Such small deflections produce big errors on the manipulator pose, when multiplied by large values (length of the links). On the other hand, most manipulator calibration techniques require expensive and/or complicated pose measuring devices, such as theodolites [MJD99]. A precise yet inexpensive solution for compensation of the stated errors of the 3DCLIMBER is desired.

B. **Error sources due to the mobility of the robot's base:** In industrial robotic arms, the base of the robot is usually fixed to a certain point. A step-by-step based climbing robot usually consists of a climbing mechanism and two grippers. During climbing, the fixed gripper is called "Base" and the moving gripper is called "Manipulator". Obviously, the base and the manipulator change their role in each step. As the manipulator movements are programmed relative to the base, errors in pose of the base will cause errors in pose of the manipulator. This error is illustrated in figure 7.12. The light figure shows the status without error, and the dark figure shows the status after the error occurs. Here, the lower gripper (G2) is the base. Due to the errors, the lower gripper is not perpendicular to the structure which causes errors on X, Z, and angle of the manipulator. As stated, these errors impair the robots autonomous climbing process and should be compensated in each
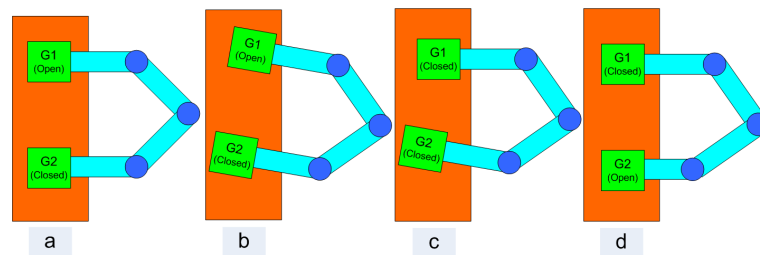
Figure 7.11: Demonstration of the tilt angle error and compensation: a -Correct status. b-After occurrence of the error. c- Error compensation for the upper gripper. d-Error compensation for the lower gripper.
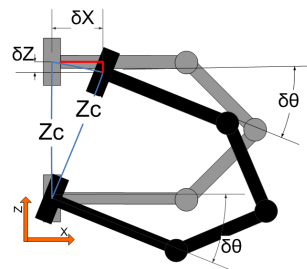
Figure 7.12: The error on the placement of the base generates a relative error on the manipulator.

step of the movement and right before grasping the pole. For simplicity of referencing in the following sections, the errors related to the general errors of the industrial robotic arms are called type A errors and those related to the mobility of the robot's base are called type B errors.

7.4.2 Angle compensation and autonomous calibration algorithm

An autonomous self-calibration algorithm is proposed in order to compensate the errors and calibrate the system in each step of the robot's movement. This algorithm requires the absolute pose of each link, in order to calculate and compensate the previously mentioned errors. The absolute pose of each link can be obtained with different strategies, namely by triangulation or by trilateration to a fixed reference system. In any of the previous cases, a reference base station is required and should be calibrated before starting the robot operation. Sometimes this is not a practical solution for outdoor industrial applications as the installation and calibration

of the observer are time consuming tasks and requires an expert. Since the 3DClimber robot is intended to operate in multiple structures and places, a solution which is embedded into the robot is highly preferred. Therefore, the proposed solution is based on an algorithm in which the absolute inclination of the links (inclination of each link relative to the horizontal) and distance of the manipulator to the structure should be measured. This method does not provide the absolute position of the robot on the structure, but it provides a precise relative pose of all links which does not contain the aforementioned error sources. Consequently, all mentioned errors can be calculated and compensated. To do so, 4 analog inclinometers have been developed, using accelerometer chips. Also Sharp range finders have been integrated to the grippers of the system. The sensors which have been applied to the system have been previously described. Here it should be noted that the inclinometers provide the absolute angle of all links including the upper and the lower grippers. In the proposed algorithm, each step of the movement is composed of three phases.

A. **Moving to the desired pose:** In the 1st phase of each step, the manipulator moves from its current pose $P_c = (Xc, Yc, Zc, \theta_c)$ to a desired pose $P_d = (Xd, Yd, Zd, \theta_d)$. In this phase no error compensation algorithm is involved. In the 2nd and the 3rd phases of each step, Type A and Type B Errors will be compensated. After execution of all three phases, the gripper which is attached to the manipulator grasps the structure and changes its role from "Manipulator" to "Base" of the robot.

B. **Compensation of Type B Error:** In the 2nd phase of each step, inclinometers will measure the angle deviation error of the robot's base $(\delta\theta)$, and, consequently, using the trajectory generating algorithm, the position of the manipulator will be changed from P_d to $P_d + (-\delta X, 0, \delta Z, \delta\theta)$, in which δZ and δX have been calculated as (figure 7.12):

$$\delta Z = 2Z_c sin(\delta\theta/2) \quad ; \quad \delta X = 2Z_c cos(\delta\theta/2)$$

This compensates the effect of the deviation of the base of the manipulator. Nonetheless, the manipulator may not yet have the desired pose for gripping due to the Type A errors.

C. **Compensation of Type A Error:** In the 3rd phase of each step, errors on positioning of the manipulator relative to the structure will be compensated. Inclinometers provide absolute angle measurement, which serves as the external feedback to encoders. This feedback addresses the problem of fine manipulation of large manipulators because the sensors are installed directly on the arm and do not contain errors related to gearing backlash, coupling mechanism, and improper placement of the base. However, for special tasks, some additional algorithms might be used. For instance, for a perfect gripping, the manipulator should be perpendicular to the structure and at a certain distance from the structure. This assures that the system will not be over defined after gripping. Therefore, in the 3rd phase of each step, the absolute angle of the manipulator and the distance of the manipulator from the structure will be measured and the relative error will be compensated. The distance between the pole and the structure is measured using range sensors (figure 6.8).

D. **The Proposed Algorithm:** Figure 7.13 shows the simplified version of the algorithm that intends to fuse the three phases in one step. To calculate the current task space position of the manipulator relative to the base, direct kinematics formulation is applied in which θ_1, θ_2 and θ_3 are calculated based on the inclinometers.

Inclinometers also provide some other useful information. As the robot should climb from bent sections, inclinometers can provide useful data about the current angle of the manipulator for grasping a $45°$ or $90°$ bent section. Figure 7.14 shows a simplified schematic of the control loop.

Figure 7.15 shows the status of the robot before and after execution of the step and after compensation of the error (only the 1st and the 2nd phases are shown here). Three important aspects of the algorithm should be noticed:

    1. There is an important difference between the 2nd and the 3rd phases of each step.

One step movement and error compensation algorithm

| 1 | Base Fix, Head Free, Get Pc={Xc,Yc,Zc,θc} & Pd={Xd,Yd,Zd,θd} (Pc & Pd: Current & desired positions of manipulator to base) |

Start

| 2 | Run trajectory planner for head (Calculate Nr. of intermediate points with Taylor method & calculate trajectory) |

Trajectory generated

| 3 | Run the trajectory |

Trajectory executed

| 4 | Read the current angle of the base and calculate error ($\delta\theta$). |

Error Calculated

| 5 | Pc= Pd   and   Pd= Pd + (-δX,0,δZ, $\delta\theta$) |

Pc, Pd

| 6 | Run trajectory planner for Pc & Pd and execute the trajectory |

Trajectory executed

| 7 | Calculate δX of head relative to structure (current pose. – desired pose) |

δX & $\delta\theta$

| 8 | Pc= Pd   &   Pd= Pd+ (-δX,0,0,-$\delta\theta$) |

Pc, Pd

| 9 | Run trajectory planner and execute trajectory |

Trajectory executed

Figure 7.13: Self-calibration algorithm.

The 2nd phase is associated with larger errors caused by the deviation angle of the base. This deviation causes relatively large errors (δX and δZ and $\delta\theta$) on position of the manipulator. The 2nd phase of the steps compensates all of these errors. For instance, considering the gripping action, if due to any other source of error (type A), the manipulator is not in the appropriate pose for gripping, then the 3rd phase of the algorithm only compensates (δX and $\delta\theta$) in order to effectively grasp the structure. The difference is that the 2nd phase tries to place the manipulator in the desired pose as much as possible, while the 3rd phase tries to place the manipulator in the precise gripping position even if the manipulator's pose differs from the desired
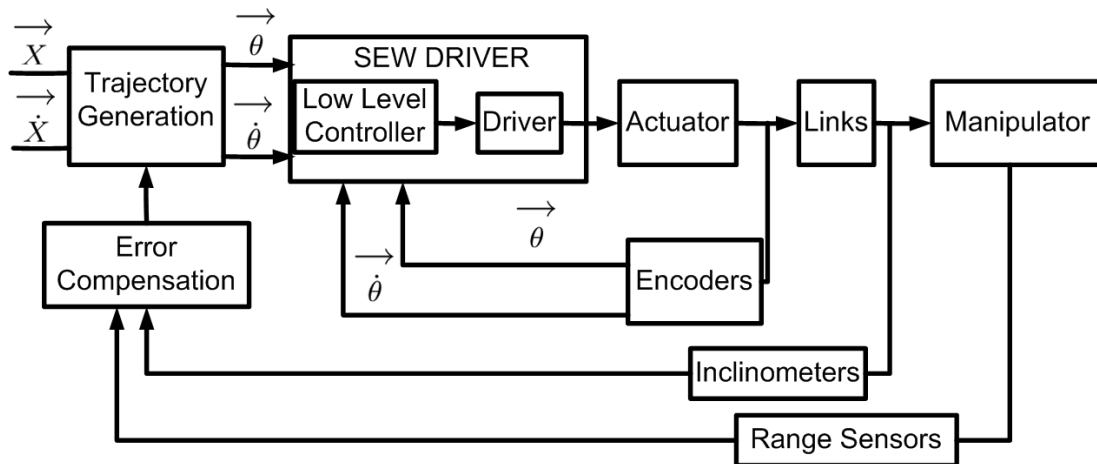
Figure 7.14: A simplified schematic of the control loop.
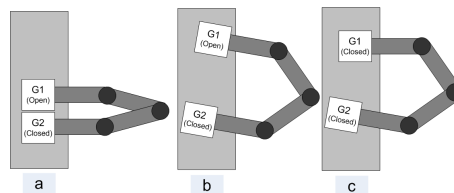
Figure 7.15: Autonomous self-calibration illustration.

pose. Therefore, if the 2nd phase is avoided, the robot can still grasp the structure, but the Z element of the manipulator will noticeably differ from the desired Z. On the other hand, the 3rd phase of the algorithm, requires to know the distance between the manipulator and the structure, which might not be always available in some specific tasks. In those cases, this phase might be eliminated.

2. The proposed algorithm (figure 7.13) is more accurate when the trajectory which should be paved is smaller. For instance, a straight line trajectory of $800\,mm$ will have an error about $30\,mm$ which will be compensated with the algorithm, but such error is not acceptable when the manipulator should also perform a specific task during the pavement of the trajectory. If we divide this trajectory into four smaller sub-trajectories of $200\,mm$, after execution of each sub-trajectory an smaller error about $7\,mm$ should be compensated.
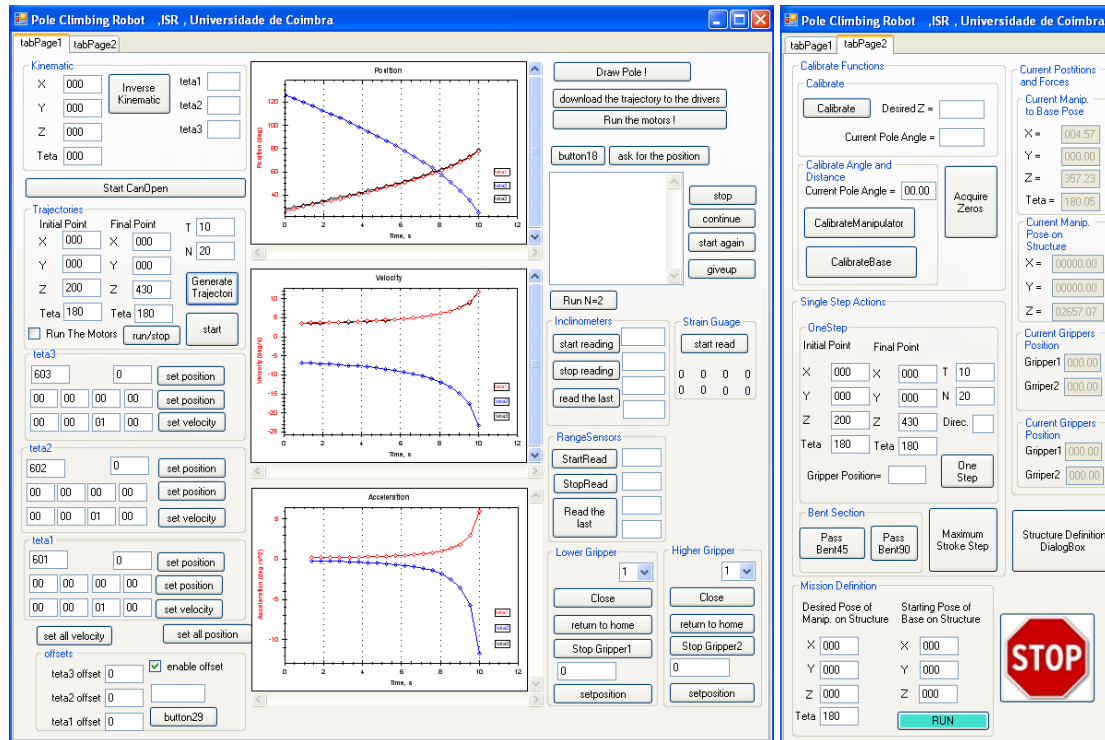
Figure 7.16: Snapshots from the user interface of the climbing robot.

7.5   User interface

A user interface, which is in fact a part of an architecture for controlling the robot is developed, but it is still under more development and is not finalized. The reason is that in the beginning, the direct control of the robot through a PC was considered but then a more advanced control architecture including a server-client based remote control of the robot was considered. Therefore, some undergraduate student projects were defined for development of the server-client based remote control of the robot which are ongoing projects and will be shortly described in the next section. Figures 7.16 shows snapshots from the first version of the user interface, and in fact it is the most reliable version used as the user interface of the 3DCLIMBER up to now.

7.6 Server-client based remote control

Remote control of the 3DCLIMBER has many advantages. Should this happen, the user can control the robot from a distance. This facilitates the inspection works and it is specially useful if the robot operation should take place in a dangerous disaster.

On the other hand, controlling climbing robots through teleoperation is a challenging task that demands a flexible and efficient user interface. Autonomous Climbing robots are often equipped with numerous sensors (proximity sensors, cameras, inertial modules, system status sensors, strain gauges, etc.) and use different climbing and gripping structures. Several initiatives have taken place that aim at defining standards, reference architectures, and middleware for the development of reusable robotic systems. JAUS (Joint Architecture for Unmanned Systems) is a set of standards, specifications, and recommendations to facilitate interoperability for unmanned systems [JAU]. The Player/Stage framework [Pla] provides the user with Player, a device server that allows the control of a wide variety of robotic sensors and actuators, and Stage, a multiple robot simulator. AuRA (Autonomous Robot Architecture) is a hybrid deliberative/reactive robot architecture developed at the Georgia Institute of Technology [AB97]. On the other hand, architectures like JAUS which have been widely used for robotic applications, were mainly concerned with unmanned vehicles. Therefore, modeling of the climbing robot and the structure that the robot should climb from is not an easy task in JAUS.

The architecture which is under development, is called RoboCom, and it is considered for general problem of tele-operation of step-by-step based climbing robots. A Master degree thesis has been conducted for development of the RoboCom architecture [Mur09]. It includes a TCP/IP based communication protocol and a GUI which serves as the client. The server side is composed of a single board computer which has the low level control applications, I/O interfaces, and wireless network adaptor. It communicates with the client through TCP/IP protocol. RoboCom architecture includes gripping and climbing classes. To introduce a new robot, one should specify the number of DOF of the climbing mechanism, the kinematics formulation, dynamics

Components	Corresponding Offset Range	Description
Core	x000h − x0FFh	Control and monitoring of the Service Connection and Robot.
Joint	x100h − x1FFh	Control and monitoring of the robot's joints.
Gripper	x200h − x2FFh	Control and monitoring of robot's grippers.
Camera	x300h − x3FFh	Control and monitoring of the robot's camera. - NOT IMPLEMENTED IN THIS VERSION -
Available	x400h − x6FFh	Offset area available for other components
Sensor	x700h − x7FFh	Control and monitoring of the robot's sensors
Available	x800h − xFFFh	Offset area available for other components

Figure 7.17: Segmentation of message codes by component.

formulation (optional), and sensors. It is possible to monitor and command a robot through the protocol. An operator may perform low level joint control, or higher level task space manipulator control. The current position of the robot's joints and manipulator is determined through reading the sensors value. RoboCom protocol only implements the host layers. In order to achieve actual client/server architecture, TCP/IP protocol is used. All messages are composed by a header and the data fields. The format of the header is common to all messages. This allows RoboCom to employ an embedded protocol. The use of an embedded protocol means that certain fields within the header provide information on how to handle the message and on how data is encoded before transmission. Figure 7.17 shows the segmentation of message codes by component.

The client applications can not directly issue commands to the robot drivers. This is done by the server application. Remote clients can only request the server to execute commands. Joints are controlled through joints properties setting. Joints are defined by six parameters (figure 7.18). The 3DCLIMBER robot was defined in the RoboCom architecture by introducing the number of DOF, the kinematics formulation, and the embedded sensors. A single board computer which contains the server program and wireless connection was installed on the robot and the robot was controlled by the client. Figure 7.19 shows the client's architecture and figure 7.20 shows a snapshot of the client which is adapted for the 3DCLIMBER robot.

Propertie	Description
ID	Joint's address ID number.
type	Type of joint:PRISMATIC or REVOLUTE.
position	Current joint position.
velocity	Current joint velocity setting.
next_position	Next joint position setting.
next_velocity	Next joint velocity setting.

Figure 7.18: Joints properties.
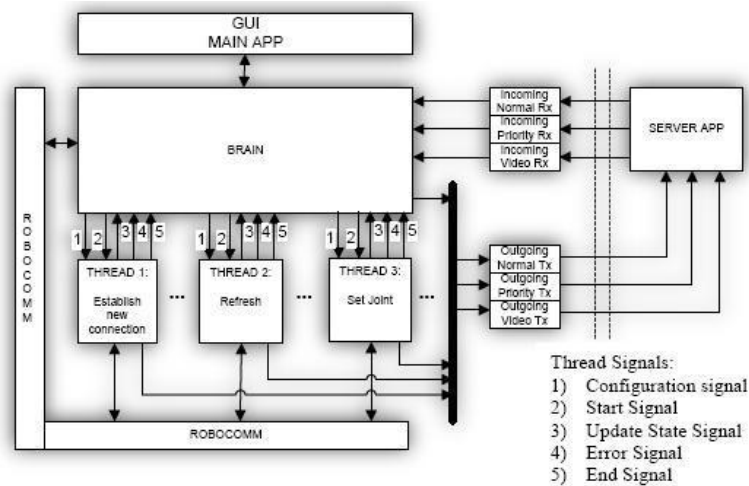
Figure 7.19: Client software architecture.

7.7 Conclusion

This chapter described trajectory generation, calibration and path planning of the 3DCLIMBER. The required level of autonomy for the 3DCLIMBER was discussed and then sensors, path planning, and control algorithms which have been applied in order to fulfill the required autonomy were presented. The electronics architecture and also the user interfaces were demonstrated. It was discussed that the existence of an architecture which allows the remote control of climbing robots generally and 3DCLIMBER specifically through TCP/IP protocol has many advantages. Consequently a master degree thesis was conducted in development of such architecture, however it is not yet fully working and has some communication problems. In addition to further development of the architecture, some other areas are open for investigation, including absolute
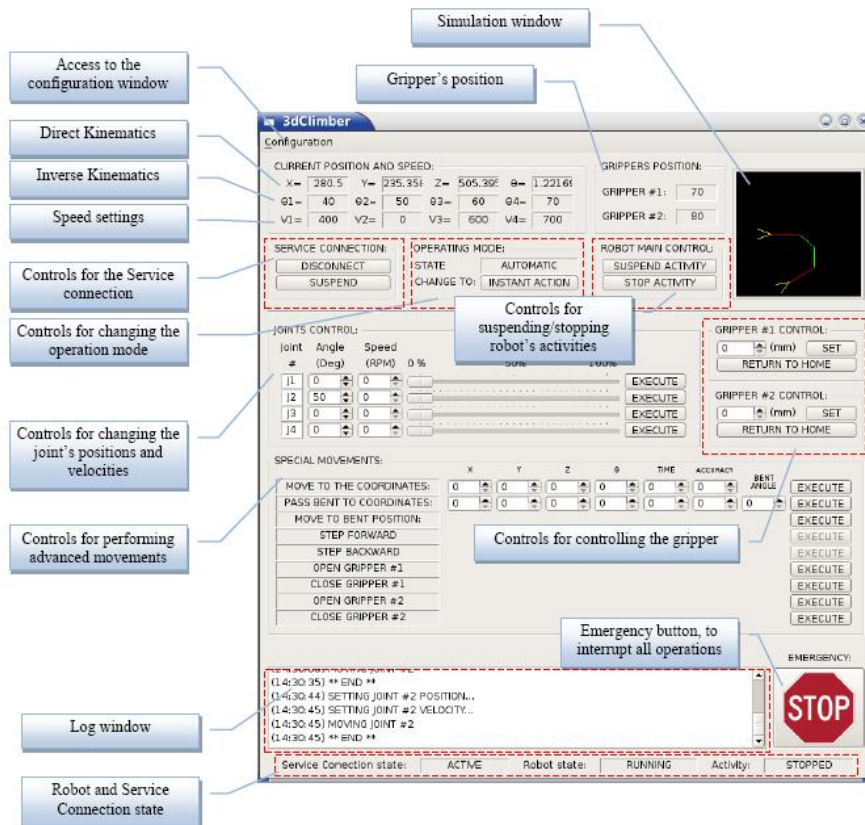
Figure 7.20: Client application GUI adapted for the 3DCLIMBER.

localization of the robot in the structure with an external camera observer or with ultrasonic transceivers through triangulation and trilateration methods.

Chapter 8

Testing and Results

"A failure will not appear till a unit has passed final inspection."

citation related to Murphy's Law.

8.1 Introduction

This chapter will explain the experiments conducted on the 3DCLIMBER, the problems revealed during the experiments and the results of the experiments. Two experiment threads were considered for this project: The first one, for the prove of the concept and discovering the possible problems and the second one after solving the problems and integration of autonomous algorithms.

8.2 First experiment

The first experiment of the robot was in fact a proof of the concept and to check and validate the design of the mechanisms (Mainly the mechanical design) as well as structural calculations. Therefore, in the first experiment still many algorithms were under development and only the

low level straight line trajectory generation algorithm was applied. Other algorithms and routines, namely for passing the bent section, calibration of the robot, start up of the robot, etc. were not yet developed and thus in this level the operator had to simulate these algorithms manually. In this case, the robot successfully climbed several steps and passed a bent section while controlled by an expert operator. This proved the concept. Furthermore, as the robot successfully could make the necessary movement and pass the bent section, it showed that the mechanical design of the mechanism, calculations, and simulations are all valid. In addition, no part failure was happened during the experiments which proved the trueness of the structure analysis. Figures 8.1 and 8.2 show some snapshots from the first experiments of the robot climbing over the structure.

On the other hand, some problems were also revealed during the first experiments, most of them were related to the positioning errors. It was decided to solve these problems before the second experiment of the robot.

One of the problems was the precise placement of the grippers before gripping. Due to some sources of errors, namely general errors of industrial large size robotic arms as well as problems related to the mobility of the robot base, some errors were adding to the manipulator position. This was fully investigated for possible solutions. Finally, some algorithms were developed and additional sensors (inclinometers and range finders) were developed and integrated. This was described in the previous section.

Besides the mentioned problems, some suggestions were made in order to promote the robot's functionality. First, an external sensor for determining a zero reference point for all degrees of freedom was necessary to implement. This would facilitate the start up process of the robot by getting the reference point automatically. Therefore, opto transistors were integrated to the robot links. Second, in the mechanical design of the system, the minimum safety factor of 2 was considered in both structural design of parts and design of the system dynamics and still in
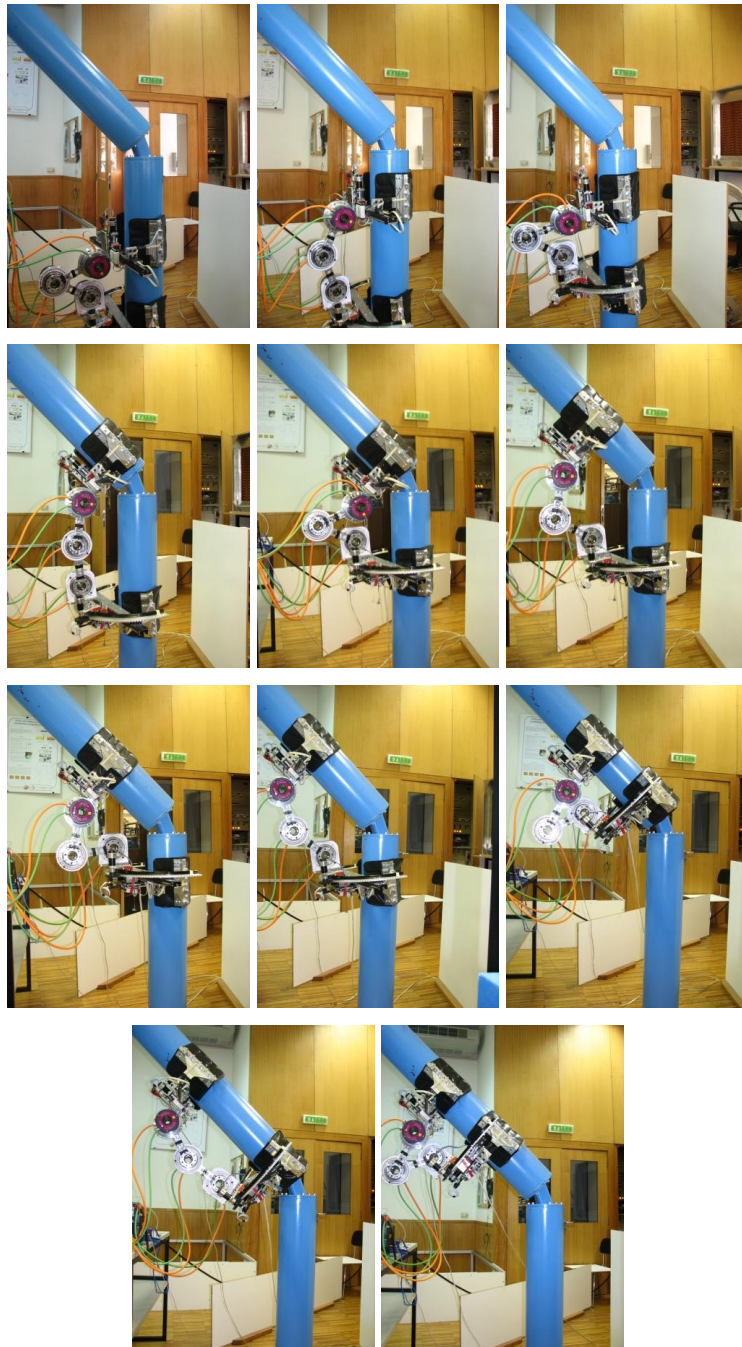
Figure 8.1: Sample snapshots of the experimental results.
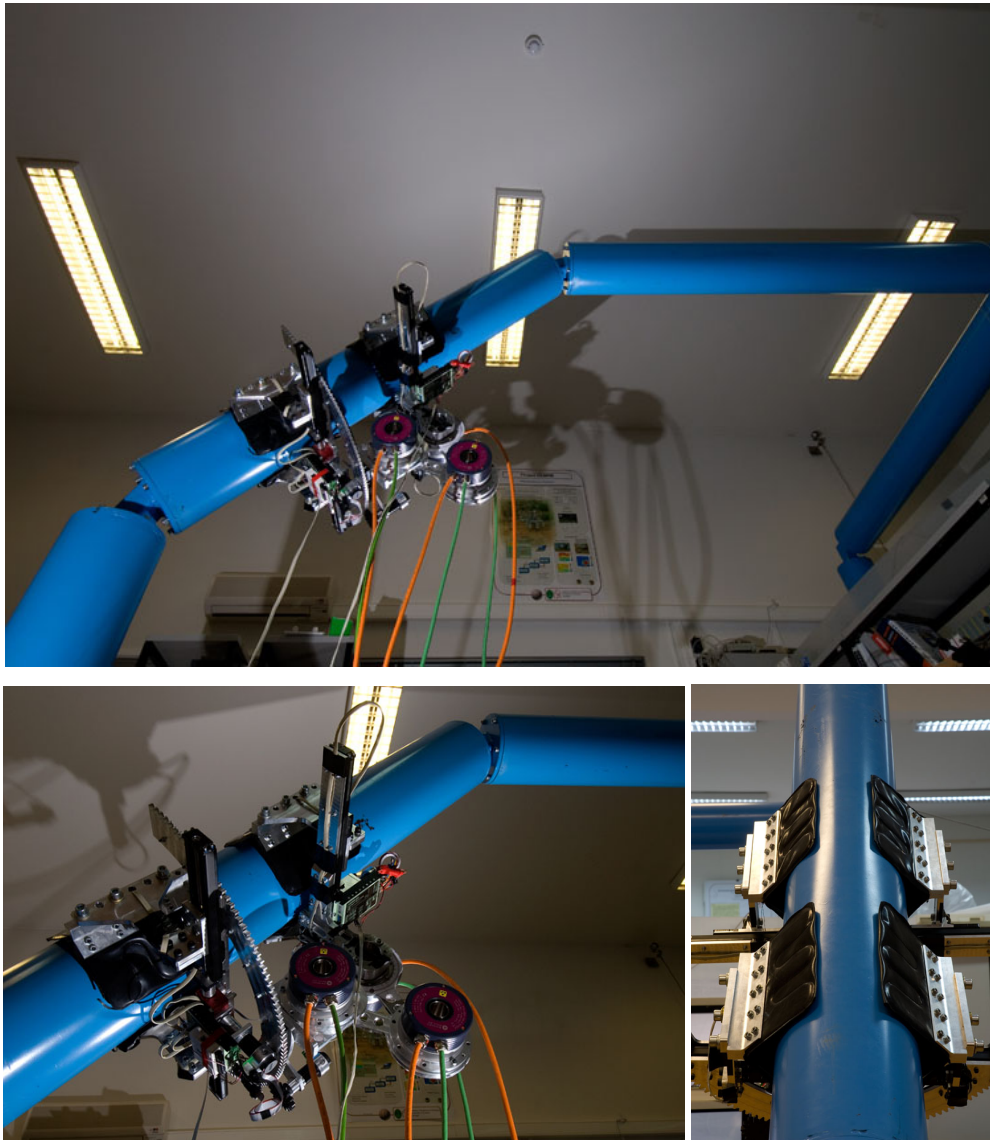
Figure 8.2: Sample snapshots of the experimental results (2).

most of the cases the FOS value was more than 3. As with this safety factor, the experiments were successful, we decided to increase the length of the links from 220 *mm* to a bigger value. Consequently, the considered FOS value for the motors torque (the ratio of the torque that motor can provide compared to the maximum required torque by joints) was reduced, but in the same time the stroke of each step increases and thus passing a 45° bend in one step would be possible. Furthermore, the length of each climbing step and thus the overall climbing speed increases. Some calculation and simulation showed that a link length of 350 *mm* makes it possible to pass a 45° bend in one step. Based on that new links were also developed and applied to the robot.

8.2.1 Safety and tolerance to power failure

One of the most important features of the robot, which was considered as one of the objectives of the project is tolerance to power failure. In other word, if any failure in the robot's power line happens, either in the actuators of the grippers or the climbing mechanism, the robot should not detach from the structure and fall down and even it should not slip down. To achieve this objective, the inertia at the output shaft of the motors were increased in order to lock the grippers in case of any power failure. This means that the multiplication of the motor inertia, gear box and the linear mechanism (Ball screws and linear guide) is big enough to avoid the grippers detachment or slippage because of the forces and torques caused by the robot weight.

To test this feature, the robot was attached to the structure and then all powers (For grippers and for actuators of the climbing structure) were disconnected. In this case the robot stayed on the structure for several days without any small slippage over the structure.

8.2.2 Test of grippers

Grippers have an effect on the robots safety (as discussed in the previous chapter), the maneuverability and also the stability of the robot. As previously mentioned, the grippers of the robot were designed in a way that a single gripper can overcome all forces and torques caused by the robot weight and reaction torques of the climbing mechanism actuators. Should this happen,

one of the grippers can detach from the structure and freely manipulate across the structure. In this case the other gripper which had grasped the structure should not slip on the structure, because this reduces the positioning accuracy. This was also tested and the test showed that the robot can stay on the pole, while only one of the grippers grasps the pole and the other gripper is set free and totally detached from the pole. A snapshot from this test is shown in figure 8.3.

3DCLIMBER can climb from structures with a minimum diameter of $200 \, mm$ to a maximum diameter of $350 \, mm$. In the other word, grippers can grasp structures with the mentioned diameters. To change these minimum and maximum values, one may use spacers to easily shift these values to smaller or bigger diameters, but the range will be always equal to $150 \, mm$. However due to the modularity of the system, the gripper can be easily changed and thus different grippers for different structure sizes or with bigger or smaller operating ranges can be used without any change on the climbing and control mechanisms.

8.3   Second experiment

The second experiments was performed after integration of the accelerometers, opto transistors, range finders, some of the mentioned high level algorithms, and also the new bigger links. In this case the robot was tested again. Figure 8.4 shows the new robot with bigger links ($350 \, mm$).

Using the opto transistor and a start up algorithm, the robot gets the zero reference points for all four motors of the climbing structure in its start up process. The strategy is that in the start up, while the upper gripper is connected, and the motors are off, the lower gripper will be free to go to an arbitrary position (the position is almost identical in all startups due to the fixed inertia of the robot parts). Then motors start to move in a pre specified direction until they find the opto transistors and indeed their zero reference points.

The error compensation algorithm has been also tested on the 3DCLIMBER robot. As stated
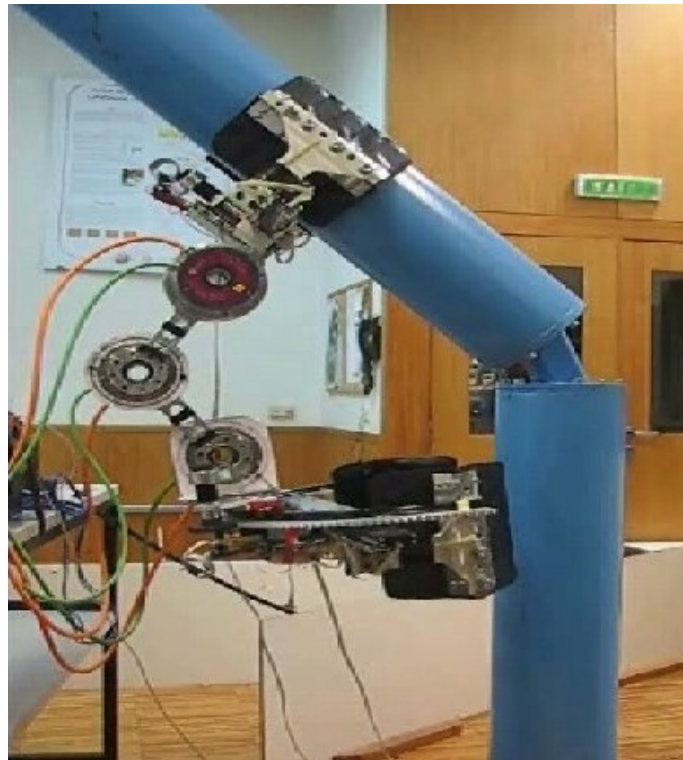
Figure 8.3: The robot can stay attached to the structure with only one gripper.
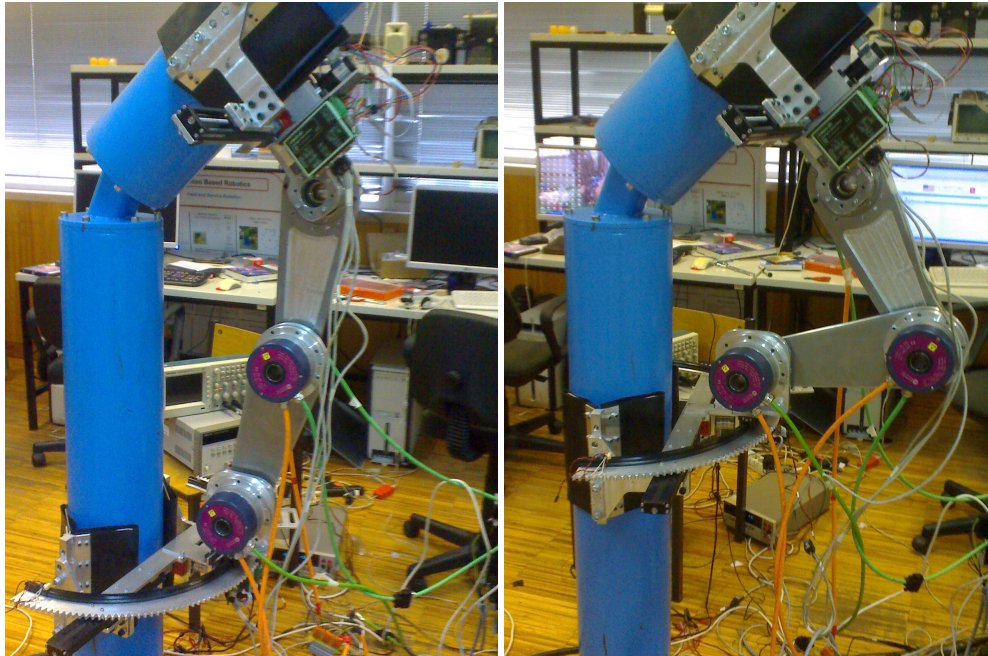
Figure 8.4: Sample snapshots of the experiments of the robot with the bigger links.

in the previous chapter, the analog accelerometer sensors provide a precision of up to $20'$ (about $0.3°$). As discussed in the previous chapter, this precision is valid even with the existence of vibrations up to 10 *Hz* during operation of the 3DCLIMBER. To attain such precision, the average value of 200 to 400 samples was calculated. To filter the effects of the mechanical vibrations of the links during operation of the 3DCLIMBER on the estimated angle, the sampling rate was set up at 100 *Hz* (10 times larger than the estimated frequency of the mechanical vibrations of the links). Using Sharp range finders, the distance between the manipulator and the structure was also estimated. Before integration of the sensors and the proposed algorithm, the base of the robot had always an angular deviation of $1 - 8°$. Due to the mentioned error sources, fine manipulation was not possible and also the gripper of the robot was not positioned correctly before gripping, adding extra constraint to the robot and leaving the system over defined. Not only was this likely to damage motors, but this error was accumulative and reached a level where the operator had to stop the robot and calibrate it manually. Taking advantage of the self-calibrating algorithm, the manipulator position was corrected in 2 phases. Using this algorithm, the 3DCLIMBER was tested on the structure. The angular deviation of the base and manipulator in the worst case were always less than $1°$, and it was not accumulating at each step. The positioning error of the manipulator on the Z direction was improved from 48 *mm* to 6.1 *mm* (values in the worst case, based on the maximum measured positioning error of the base). The worst case value was measured on the edges of the manipulator's workspace, where maximum torques are applied to the base of the robot, and geometrical parameters which are multiplied by the angular deviations are at their maximum. In most of the robot's workspace an accuracy of 3 *mm* was easily obtained.

Table 8.1 shows the main characteristics of the first version of the robot and table 8.2 shows the main characteristics of the second version with bigger links. The second version of the robot with bigger links is about 4 *kg* heavier than the first version and has a 20 *cm* bigger climbing step. Even both versions pass a $90°$ bend in a single step, but for a $45°$ bend, the first robot takes

Table 8.1: Main characteristics of the robot with 220 *mm* links

Degrees of Freedom	4
Quantity of Motors	6
Climbing Procedure	Step by Step
Weight (kg)	42
Material of the Parts	Aluminium 7075-T6
Robot Size (m)	$0.5 \times 0.6 \times 0.5$
Extended Robot Size (m)	$0.5 \times 0.6 \times 0.85$
Each step length (m)	0.35
Climbing Speed (m/min)	0.8
Minimum diameter of the pole that gripper is able to grasp	$200\,mm$
Maximum diameter of the pole that gripper is able to grasp	$350\,mm$

Table 8.2: Main characteristics of the robot with 350 *mm* links

Weight (kg)	46
Robot Size (m)	$0.5 \times 0.6 \times 0.55$
Extended Robot Size (m)	$0.5 \times 0.6 \times 1.10$
Each step length (m)	0.55
Climbing Speed (m/min)	1.10

3 step to pass the bend section while the second version can pass it in a single step.

Table 8.3 shows some of the improvements on the robot performance after integration of self-calibration algorithms and sensors.

8.4   Limitations and problems

Design of climbing robots faces many problems which is not the case for land machines, robots, and mechanisms. The most important problem is weight optimization of all parts. On the other hand, it should be noted that a robot which can climb from bends and branches faces much more problems than the one which can just climb a straight poles. Adding to them the problems concerned with the precise manipulation, it can be stated that the development of the 3DCLIMBER is similar to the development of an articulated precise industrial arm, which its base is not fixed

	Before integration	After integration
Angular error on placing the gripper on the structure	$1° - 8°$	$1°$
Positioning error type	Accumulative	Reset at each step
Maximum positioning error of the manipulator in the worst case	$48mm$	$6.1mm$

Table 8.3: Improvements on the robot's performance after integration of self-calibration algorithms and sensors

and contains errors and also should be light, furthermore the problem of gripping the structure should be addressed.

Consequently, the development of this robot includes the development of novel systems and algorithms. For instance, the problem of precise manipulation of flexible arms has been addressed previously by integration of strain gauges, but in 3DCLIMBER, we integrated inclinometers which not only helps compensating external errors related to the flexibility of the links, but also provides the estimation on the absolute angle of the links and grippers. This contributes precise positioning of the grippers which results in efficient gripping. Away from that, the size of the system imposed additional problems. As the objective of the project was to develop an industrial size robot with real industrial applications, the developed structure for tests and the robot itself were very large. Also operating the $560V$ actuators and their associated drivers face more problems than operating the small DC motors for small applications. Another remarkable problem was human resources. My personal background is mechanical engineering and I was requiring students to help in development of boards, small electrical sensors, etc. Unfortunately, students do not wish to involve in practical projects easily and even if they involve, they are not easily integrated into previously started projects and most of them prefer a personal project than a group work. Due to the lack of human resources and funding, I involved in many different

areas, ranging from conceptual and detailed mechanical design, installation, and calibration to design of the control system, integration of sensors, and development of the user interface.

Chapter 9

Biological Inspired Designs and Actuators

9.1 Introduction

Biological engineering, the engineering discipline that connects engineering and biology, encompasses both "connecting engineering to biology" and "connecting biology to engineering" in the engineering design process.

Both biologically inspired designs and biologically inspired actuators, have been considered in the conceptual and detailed design of the 3DCLIMBER. However to avoid the complexity and maintain conformity, it was not described in the previous chapters. In the other word, this analysis was performed in parallel with the conceptual and detailed design stages, but it is presented in this chapter for the sake of conformity. Two main research questions which have been investigated in the early stages of the 3DCLIMBER design were:

1. How much can the design of the 3DCLIMBER benefit from inspiration, anatomical specializations, and morphology of climbing animals? (Biologically inspired design.)

2. What are the advantages and disadvantages of the application of biological inspired actuators?

The former question was mainly studied during the conceptual design stage, and the latter during the detailed design stage.

9.2 Biologically inspired design

There are a diverse range of climbing animals; Animals that spend much of their time moving on steep, vertical, or overhanging surfaces and have appropriate adaptations for such scansorial locomotion. Climbing animals can be roughly divided into two groups: Those animals which move steep, vertical, or overhanging rock surfaces - rockface locomotion and those who move among tall vegetation - arboreal locomotion. These two environments may produce quite different methods of climbing. However, in some cases the climbing methods are similar, especially for small animals for which a rockface and a tree trunk may present similar problems

Figure 9.1: Gecko (Left) and opossum (Right) use balancing, clinging, and sticking techniques for climbing over trees.

for locomotion [Bri09]. PCRs may inspire more from the arboreal locomotion group, and their anatomical specializations, namely:

1. Balancing, clinging, and sticking; Examples: tree gecko, and opossum (figure 9.1).

2. Hanging; Examples: sloths (figure 9.2).

3. Leaping and gliding; Examples: bushbabies (figure 9.3).

4. Body clasping; Examples: Tree-kangaroos, coconut crabs, tree snakes, and goanna (figure 9.4).

5. Clasping with hands/feet; Examples: monkeys, squirrels, birds, and chameleons (figure 9.5).

6. Brachiating; Examples: Spider monkeys and gibbons (figure 9.6).

To discuss about anatomical specializations of animals, besides the climbing techniques, the gripping and supporting techniques which make it possible for climbing animals to hold themselves attach to the climbing surface, should be taken into account. Arboreal animals include some common aspects. They frequently display elongated limbs, in order to assist them in
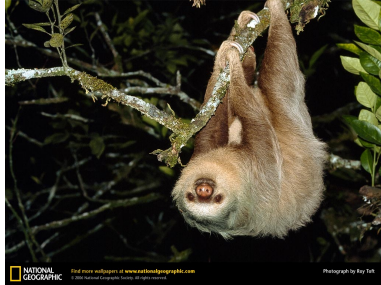
Figure 9.2: Sloths can hang from a branch.

Figure 9.3: Bushbabies leap up and glide down the tree.

Figure 9.4: Tree-kangaroos, goannas, coconut crabs, and tree snakes use body clasping techniques to attach themselves to the tree.

crossing gaps, reaching fruit or other resources, testing the firmness of support ahead, and in some cases, brachiation. However, some species of lizard display reduced limb size, in order to avoid the limb movement being obstructed by impinging branches. Many arboreal species have

Figure 9.5: Monkeys, squirrels, birds, and chameleons, clasping with their hands and feet.

Figure 9.6: Spider monkeys and gibbons can brachiate over trees and swing from one hold to the next.

prehensile tails, such as chameleons, spider monkeys, and possums, in order to grasp branches. In the spider monkey and crested gecko, the tip of tail has either a bare patch or adhesive pad, respectively, resulting in increased friction. Besides, claws can be used to interact with rough substrates and re-orient the direction of forces the animal applies. This is what allows squirrels to climb tree trunks that are so large as to be essentially flat, from the perspective of such a small animal. Adhesion is an alternative to claws, which works best on smooth surfaces. Wet

Figure 9.7: Humans use different techniques and additional tools to climb trees.

adhesion is common in tree frogs and arboreal salamanders, and functions either by suction or by capilary adhesion. Dry adhesion is best typified by the specialized toes of geckos, which use van der Wals forces to adhere to many substrates, even glass. Frictional gripping is used by primates, relying upon hairless fingertips. Squeezing the branch between the fingertips generates frictional force which holds the animal's hand to the branch. However, this type of grip depends upon the angle of the frictional force, thus upon the diameter of the branch, with larger branches resulting in reduced gripping ability. Animals other than primates which use gripping in climbing include the chameleon, which has mitten-like grasping feet, and many birds which grip branches in perching or moving about.

Brachiation is a specialized form of arboreal locomotion, used by primates to moves very rapidly while hanging beneath branches. It involves swinging with the arms from one handhold to another. Only a few species are brachiators, and all of these are primates; it is a major means of locomotion among spider monkeys and gibbons, and is occasionally used by female orangutan. Gibbons are the experts of this mode of locomotion, swinging from branch to branch with distances up to 15m (50ft), and travelling at speeds of as much as 56 km/h (35 mph). The adaptation for climbing is unique for each group of arboreal animals. All climbers must have strong grasping abilities, and they must keep their center of gravity as close as possible to the object being climbed. Because arthropods are generally small and, thus, not greatly affected by the pull of gravity, they show little specific structural adaptation for climbing. In contrast, the larger and heavier-bodied vertebrates have many climbing specializations. In both arthropods and vertebrates, however, no leg is moved until the others are firmly anchored [Bri09]. As the objective of the 3DCLIMBER project, was defined as development of an industrial robot, and the robot should be able to carry relatively heavy test and inspection devices, body and hand clasping and brachiating were more appropriate sources of inspiration, due to existence of bigger animals in this group e.g. tree-kangaroos, monkeys, goannas, and gibbons.

- **Brachiating:** A couple of researches has been conducted on brachiating robots. Fukuda et al. [FHK91] proposed and simulated a brachiating robot design. Saito and Fukuda (1996) [SF96] extended this work to create a three-dimensional robot with proportions that closely resemble a siamang. The robot consists of 12 DOF controlled by 14 motors, two of which are responsible for grasping. This robot is able to initiate brachiation from a stationary hanging position and continue moving beneath a horizontal series of ladder-like rungs. Kajima et al. (2003) [KHF03] constructed an even more complex robot consisting of 19 links and 20 actuators, called "Gorilla Robot II". It was designed to be able to walk bipedally or quadrupedally and brachiate. It has the approximate proportions of a siamang and weighs 20 *kg* [Ber04]. According to the studies [ULB03, UB03, CBL00],

the reason that the gibbons who weight usually less than 10 kg, can brachiate on 56 km/h is that they do not generate torques on their shoulders and even the amount of torque on their handhold is surprisingly less than 2 $N.m$ [CBL00]. Gibbons use potential to kinetic energy conversions and vise versa for accelerating and decelerating. This method might be studied in order to reduce the amount of the necessary torque on joints, thus reducing the size of the motor and consequently reducing the total weight of the system. For the objectives of the 3DCLIMBER, fast arboreal locomotion between many pipes was not the main consideration and rather a precise and stable locomotions in a single 3D structure was preferred. Therefore brachiating was not considered as an option for the 3DCLIMBER design.

- **Body and hand clasping**: As it can be seen in figures 9.4 and 9.5, body clasping technique takes advantage of hands and other parts of body like as tail in order to clasp a tree, climb across it, and to always keep their center of gravity closer to the trunk. Hand clasping group mainly use their hand and their feet. In both groups hands and feet are both used for clasping and locomotion.

9.2.1   Design inspiration

In the conceptual design stage, the morphology of climbing animals was studied and considered as a source of design inspiration. Most of the climbing animals, use a step-by-step based climbing in which they first fix a part of their body and then move up the other part of the body. In the next step the fixed part and the moving part change their role. The same strategy is used in the 3DCLIMBER. To clasp the trunk, they clutch the trunk between their fingertips. This is done by rotating their limb around the revolute joint of the shoulder. Clutching the branch between the fingertips generates frictional force which holds the animal's hand to the branch. However, this type of grip depends upon the angle of the frictional force, thus larger branches result in reduced gripping ability. To avoid this and to maintain the same grasping force, the design of the 3DCLIMBER gripper was based on prismatic motion and not revolute rotation. In this way

the gripping force is equal in all working range of the gripper.

For climbing over the structure, biological inspired designs were proposed in the conceptual design steps. As demonstrated in the conceptual design chapter, one of the concepts consisted of 4 arms, similar to what exists in most of climbing animals. However, further analysis revealed that this design leads to a heavier robot compared to the current single arm design. This is mainly due to the existing limits in the current technology of the actuators. The following simple calculation shows how far is the current technology from a biological arm. A human arm consists of seven degrees of freedom (not considering the fingers). According to Clauser [CMW69], the average mass of the human arm is about 3.2 kg with a standard deviation of 0.464 kg. Another analysis [KK98] on 44 male basketball players showed that the average value of their pick elbow torque on flexor is 103 $N.m$ and their shoulder joint is 160 $N.m$. On the other hand, a brushless motor equipped with a harmonic drive reduction which is used in the 3DCLIMBER, can deliver about the same torque, weighs 4.2 kg. As it can be seen, with the current technology driving one DOF of the arm requires an actuator heavier than the total arm. Therefore in design of the climbing mechanism, the minimum DOF which could perform the necessary objectives was considered.

On the other hand, application of biologically inspired actuators rather than electrical motors was also considered in order to reduce the weight of the robot. This part will be discussed in the next section.

9.3 Biologically inspired actuators

The second research question of this section was about biologically inspired actuators.
One of the major research areas in the biological inspired robots is biologically inspired actuators. Animals use their muscles to generate force for their movements.
Biologically inspired actuators, are actuators which can insert force or torque in a similar way

to the muscles. Pneumatic Artificial Muscles also known as "PAM", "PM", and McKibben artificial muscle, are the most similar artificial actuators to animal muscles. 9.8. "PAM" is famous as a very light actuator in the current literature. The reason stated in the literature for such a claim is their lower "power to weight" ratio compared to other types of actuators namely pneumatic cylinders and electrical motors. Consequently, application of PAMs rather than Electrical motors was considered in the design phase. However, the result of kinematics, workspace, and dynamic analysis of the climbing mechanism by application of PAMs showed that the application of PAMs will significantly increase the total weight of the robot compared to application of electrical actuators. Therefore, we made a more general analysis, comparing PAMs with electrical motors. A Pneumatic Muscle is an interesting actuator, developed in late 1950's for use in prosthetics. It shares many properties with actual muscles [CMCG95, NPG63] and is readily applicable to construction of biomechanically realistic skeletal models [CH96]. These actuators consist of a rubber bladder encased in mesh braid (with flexible yet inextensible strands) that is rigidly attached at either end to fittings (figure 9.8) [AKBQ06]. The physical configuration of the muscle gives the muscle its variable-stiffness spring like characteristics, non-linear passive elasticity, physical flexibility, and very light weight compared to other kinds of artificial actuators [CH96]. The latter is the most repeated advantage of PMs in the literature review expressed as "force to weight ratio" [CMCB97, KH00, TL00, VVHDL02], or "power to weight ratio" [HW90, TC00, MCBC95, NS02]. Current literature states that PMs have two significantly important characteristics:

- A power/weight ratio of about 1 W/g.

- A power/volume ratio of about 1 W/cm^3.

Both these ratios are about five times higher in comparison with an electric motor or a hydraulic actuator. Of course, a gas supply must be included in the total PM system, so this must be factored i when comparing the systems performance [RRPB03].
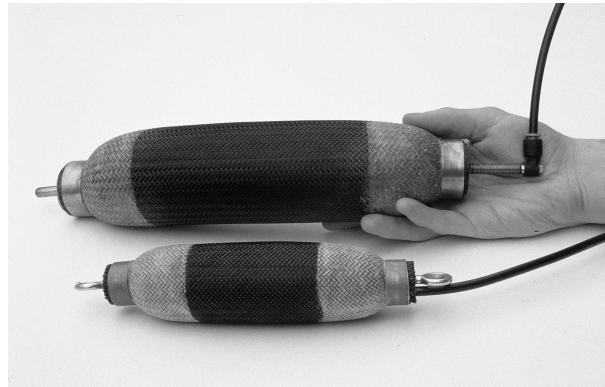
Figure 9.8: McKibben pneumatic actuators relaxed (top) and inflated (bottom) [rc08].

Due to consideration of PMs as light actuators in current literature, many robots were developed using PMs [AKBQ06, KAB02, VVvH$^+$05]. On the other hand, the "power to weight ratio" is not the only factor which should be evaluated when comparing the weight of a particular system. Having a lower power to weight ratio does not necessarily mean that using PMs would lead to a lighter system since many other factors should be considered. On design process of a revolute joint, the actuator should be able to deliver the required torque of "τ" in a specific angle of "α". Usually an electrical motor is coupled with a reduction gearing which might be heavier than the motor itself. Although the electrical motor provides the same power as the motor plus the reduction gearing, the power to weight ratios are different. Moreover, a pneumatic muscle may have a high power to weight ratio but it can apply a big force in a short stroke while a bigger stroke might be required. Therefore, an analysis on the amount of the output torque of motors, and output force and stroke os PMs can lead to more realistic results than comparing their power to weight ratio.

Another important parameter which was also neglected in the literature for the comparison between actuators is that driving a joint by pneumatic muscles require at least 2 PMs, as one PM only exerts force in one direction. Therefore for a fair comparison between the weight of the PMs and other actuators, namely pneumatic cylinders or electrical motors to be used in a spe-

cific system, the weight of the PM should be multiplied by 2. There might exist applications which do not require insertion of force (or torque) in both directions, but normally in robotics applications like an articulated arm, the torque control of the joints in both directions is required.

Plettenburg also questioned consideration of the PMs as one of the lightest actuators only due to their lower power to weight ratio compared with other actuators [Ple05]. He used the energy to weight ratio for comparison between PMs and pneumatic cylinders and concluded that PMs have a somewhat better energy to mass ratio compared to standard industrial cylinders, but a re-design of piston in cylinder actuators shows the energy to mass ratio of these cylinder actuators to be superior to pneumatic artificial muscles. But this research did not consider the fact that the weight of PMs should be multiplied by two to be able to drive a system in both directions.

Therefore, as it seems that previous comparisons between PMs and other actuators, were not precise, we made a comparison study between PMs and electrical actuators. The comparison is based on a single DOF revolute joint. To drive such a joint the actuator should be able to deliver a specific torque in a specific travel angle. Then the weight of the PMs which can drive such a joint and the weight of an electrical motor which can drive the same joint were estimated and compared. This procedure was repeated for a range of torques and travel angles and the selected data is presented as graphs and discussed.

9.3.1   Comparison procedure

A reliable method for comparison between the two types of actuators is to consider a specific system to be derived by both actuators and then compare the weight of the actuators. To do so, a one DOF joint is considered as it is shown in figure 9.9. The first link is fixed to the base, and the second link is derived by the joint. The objective is driving the revolute joint.

To drive the joint either an electrical motor or two PMs as flexor and extensor (figure 9.10) can be used. The joint should insert a torque equal to τ $N.m$ in a circular path of α radian. A com-
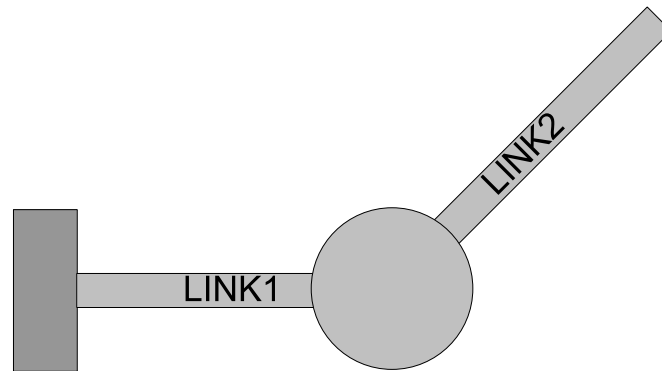
Figure 9.9: The one DOF joint considered for the comparison study.

Figure 9.10: A rotational joint derived by two PMs as extensor and flexor.

parison between the $\tau.\alpha$ values for a range of torques and travel angles of PMs and electrical motors was performed and graphs showing the weight of each system for a range of $\tau.\alpha$ were extracted.

It should be mentioned that the "energy to mass" ratio introduced in [Ple05], is more comprehensive than "power to weight" ratio for comparison between the weight of actuators, since the "energy to mass" ratio considers the torque and the travel angle of the actuator which are the most important parameters in selection of an actuator for a specific application. On the other

hand, an electrical motor can apply an equal force during the rotation of the joint but a PM exerts a bigger force at the beginning of its stroke and a smaller force at the end of its stroke. The "energy to mass" ratio integrals the force in the domain of the contraction. But to select an actuator for a revolute joint in an articulated robotic arm, the designer usually looks for the amount of the torque that the actuator can provide. The energy that a system can provide does not state the amount of torque that it can provide in a certain point of the workspace. Furthermore, the whole energy that an actuator generates may not be required by the joint and therefore our approach considers the amount of torque that the actuator can provide in a travel angle equal to the stroke that is demanded by the actuator.

Electrical Motors

Electrical motors are usually coupled with a reduction gearing in order to increase their torque and decrease their rotation speed. The efficiency and the weight of gearing systems for a specific reduction ratio vary according to the type of the gearing system. Harmonic Drive reduction systems are proved to be one of the most efficient and lightest solutions for gearing systems [LLC08]. Thus, the motors used in this study were selected from the Harmonic Drive products. The data of rotation velocity, nominal torque, maximum torque, and weight of more than 40 electrical rotary actuators (the combination of the electrical motor and the reduction gearing) were collected from Harmonic Drive catalogue. For this study the nominal torque of the actuators was considered for analysis. In contrast with PMs which have a limited stroke, electrical rotarty actuators can rotate continuously and therefore the travel angle α is infinite and consequently the $\tau.\alpha$ value is also infinite. This value is only limited by the travel angle demanded by the joint for a specific application. Thus, the nominal torque of the motor was multiplied by α values in a range of 1 to 5 radian, to calculate the $\tau.\alpha$ value. Therefore, depending on the required travel angle, one may select the appropriate curve in the graph shown in figure 9.13.
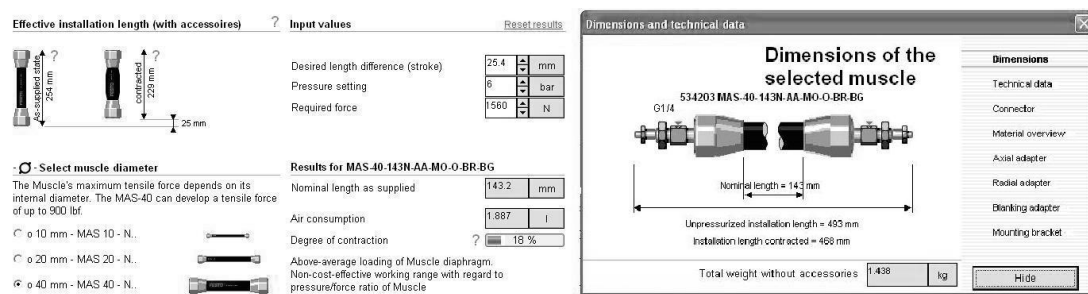
Figure 9.11: A screen shot from the MuscleSim package [FES08].

Pneumatic Muscles

Festo PMs were considered for the comparison due to the existence of a simulation package, MuscleSim, which provides the information about the weight, force, contraction, and length of the Pneumatic Muscles. Figure 9.11 shows a screen shot from the MuscleSim package. An earlier simple analysis made by the authors, showed that PMs from different suppliers, show very similar characteristics in practice, and thus using products from other companies will not change the results of this analysis. To drive the joint, two PMs as flexor and extensor are required (figure 9.12). The $\tau.\alpha$ value of the joint is always equal to the $F.s$ value of the pneumatic muscle, in which "s" is the stroke of the PM, and F is the contraction force at the maximum stroke. The reason is that the PM should rotate the second link via a lever and the longer the lever the higher the torque and the smaller the travel angle and vice versa. But the $F.s$ value for each PM remains constant and equal to the $\tau.\alpha$ value that it can deliver. Thus the $F.s$ value and the weight of 16 PMs with different lengths and outer diameters of 20mm and 40mm were obtained using MuscleSim package. A maximum contraction of 20 percent and a working pressure of 6 bars were considered for all PMs. Then the weight of each PM was multiplied by 2, as 2 PMs are required for driving the joint in both directions.
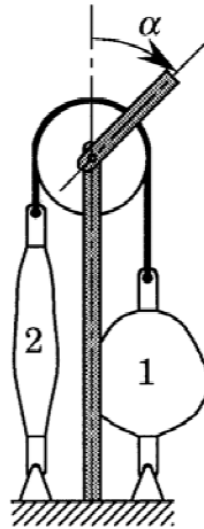
Figure 9.12: Two pneumatic muscles are required to drive a revolute joint in both directions [OL02].

9.3.2   Comparison

Figure 9.13 shows the $\tau.\alpha$ values against the weight for PMs and also for electrical rotary actuators with the output speed of 30 rpm and figure 9.14 shows the same graph for the rotatry actuators with the output speed in a range of 40 to 60 rpm. Each chart includes 6 curves, one curve for PMs, and five curves for electrical motors for travel angles of 1 to 5 radians.

 As it can be seen in figure 9.13, for low $\tau.\alpha$ values the PM curve is almost matching with the curve of the rotary actuator, if a travel angle of 1 radian is required, and for higher $\tau.\alpha$ values it matches the curve with the travel angle of 2 radians. A rough conclusion is that a PM system is lighter than the rotary actuator if the required travel angle for the joint is lower than 1 radians. But other factors should be considered for the actuator selection which will be discussed in the next section. Comparing the chart in figure 9.14 with the chart in figure 9.13, it can be concluded that for higher velocity requirements, the situation changes in favor of PMs. It means that for higher velocity requirements electrical motors provide lower $\tau.\alpha$ values. The final conclusion is that the rate of the increase in the value of $\tau.\alpha$ against the increase on the weight of the actuator in PMs is superior than those of rotary electrical actuators.
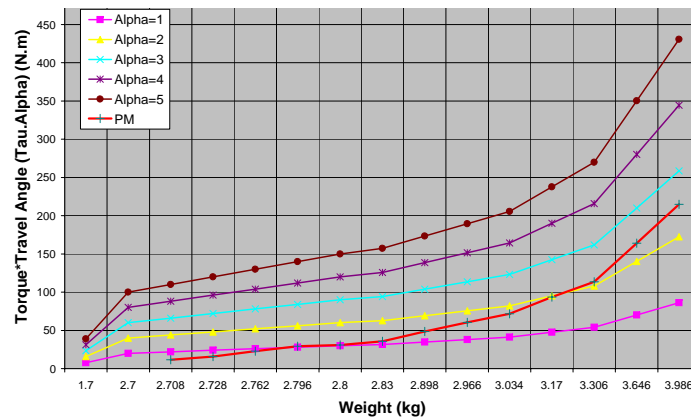
Figure 9.13: The $\tau.\alpha$ values for PMs (red) and electrical rotary actuators with 30 rpm rotational speed and travel angles of $\alpha = 1$ to $\alpha = 5$ against the weight of the actuators.

Installation Length

In a multi joint serial arm, the electrical rotary actuator is either directly coupled to the joint or installed on the base of the robot. In the second case, the motion is usually transferred with belts. But PMs are long actuators which are usually installed on the previous link of the joint (figure 9.12). Therefore, this link should be long enough so that the PM can be installed on that. On the other hand, longer links are not desired because they impose higher torque requirements to their previous joints. Thus if for a certain $\tau.\alpha$ value, the PM actuator is lighter than the electrical motor according to the presented charts, they can be used in the arm provided that the previous link of the joint is long enough to allow the installation of the PM. To facilitate the decision making process, the installation length of the PM samples was calculated using the MuscleSim and then a graph was extracted from those data which shows the installation length against each $\tau.\alpha$ value. The graph is shown in figure 9.15. It can be seen that the installation length is increasing with the increase of $\tau.\alpha$ values. The minimum possible installation length for a PM with a 20 *mm* diameter in Festo products is 145 *mm* considering the connections. On the other hand, for many types of biologically inspired robotic applications namely humanoid robots and mobile legged robots, the length of the links hardly exceeds 300mm. This restricts the usage of PMs in robotic applications. It should be mentioned that according to figure 9.13
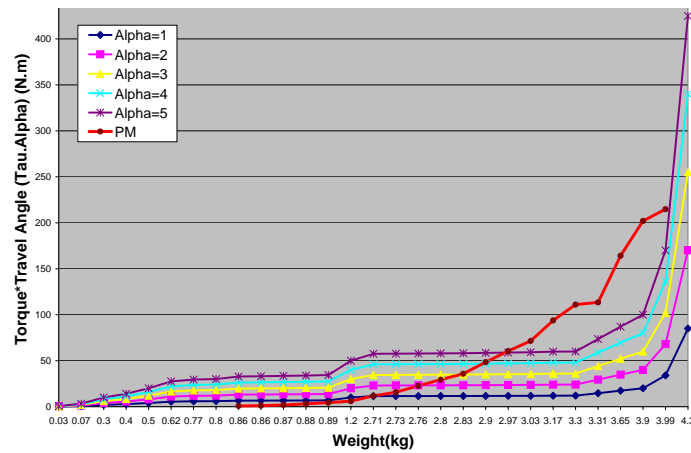
Figure 9.14: The $\tau.\alpha$ values for PMs (red) and electrical rotary actuators with 40 to 60 rpm rotational speed and travel angles of $\alpha = 1$ to $\alpha = 5$ against the weight of the actuators.
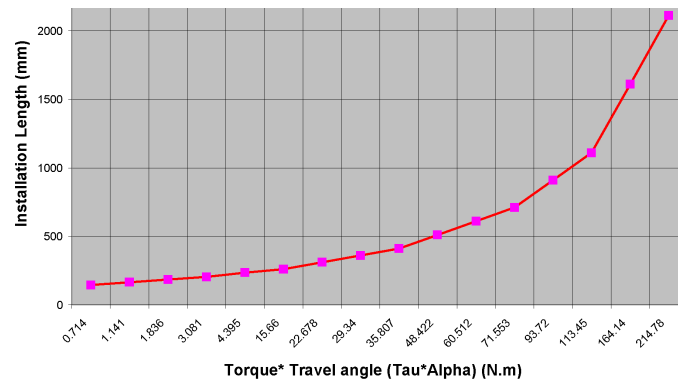
Figure 9.15: The installation length of pneumatic muscles against their $\tau.\alpha$ value.

for lower $\tau.\alpha$ values, the PM is a lighter solution than electrical rotary actuator provided that the required travel angle is less than 1 radian. According to figure 9.15 for an installation length of 300 mm, $\tau.\alpha = 22.6$ N.m, and according to figure 9.13 in this case the PM is a lighter solution if the required travel angle is less than 0.8 radian (equal to 45°).

9.3.3   Numerical example

To clarify the comparison study, a numerical example from the 3DCLIMBER climbing mechanism is presented. The schematic drawing of the climbing structure is shown in figure 4.2. According to the kinematics analysis, the optimum length of the 3rd link is 350 *mm* and the 3rd

joint demands for $\tau.\alpha = 250\,N.m$. A travel angle equal to 1.75 radians with an output speed of 60rpm is also desired. FHA-25C-160H Harmonic Drive rotary actuator can provide this value and weights 4.2 kg. The weight of the rotary actuator can also be estimated from figure 9.14. From the same chart it can be seen that a PM with the same $\tau.\alpha$ value weights slightly more than 4 kg. But figure 9.15 shows that the length of such a muscle is about 2500 mm which is 10 times more than the length of the 3rd link and consequently this PM can not be installed on the arm. There exist possibilities of installing the PAM in other places and not directly on the link, but a PAM with a length of 2500 mm is definitely very difficult to install on the 3DCLIMBER robot.

Parallel Configuration of PMs

PMs may be connected in parallel to have a greater $\tau.\alpha$ value in a shorter length, the final actuator, however, becomes spacious. Therefore, we analyzed the possibility of utilizing such configuration in the same numerical example. Thus a PM which can be fitted in 250mm should be selected. From figure 9.15, it can be seen that a pair of PMs with a 250mm setup length can deliver $\tau.\alpha = 20\,N.m$, and weighs 2.7 kg (figure 9.13). To deliver $\tau.\alpha = 250\,N.m$, 12 pairs of PMs should be connected in parallel. The total weight would be 32.4 kg which is about 8 times heavier than that of the FHA-25C-160H Harmonic Drive rotary actuator.

9.3.4 Discussion about biologically inspired actuators

As a rough conclusion from figure 9.13, if the required travel angle is more than 2 radians, electrical motors are lighter solutions and for a travel angle in the range of [0.7-2] it depends on the required torque. Eventually, if the application demands for a travel angle of less than 0.7 radian, then the PM solution might be slightly lighter than the electrical rotary actuator solution.

To see if PMs are a better solution than an electrical rotary actuator for a specific application one may use the graph showed in figure 9.13 and if PMs were lighter than it, the graph presented in figure 9.15 might be used in order to see if the geometry of the mechanism allows for installation

of the PM with the specific $\tau.\alpha$ value or not.

As it can be seen in figure 9.13 and figure 9.14, the difference between the weight of electrical rotary actuators and the weight of PMs is small, and therefore by changing one of the parameters of the comparison the curves might change. For example, considering 10 percent contraction instead of 20 percent, may slightly change the charts in favor of PMs. This study showed that PMs are not lighter than electrical rotary actuators as it is claimed in the current literature, and the weight of PMs and electrical rotary actuators are very similar for a big range of $\tau.\alpha$ values, provided that the design of the mechanism allows the installation of long PMs.

The fact that PMs require a big installation length, may make them unsuitable for many applications. For multi joint robotic arms, the length of each link is determined by many factors namely the geometrical constraints and the driving torque of its previous joints, and usually is determined before selection of actuators for the system, thus it can not be increased to fit the installation length of the PMs. But electrical rotary actuators do not have such restrictions. Eventually, the fact that the current literature is considering PMs as lighter solutions than electrical motors for robotics applications is highly questionable as they just consider the power/weight ratio of actuators which is not the main factor in the selection of a light actuator for a specific application. The point that a pneumatic muscle can only exert force in one direction is also neglected in the literature. Taking into account the other common problems on the control of pneumatic systems and also the weight of the gas reservoir on mobile robots make PMs even more unfavorable. The result of the analysis about PAMs has been published in [TMdA08a].

9.4   Conclusion

This chapter analyzed integration of biologically inspired design and actuators in the 3DCLIMBER in order to reduce the weight of the robot and increase the efficiency. The analysis was performed in the conceptual and detailed design phases of the project, but it is presented in this

chapter in order to maintain conformity. In order to evaluate the possibility of taking advantages of biological inspiration for promoting the 3DCLIMBER design, two main research questions were considered to be answered. Some studies and analyses were conducted which led us to the following answers:

1. Biologically inspired design, can be a source of inspiration in the design of climbing and gripping mechanisms. But due to limitations of the current technologies the exact emulation of climbing animals is not possible. Animals take advantage of numerous degrees of freedom in their arm and body, and also a big torque to weight ratio compared to current actuators technology. The gripping mechanism of the 3DCLIMBER is inspired by the climbing animals which clasp the structure by their hands and feet like monkeys.

2. Biologically inspired actuators, can not reduce the overall weight of the system. Our study showed that the current technology of PAMs, the most known biologically inspired actuators, is applicable for applications which demand for low stroke and torque.

Chapter 10

Conclusions and Future Works

The Plan of the 3DCLIMBER project is to develop an industrial PCR able to climb over 3D-complex human-made structures including T-junctions and perform test and maintenance tasks in those structures and also be able to semi-autonomously climb over 3D structures and perform in target tasks assisted by a remote operator. Such robot can have a high potential economic impact in several practical applications, including construction, testing, repairing, and maintenance of 3D complex human-made structures, namely electrical energy poles, nuclear and petrochemical plants, shipyards, selective cutting of tree branches, etc.

A fundamental difference between a climbing machine and a general ground based mobile robot is that the climber should support its own weight in the operating environment. On the other hand, climbing over 3D structures is more problematic than climbing on walls due to the lack of regular surfaces where vacuum or similar methods can be used for gripping. During the last decade, many wall climbing robots have been developed but only a few pole climbing robots were introduced. Furthermore as mentioned in the literature review, even these few developments on pole climbing robots mainly tried to address the climbing problem and not the manipulation problems. The developed robots were unable to pass either bends or T-junctions.

To design the 3DCLIMBER, some concepts were introduced and discussed and the best one

(regarding the project objectives) was developed. Weight optimization was considered as a key issue in design of custom design parts and selection of commercial parts and actuators. Then necessary sensors were integrated and a control application and a GUI was developed with $C\sharp$. An industrial size test structure was also developed and the robot was tested on that. The first test of the robot validated the concept and mechanical design of parts and mechanisms. Based on the success of the first experiment, the factor of safety was decreased in some designs but the climbing speed was increased. Also by integration of new sensors the manipulation precision was significantly increased and some gripping problems were solved. Self-calibration algorithms were also integrated, which significantly promoted the reliability of the performance for autonomous navigation.

In addition to the optimized design of the robot which led to a lighter robot compared to previously developed PCRs, the main improvement of this robot in comparison with the previously developed PCRs is its greater maneuverability and safety. First of all, the specific Z-axis rotation mechanism, provides fast manipulation around the structure which is necessary for inspection purposes and furthermore facilitates and accelerates locating the climbing mechanism below a specific bent section in T-junctions. The second reason which increases the maneuverability and safety are grippers. Long V-shaped grippers with their high inertia system (due to high ratio gearbox and low pitch ball screw of the rotational to linear transformation mechanism), allow the robot stay safely on the structure with only one of the grippers, while the other gripper can take the role of a manipulator and manipulate over the pole freely. Moreover, the grippers are tolerant to power failure meaning that they keep their last position in case of power failure without sliding on the structure. The third factor contributing to the improvements on the maneuverability is better manipulating accuracy. High accuracy is generally difficult to obtain in large manipulators due to well known error sources, but is even more difficult considering the fact that the base of the robot is not fixed and contains accumulative errors. This problem was addressed by integration of a self calibration algorithm and low cost redundant sensors such as

accelerometers and range sensors.

10.1   Future works and novel concepts

The current version of the 3DCLIMBER can reliably climb from 3D structures and manipulate on the structure with an acceptable accuracy. Yet, the project is not finished and still many areas can be explored. At the end of this thesis, I would like to not only explain the future works, but also to categorize the possible developments which can be considered for the continue of this project. Some suggestions are integration of new systems for the further development of the current version of the 3DCLIMBER. These suggestions do not change the mechanical design of the robot. The second category of suggestions introduces new concepts which can be developed separately or can be integrated to the 3DCLIMBER in order to promote its functionality. The second category does include some changes on the mechanical design of the parts and systems. In any case these suggestions are results of many hours of discussion between members of the team, and consequently are mature ideas rather than some pure undiscussed concepts.

In summary, research objectives of the team in the current status can be divided into 2 sections; First, completing and automating the current robot and second, evolution of the mechanical design. Consequently, following goals are considered for further developments:

10.1.1   A lighter climbing robot

- **Dedicated drivers:** Commercial motor drivers are multi purpose drivers and therefore are heavy. On the other hand, each driver is for one motor and as the robot uses 3 motors from the same type, some parts in all drivers are common (i.e. AC to DC converters). Therefore, development of dedicated drivers by application of commercial driver parts, would decrease the weight of the drivers and consequently the weight of the robot.

- **Novel designs:** Possible approaches for reducing the weight of the robot through lighter gripper and climbing mechanism design, and application of lighter non metallic materials

in the design should be examined.

10.1.2 Gripping mechanisms

The current gripper is a specific design for gripping circular profiles but is relatively heavy (About 10 kg each). On the other hand, some other approaches and designs should be analyzed in order to find probable solutions which are either lighter or offer more advantages. For instance, possibility of integrating semi flexible materials, that have compliance, flexibility, and enough rigidity for grasping can be studied. Combination of such materials with tactile sensors provides many advantages. For instance, compliance is necessary at the end effector (here gripper) in order to compensate small errors. This compliance can be considered by compliant materials or compliant mechanisms. Current gripper design is rigid which offers some advantages such as easier control, but integration of a gripper with some degree of compliance may address some of positioning problems, and thus should be investigated.

Here two gripping concepts are briefly introduced:

- **Biomimetic gripping mechanisms:** The Biomimetic approaches for climbing robot have been recently studied [MS06, GSC$^+$05, AMS08]. However these research are dedicated for small scale climbing robots in a gecko scale. For industrial and large scale robots, Biomimetic solutions can be studied through investigating the techniques used by large scale animals. A number of researches have been conducted on large scale Biomimetic climbing robots [YSHF08, SMA08], which have tried patterning human and monkeys climbing strategies to a robot for climbing poles and ladders. Even though the general ideas of the developed robot in [YSHF08, SMA08] are biomimetic, but the gripper designs are for climbing from structures with specific design and are not applicable to the 3DCLIMBER. Therefore, a research might be conducted on Biomimetic approaches for grasping the poles and upon reaching a successful light gripper design, it might be developed. Anyway during this project, a research was performed about climbing animals, but

this is a vast research area and can be explored more.

A problem associated with biological solutions for grippers is excessive degrees of freedom. A simplified Biomimetic solution can also be considered. Figure 10.1 shows a gripper concept consisting of several links which are connected through a revolute joint. It is inspired by human arm while encircling a pole or a palm tree. However, for circular profiles the angle of all revolute joints can be equal. Consequently, each gripper (both right and left arms) can be controlled by a single motor. Using gear mates or belts, revolute joints can be connected to each other and only the final joint will be derived by a motor.

- **Wheel gripper:** Another approach for fast pole climbing is using wheels. Continuous motion PCRs which use tires both for climbing and gripping to the pole are faster and lighter than step-by-step motion PCRs. Their main drawback is the lack of maneuverability. If one robot aims to perform more complicated tasks, namely welding, testing, or painting of pipes, then a step-by-step based design is a better choice. Integration of a dedicated designed wheel in the current design which acts as both grippers and for climbing along straight pole, will lead to a hybrid design with high climbing speed in straight poles as well as good maneuverability for passing bents and branches and maintenance. Another very important issue, which can be added by integration of wheels through a comprehensive design, would be navigation on the terrain. If such an integrated design can be designed and developed in a way that the climbing robot could also navigate on terrain, it would significantly increase the usability of the robot for real applications. In a petrochemical plant where many pipes with bents and branches exist, a robot should be able to navigate on terrain autonomously, reach to the specific pole and then climb from the pole. Using Hub motors technology, in which a brushless electrical motor is embedded inside a wheel would facilitate integration of wheels. Figures 10.2,10.3, and 10.4 show a concept for integration of wheels.
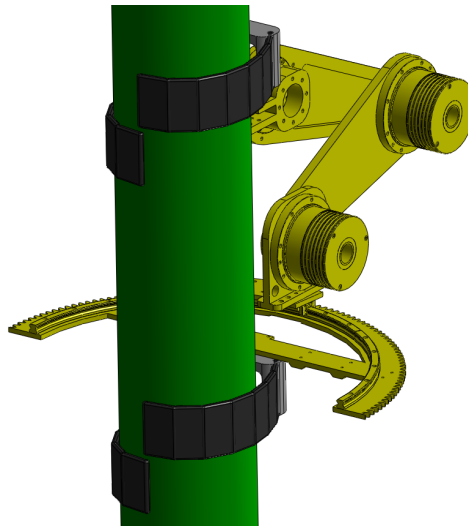
Figure 10.1: The conceptual design model of the one-DOF biologically inspired gripper concept.
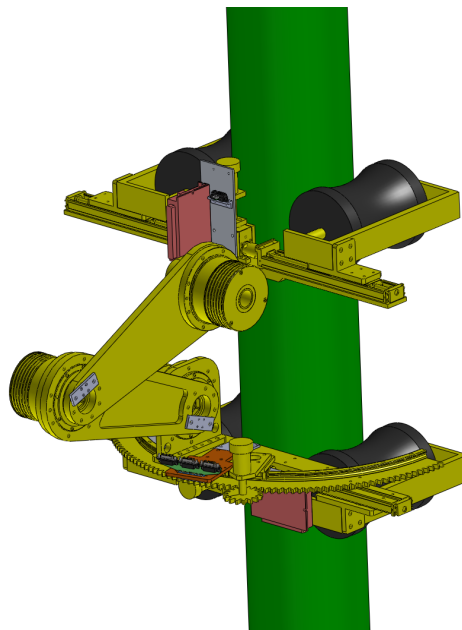
Figure 10.2: Integrated wheel increases the climbing speed

10.1.3   Server-client based remote control

As previously described, an architecture for the server-client based remote control of the 3DCLIMBER robot is under development. For a reliable communication between the server and the client ap-
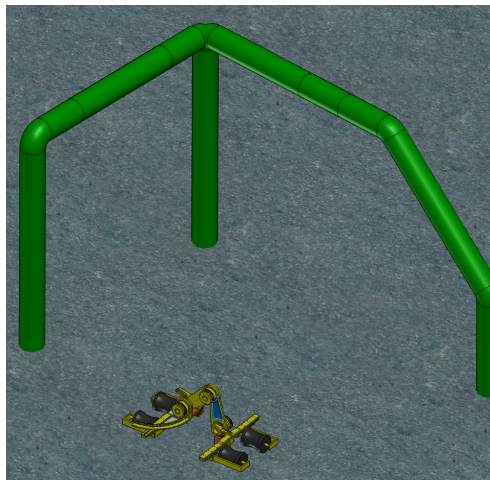
Figure 10.3: Wheels might help the robot moving on the ground.
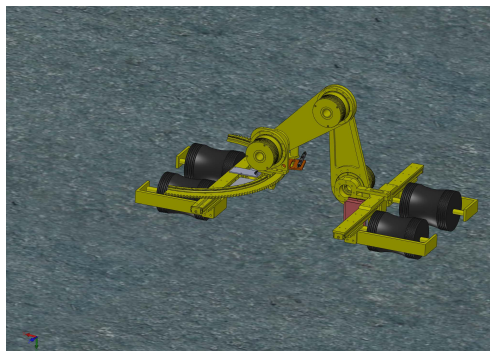
Figure 10.4: Close view of the robot model moving on the ground.

plications through TCP/IP protocol, the application should be tested and validated. Therefore, the validation of the application and its implementation on the 3DCLIMBER can be considered as one of the actions with the highest priority.

10.1.4 Absolute localization on the structure

Recently, the necessary hardware and software for the 3D localization of an object through trilateration methods using ultrasonic transceivers was developed under undergraduate projects. These systems can be used for localization of all types of mobile robots including the 3DCLIMBER. Consequently, application of one of this systems to the 3DCLIMBER is under study. Should

this happen, the server application can automatically locate the robot in a multi-branch structure and report the position.

10.1.5   Optimization of the gait generation

Currently the gait generation for controlling the 3DCLIMBER is not optimized. As an example, while the manipulator is moving above, the upper gripper remains open until the end of the movement. It means that these two actions are performed consecutively while it might be possible that some of their time lines coincide i.e. a part of both actions could be achieved simultaneously.

10.2   Main contributions and publications

Main contributions of this project are listed as below:

- Design of a benchmark for evaluation of pole climbing robots: A benchmark not only helps to compare different robots with the same application, but it also helps for a better perception of the problem which result in a better solution. The proposed benchmark for PCRs was the first one and up to now it is the only benchmark designed for PCRs and it was published as a book chapter in [TMdA08b]. The benchmark is designated for a wide range of PCR applications, so that one may find the best mechanism for a specific application by adjusting the weight factors.

- Design and introduction of 4 novel concepts for PCRs: These designs were not developed previously, being a source of novel ideas for conceptual design of PCRs [TMdAZ06].

- A detailed analysis on minimum DOF that a PCR requires in order to scan a 3D structure [TMdA06a]: This analysis is a source for anyone who intends to design a PCR able to pass bends and T-junctions. As a result of this study a minimum of 4 degrees of freedom are necessary for climbing across the 3D scaffolds. It also revealed that the determined 4 degrees of freedom are enough for scanning the whole structure surface. Previously

developed PCRs which were claimed that are able of passing bends had 6 degrees of freedom [BGA02, SSA$^+$06]. Extra degrees of freedom makes a robot massive and not necessarily increases its efficiency.

- Detailed design, optimization, kinematics, and dynamic analysis, development, and control of the 3DCLIMBER which can climb and manipulate on 3D structures with bends and branches [TMMdA08]: The robot fulfills all of the project objectives, being able to pass bends and T-junctions, operate in a range of cross section sizes, and overcome the step changes on the cross section. It is very tolerant to power failures and after grasping the structure, it can stay on the structure with the actuator's power disconnected.

- Development and integration of a self-calibration algorithm for the 3DCLIMBER which can be also used for other step by step based pole climbing robots: Accelerometers were integrated for the first time to climbing robots in order to measure the absolute inclination of the grippers and links from the horizon. This information helped to calibrate the gripper pose after each step, compensate the positioning errors of the manipulator (errors related to the placement of the base and also well known large manipulator errors), and perform precise manipulation. Integration of the sensors and the relative algorithms reduced the worst case positioning error of the robot from 48mm to 6.1mm [TMdA09].

- An analysis on arboreal locomotion of climbing animals, their gripping mechanisms and their climbing mechanisms [TMB10].

- A comparison analysis between pneumatic muscles and electrical motors: This analysis showed that pneumatic muscles are not appropriate for a wide range of robotic applications. Current literature persists that pneumatic muscles are lighter then electrical actuators considering that they have a lower power to weight ratio. In an article [TMdA08a], it was demonstrated that the "power to weight ratio" parameter is not a good parameter for comparison between the actuator weights. We showed in some charts that only in a

small range of applications which require short stroke or rotation the pneumatic muscles are lighter than electrical actuators and in a wider range of applications they are heavier.

Appendix A

Technologies

Commercial drivers, sensors, electronics, standard and non-standard mechanical components, etc. which have been integrated in the 3DCLIMBER robot are presented in this appendix.
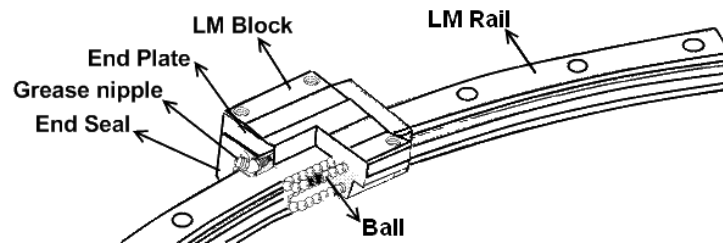
Figure A.1: Construction of the HCR guide and the slider.
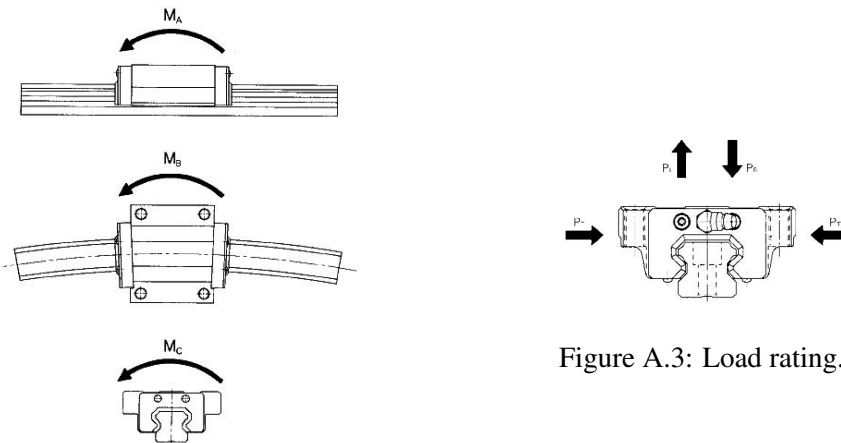
Figure A.3: Load rating.

Figure A.2: Permissible moments.
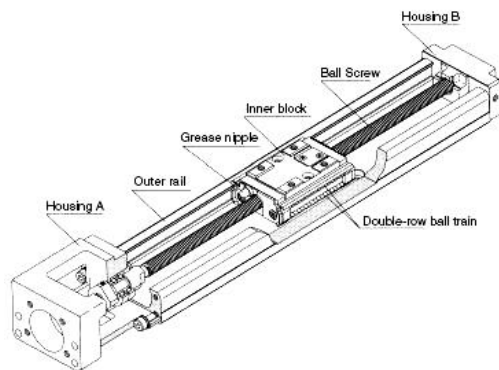
Figure A.4: The construction of the kr2602 THK guide.
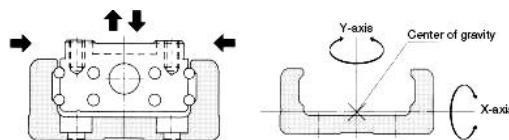
Figure A.5: Permissible forces and moments on kr2602 linear guide.
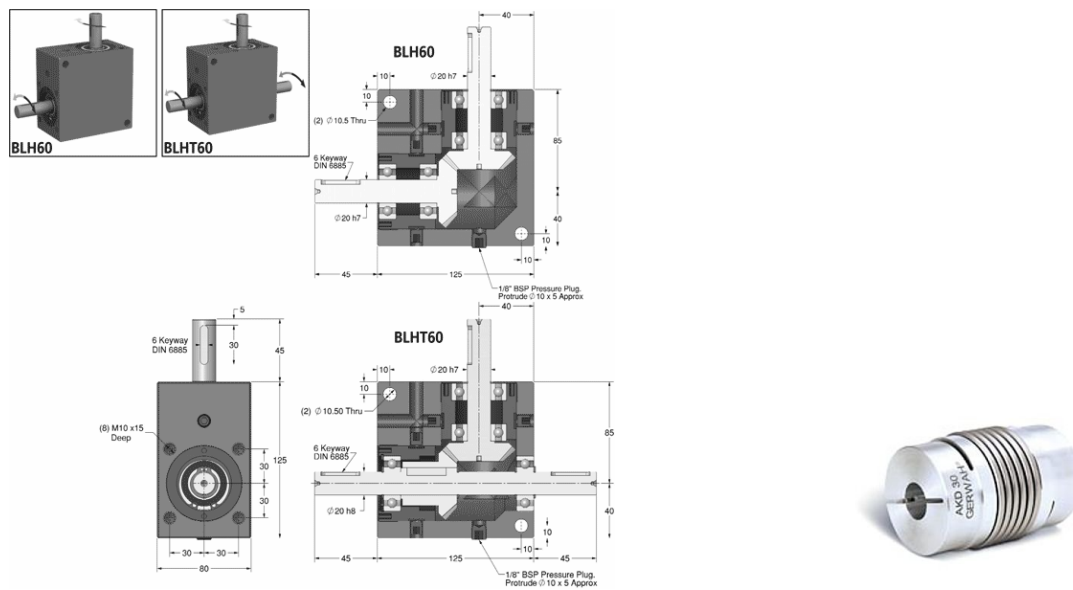
Figure A.6: The bevel gear (Left) and the coupling (Right) which have been used for the 3DCLIMBER'S grippers.
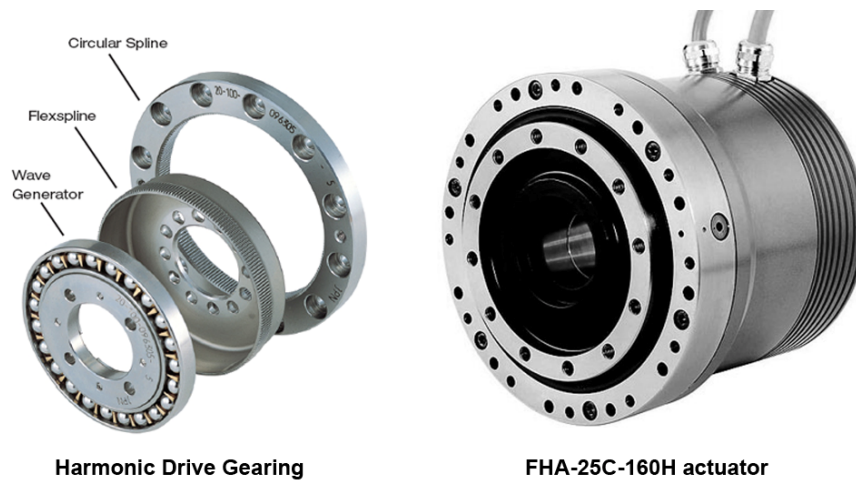
Figure A.7: The harmonic drive gearing technology (left) and the FHA-25C-160H actuator(right).
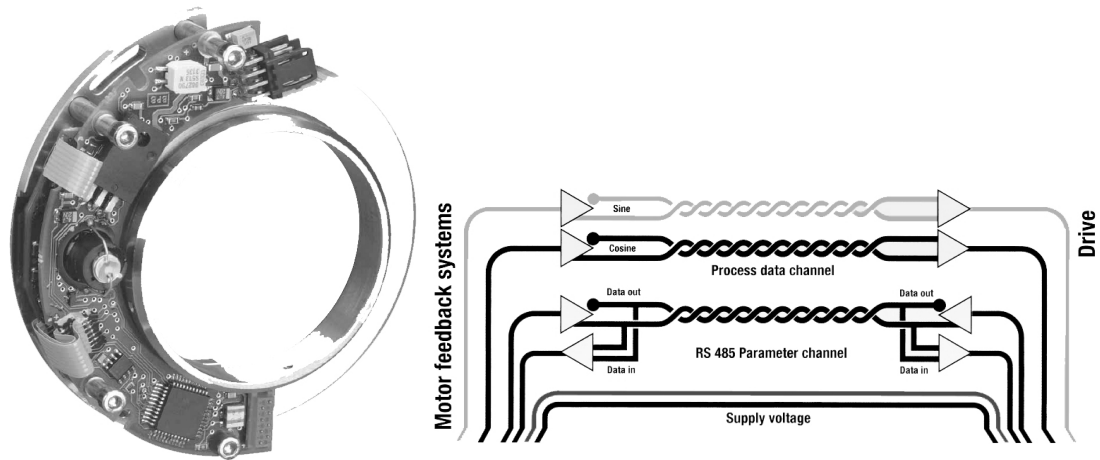
Figure A.8: SICK/STEGMANN sine/cosine encoder with HIPERFACE interface.

Figure A.9: IBL2403 DC motor driver from TECHNOSOFT.

Figure A.10: NI USB-6009 data acquisition from National Instrument.

Figure A.11: MDX 60/61B driver from SEW is used for control of AC motors of the 3-DOF serial arm

Appendix B

Notation

The following table summarizes the notation used in this thesis.

θ_n	Angular position of the nth joint.
ω_n	Angular velocity of the nth joint.
α_n	Angular acceleration of the nth joint.
I_n	Moment of inertia of the nth link.
m_n	Weight of the nth link.
s_{123}	$\sin(\theta1 + \theta2 + \theta3)$
c_{123}	$\cos(\theta1 + \theta2 + \theta3)$
$l_0, l_1, l_2 and l_3$	Length of the 4-DOF climbing mechanism links.
^4_0T	Transform matrix between the 4th and the 1st coordinate systems.
P_x, P_y, P_z, θ	Cartesian representation of the manipulator position relative to the base.
P_c	Current position of the manipulator relative to the base.
P_d	Desired position of the manipulator relative to the base.
τ_1, τ_2, τ_3	Driving torques of the 3-DOF serial arm.

Appendix C

Publications

[1] M.Tavakoli, L. Marques, and A.T. de Almeida. Development of an Industrial Pipeline Inspection Robot. Journal of Industrial Robots, Volume 37, Number 3, 2010 , pp. 309-322

[2] M.Tavakoli, L. Marques, and A.T. de Almeida. 3DCLIMBER: Climbing and Manipulation over 3D Structures, accepted by Journal of Mechatronics

[3] M.Tavakoli, L. Marques, and A.T. de Almeida. A Low Cost Method for Self Calibration of Climbing Robots, submitted to the Journal of Robotica (Under review)

[4] M.Tavakoli, L. Marques, and Fabio Bonsignorio, Biomimetic inspiration in climbing robots, CLAWAR2010, the 13th International Conference on Climbing and Walking Robots, Japan, 31 August- 3 September 2010

[5] M.Tavakoli, L. Marques, and A.T. de Almeida. Self Calibration of Step-by-Step Based Climbing Robots. In IEEE/RSJ International Conference on Intelligent Robots and Systems, IROS 2009, MO,USA, October 11 to 15 2009.

[6] M. Tavakoli, L. Marques, and A.T. de Almeida. A comparison study on pneumatic muscles and electrical motors. In 2008 IEEE International Conference on Robotics and Biomimetics ROBIO 08, Bangkok,Thailand, February 22 -25, 2009.

[7] M.Tavakoli, L. Marques, and A.T. de Almeida. Propose of a Benchmark for Pole Climbing Robots, Book Chapter, volume 44 of Springer Tracts in Advanced Robotics. Springer Berlin / Heidelberg, 2008.

[8] M. Tavakoli, A. Marjovi, L. Marques, and A.T. de Almeida. 3DCLIMBER: A climbing robot for inspection of 3D human made structures. In IEEE/RSJ International Conference on Intelligent Robots and Systems, IROS 2008, pages 41304135, Nice, France, 2008.

[9] M.Tavakoli, Lino Marques, Anibal T. de Almeida, "A comparison study on pneumatics muscles and electrical motors using the 3DCLIMBER as a case study" CLAWAR 2008, 8-10 September, Coimbra, Portugal

[10] M.Tavakoli, Lino Marques, Anibal T. de Almeida, "Path Planning for the"3DCLIMBER", CLAWAR 2007, 16-18 May 2007, Singapore

[11] M. Tavakoli, L. Marques, and A.T. de Almeida. Design and simulation of a novel pole climbing and manipulating robot. In Advances in Climbing and Walking Robots : Proceedings of the 9th International Conference, Brussels, Belgium, September 2006. CLAWAR.

[12] M. Tavakoli, L. Marques, and A.T. de Almeida. Pole climbing and manipulating robots: Assessment of different design categories. In Proc. 37th Intl. Symp. on Robotics, Munich, Germany, May 2006.

[13] M. Tavakoli, L. Marques, A.T. de Almeida, and M.R. Zakerzadeh. Climbing robots for human made 3d structures. In Advances in Climbing and Walking Robots: Proceedings of the 9th International Conference CLAWAR 2006, Brussels, Belgium, September 2006

Bibliography

[AB97]   R.C. Arkin and T. Balch. Aura: Principles and practice in review. *Journal of Experimental & Theoretical Artificial Intelligence, 9*, 2(3):175–189, 1997.

[ABG$^+$99] M. Abderrahim, C. Balaguer, A. Gimenez, JM Pastor, and VM Padron. ROMA: a climbing robot for inspection operations. *In Proceedings of IEEE International Conference on Robotics and Automation*, 3, 1999.

[AKBQ06] KS Aschenbeck, NI Kern, RJ Bachmann, and RD Quinn. Design of a quadruped robot driven by air muscles. In *The First IEEE/RAS-EMBS International Conference on Biomedical Robotics and Biomechatronics, BioRob 2006*, pages 875–880, 2006.

[AMS08] B. Aksak, M.P. Murphy, and M. Sitti. Gecko inspired micro-fibrillar adhesives for wall climbing robots on micro/nanoscale rough surfaces. In *IEEE International Conference on Robotics and Automation, ICRA 2008*, pages 3058–3063, 2008.

[AOT01] H. Amano, K. Osuka, and T.-J. Tarn. Development of vertically moving robot with gripping handrails for fire fighting. In *IEEE/RSJ Int. Conf. on Intelligent Robots and Systems*, pages 661–667, Maui, USA, Oct-Nov 2001.

[ASAR03] M. Almonacid, R. Saltaren, R. Aracil, and O. Reinoso. Motion planning of a climbing parallel robot. *IEEE Transactions on Robotics and Automation*, 19(3):485–489, 2003.

[ASS99] R. Aracil, R. Saltarén, and J.M. Sabater. TREPA, Parallel Climbing Robot for Maintenance of Palm Trees and Large Structures. *Proc. 2nd International Workshop & Conference on climbing & walking robots (CLAWAR)*, pages 453–461, 1999.

[BAH05] A. Baghani, M.N. Ahmadabadi, and A. Harati. Kinematics modelling of a wheel-based pole climbing robot (UT-PCR). In *Proc. IEEE Int. Conf. on Robotics and Automation*, Barcelona, April 18-22 2005.

[BDM00] D. Bevly, S. Dubowsky, and C. Mavroidis. A simplified cartesian-computed torque controller for highly geared systems and its application to an experimental climbing robot. *Journal of Dynamic Systems, Measurement, and Control*, 122:27, 2000.

[Ber04] J.E.A. Bertram. New perspectives on brachiation mechanics. *American Journal of Physical Anthropology*, 125, 2004.

[BGA02] C. Balaguer, A. Gimenez, and M. Abderrahim. ROMA robots for inspection of steel based infrastructures. *Industrial Robot: An International Journal*, 29(3):246–251, 2002.

[BGP+00a] C. Balaguer, A. Gimenez, J. Pastor, V. Padrón, and M. Abderrahim. A climbing autonomous robot for inspection applications in 3d complex environments. *Robotica*, 18:287–297, 2000.

[BGP+00b] C. Balaguer, A. Giménez, JM Pastor, VM Padrón, and M. Abderrahim. A climbing autonomous robot for inspection applications in 3D complex environments. *Robotica*, 18(03):287–297, 2000.

[BHdP09] F. Bonsignorio, J. Hallam, and A. del Pobil. Defining the Requisites of a Replicable Robotics Experiment. In *RSS2009 Workshop on Good Experimental Methodologies in Robotics*, 2009.

[Bri09] Encyclopædia Britannica. Locomotion http://www.britannica.com/EBchecked/topic/345861/locomotion. Encyclopædia Britannica Online, March 2009.

[CBL00] Y.H. Chang, J.E.A. Bertram, and D.V. Lee. External forces and torques generated by the brachiating white-handed gibbon (Hylobates lar). *American Journal of Physical Anthropology*, 113(2):201–216, 2000.

[CH96] C.P. Chou and B. Hannaford. Measurement and modeling of McKibben pneumatic artificial muscles. *IEEE Transactions on Robotics and Automation*, 12(1):90–102, 1996.

[CJS84] R.H. Cannon Jr and E. Schmitz. Initial experiments on the end-point control of a flexible one-link robot. *The International Journal of Robotics Research*, 3(3):62, 1984.

[CMCB97] DG Caldwell, GA Medrano-Cerda, and CJ Bowler. Investigation of bipedal robot locomotion using pneumatic muscleactuators. *IEEE International Conference on Robotics and Automation*, 1, 1997.

[CMCG95] D. G. Caldwell, G. A. Medrano-Cerda, and M. Goodwin. Control of pneumatic muscle actuators. *IEEE control system magazine*, 15(1):40, 1995.

[CMW69] C. E. Clauser, J. T. McConville, and Young J. W. Weight, volume and center of mass of segments of the human body. Technical Report AMRL TR 69-70, Wright-Patterson Air Force Base, Ohio (NTIS No. AD-710 622), 1969.

[Co.08] THK Co. http://www.thk.com/technical/download/e.html. Web reference, May 2008.

[Co.09] STEGMANN Co. http://www.stegmann.com/ltr2/access.php?file=pdf/4111.pdf. Web reference, May 2009.

[CPA+98] J. C., M. Prieto, M. Armada, , and P. G. de Santos. A six-legged climbing robot for high payloads. In *IEEE Int. Conf. on Cont. App*, pages 446–450, Trieste, Italy, Sept. 1998.

[Cra89] J.J. Craig. *Introduction to Robotics: Mechanics and Control*. Addison-Wesley Longman Publishing Co., Inc. Boston, MA, USA, 1989.

[Dil04] R. Dillmann. Benchmarks for robotics research. In *EURON*, Brussels, Belgium, 2004.

[dP06a] Angel P. del Pobil. Benchmarks in robotics research. In *IEEE/RSJ Int. Conf. on Intelligent Robots and Systems*, pages 1178–1185, Beijing, China, 2006. Workshop on benchmarks in robotics research.

[dP06b] Angel P. del Pobil. Why do we need benchmarks in robotics research. In *IEEE/RSJ Int. Conf. on Intelligent Robots and Systems*, Beijing, China, 2006. Workshop on benchmarks in robotics research.

[DT02] H. Dulimarta and R. L. Tummala. Design and control of miniature climbing robots with nonholonomic constraints. In *World Congress on Intelligent Control and Automation*, Shanghai, P.R.China, June 2002.

[ESL06] V. Etxebarria, A. Sanz, and I. Lizarraga. Control of a lightweight flexible robotic arm using sliding modes. *Arxiv preprint cs/0601054*, 2006.

[FES08] FESTO. Festo http://www.festo.com. Web reference, May 2008.

[FGL87] K.S. Fu, R.C. Gonzalez, and C.S.G. Lee. *Robotics: control, sensing, vision, and intelligence*. McGraw-Hill, Inc. New York, NY, USA, 1987.

[FHK91] T. Fukuda, H. Hosokai, and Y. Kondo. Brachiation type of mobile robot. In *Fifth International Conference on Advanced Robotics, ICAR.*, pages 915–920, 1991.

[GSC⁺05] Matthias Greuter, Gaurav Shah, Gilles Caprari, Fabien Tâche, Roland Siegwart, and Metin Sitti. Toward micro wall-climbing robots using biomimetic fibrillar adhesives. In *Proceedings of the 2005 IEEE International Conference on Robotics and Automation*, Barcelona, Spain, April 2005.

[GW62] V.E. Gough and S.G. Whitehall. Universal tyre test machine. *Proc. FISITA 9th Int. Technical Congress*, pages 117–137, 1962.

[HH01] H. Hosokai and F. Hara. Manoeuvrability passing over obstacles on a pipeline by a pipeline inspection. In *International Conference on Climbing and Walking Robots (CLAWAR 01)*, Karlsruhe, Germany, 2001.

[HKL⁺09] G. C. Haynes, Alex Khripin, Goran Lynch, Jon Amory, Aaron Saunders, Alfred A. Rizzi, and D. E. Koditschek. Rapid pole climbing with a quadrupedal robot. In *Proceedings of the IEEE International Conference on Robotics and Automation*, pages 479–485, 2009.

[HNT91] S. Hirose, A. Nagabuko, and R. Toyama. Machine that can walk and climb on floors, walls, and ceilings. In *Proc. IEEE Int. Conf. on Advanced Robotics*, pages 753–758, Pisa, Italy, June 1991.

[HOMS99] S. Hirose, H. Ohno, T. Mitsui, and K. Suyama. Design of in-pipe inspection vehicles for φ25, φ50, φ150 pipes. In *IEEE International Conference on Robotics and Automation*, volume 3, Detroit, MI, USA, 1999.

[HPC01] S. Hanks, M. E. Pollack, and R. Cohen. Benchmarks, test beds, controlled experimentation, and the design of agent architectures. In *AI Magazine*, volume '14, 2001.

[HW90] B. Hannaford and JM Winters. Actuator properties and movement control: biological and technological models. *Multiple Muscle Systems: Biomechanics and Movement Organization*, pages 101–120, 1990.

[Ins09] National Instrument. http://sine.ni.com/nips/cds/view/p/lang/en/nid/14605. Web reference, May 2009.

[JAU] JAUS. http://www.jauswg.org.

[JME01] A. Jacoff, E. Messina, and J. Evans. Reference test arenas for autonomous mobile robots. In *14th International FLAIRS Conference*, Florida, 2001.

[KAB02] T. Kerscher, J. Albiez, and K. Berns. Joint control of the six-legged robot airbag driven by fluidic muscles. In *RoMoCo '02, In Proceedings of the Third International Workshop on Robot Motion and Control*, pages 27– 32, Poland, November 2002.

[KH00] G.K. Klute and B. Hannaford. Accounting for Elastic Energy Storage in McKibben Artificial Muscle Actuators. *Journal of Dynamic Systems, Measurement, and Control*, 122:386, 2000.

[KHF03] H. Kajima, Y. Hasegawa, and T. Fukuda. Learning algorithm for a brachiating robot. *Applied Bionics and Biomechanics*, 1(1):57–66, 2003.

[KK98] B. Krzysytof and M. Klossowski. Muscle torque of male basketball players playing at different floor positions. In *16 International Symposium on Biomechanics in Sports*, Konstanz - Germany, July 1998.

[LL03] J. Lin and FL Lewis. Two-time scale fuzzy logic controller of flexible link robot arm. *Fuzzy Sets and Systems*, 139(1):125–149, 2003.

[LLC08] Harmonic Drive LLC. http://www.harmonicdrive.net/products/actuators/fha/. Web reference, May 2008.

[LMLW09] P. Li, S. Ma, B. Li, and Y. Wang. Design and Motion Analysis of an In-pipe Robot with Adaptability to Pipe Diameters. *Jixie Gongcheng Xuebao (Chinese Journal of Mechanical Engineering)*, 45(1):154–161, 2009.

[LWP80] J.Y.S. Luh, M.W. Walker, and R.P.C. Paul. Online computational scheme for mechanical manipulators. *Journal of Dynamic Systems Measurement and Control*, 102:69–76, 1980.

[LXGL07] J. Luo, S. Xie, Z. Gong, and T. Lu. Development of cable maintenance robot for cable-stayed bridges. *Industrial Robot: An International Journal*, 34(4):303–309, 2007.

[MCBC95] G.A. Medrano-Cerda, C.J. Bowler, and D.G. Caldwell. Adaptive position control of antagonistic pneumatic muscle actuators. *IEEE/RSJ International Conference on Intelligent Robots and Systems*, 1:378–383, 1995.

[MDM04] M.A. Meggiolaro, S. Dubowsky, and C. Mavroidis. Error identification and compensation in large manipulators with application in cancer proton therapy. *Revista Brasileira de Controle & Automação*, 15(1):71–77, 2004.

[MJD99] M.A. Meggiolaro, P.C.I. Jaffe, and S. Dubowsky. Achieving fine absolute positioning accuracy in large powerful manipulators. In *Proc. IEEE Int. Conf. on Robotics and Automation*, 1999.

[MNA06] S. Mahdavi, E. Noohi, and M.N. Ahmadabadi. Path planning of the Nonholonomic Pole Climbing Robot UT-PCR. *Robotics and Biomimetics, 2006. ROBIO'06. IEEE International Conference on*, pages 1517–1522, 2006.

[mot08] Maxon motor. http://www.maxonmotor.co.uk/maxon_motor_products_EC.htm. Web reference, May 2008.

[MS06] Carlo Menon and Metin Sitt. A biomimetic climbing robot based on the gecko. *Journal of Bionic Engineering*, 3(3):115–125, September 2006.

[Mur09] Carlos Jorge F. Murtinheira. Teleoperation of a 3d structure climbing robot. Master's thesis, Department of Electrical Engineering, Universoty of Coimbra, Coimbra, Portugal, January 2009.

[Neu94] W. Neubauer. A spider-like robot that climbs vertically in ducts or pipes. In *IEEE/RSJ Int. Conf. on Intelligent Robots and Systems*, pages 1178–1185, Munich, 1994.

[NH94] A. Nagakubo and S. Hirose. Walking and running of the quadruped wall climbing robot. In *Proc. IEEE Int. Conf. on Robotics and Automation*, pages 1005–1012, San Diego, CA, USA, May 1994.

[NPG63] V.L. Nickle, J. Perry, and A.L. Garrett. Development of useful function in the severely paralyzed hand. *The Journal of Bone and Joint Surgery*, 45(5):933, 1963.

[NS02] N. Nakamura and M. Sekiguchi. Developing a Robot Arm using Pneumatic Artificial Rubber Muscles. *Power Transmission and Motion Control: PTMC 2002*, 2002.

[OL02] F. Oaerden and D. Lefeber. Pneumatic artificial muscles: actuators for robotics and automation. *European Journal of Mechanical and Environmental Engineering*, 47(1):11–21, 2002.

[OO05]   T. Oya and T. Okada. Development of a steerable, wheel-type, in-pipe robot and its path planning. *Advanced Robotics*, 19(6):635–650, 2005.

[Pla]   Player/Stage. http://playerstage.sourceforge.net.

[Ple05]   DH Plettenburg. Pneumatic Actuators: a Comparison of Energy-to-Mass Ratio's. *9th International Conference on Rehabilitation Robotics, ICORR 2005.*, pages 545–549, 2005.

[Rac02]   M. Rachkov. Control of climbing robot for rough surfaces. In *IEEE Int. Workshop on Robot Motion and Control*, pages 101–105, Poland, Nov. 2002.

[RC05]   S. Roh and H.R. Choi. Differential-drive in-pipe robot for moving inside urban gas pipelines. *IEEE Transactions on Robotics*, 21(1):1–17, 2005.

[rc08]   Shaddow robot company. http://www.shadowrobot.com/. Web reference, May 2008.

[RJGB06]   J.C. Resino, A. Jardón, A. Gimenez, and C. Balaguer. Analysis of the Direct and Inverse Kinematics of ROMA II Robot. *Proceedings of the 8th International Conference on Climbing and Walking Robots (CLAWAR06)*, pages 869–874, 2006.

[RKL$^+$09]   S. Roh, D.W. Kim, J.S. Lee, H. Moon, and H.R. Choi. In-pipe robot based on selective drive mechanism. *International Journal of Control, Automation and Systems*, 7(1):105–112, 2009.

[Rob08]   Robotbooks. Robot materials. http://www.robotbooks.com/robot-materials.htm, june 2008.

[RP97]   T. Rossmann and F. Pfeiffer. Control of an eight legged pipe crawling robot. In *Int. Symp. on Experimental Robotics*, pages 353–346, Barcelona, 1997.

[RPRC01]   S. W. Ryu, J. J. Park, S. M. Ryew, and H. R. Choi. Self-contained wall-climbing robot with closed link mechanism. In *IEEE/RSJ Int. Conf. on Intelligent Robots and Systems*, pages 839–844, Hawai, USA, Oct-Nov 2001.

[RRPB03]   DB Reynolds, DW Repperger, CA Phillips, and G. Bandry. Modeling the Dynamic Characteristics of Pneumatic Muscle. *Annals of Biomedical Engineering*, 31(3):310–317, 2003.

[RSAS00]   Z. Ripin, T. B. Soon, A. Abdullah, and Z. Samad. Development of a low-cost modular pole climbing robot. In *Conference on Trends in Electronics, TENCON00*, pages 196–200, Kuala Lumpur, Malaysia, 2000.

[S.A08]   MEDEX Loncin S.A. http://www.medex.be/en/GemX-160_NDT.pdf. Web reference, May 2008.

[SARS05]   R. Saltaren, R. Aracil, O. Reinoso, and MA Scarano. Climbing parallel robot: a computational and experimental study of its performance around structural nodes. *see also IEEE Transactions on Robotics and Automation*, 21(6):1056–1066, 2005.

[SAS+99]   R. Saltarén, R. Aracil, J.M. Sabater, O. Reinoso, and L.M. Jimenez. Modelling, simulation, and conception of parallel climbing robots for construction and service. *2nd International Conference on Climbing and Walking Robots*, pages 253–65, 1999.

[sC08]   Msc software Co. http://www.mscsoftware.com/success/details.cfm?Q=286&sid=206. Web reference, May 2008.

[SE09]   SEW-EURODRIVE. http://www.sew-eurodrive.com/produkt/A43.htm. Web reference, May 2009.

[SF96]   F. Saito and T. Fukuda. A First Result of The Brachiator III— A New Brachiation Robot Modeled on a Siamang. In *Artificial life V. Cambridge, MA: MIT Press.*, pages 354–361, 1996.

[Sit08]   NDT Services Site. http://www.ndtservices.co.in. Web reference, May 2008.

[SMA08]   A. Sadeqi, H. Moradi, and M.N. Ahmadabadi. A human-inspired pole climbing robot. In *IEEE/RSJ International Conference on Intelligent Robots and Systems, IROS 2008*, pages 4199–4199, Nice, France, 2008.

[SSA+00]   R. Saltarén, J. Sabater, J. Azorin, O. Reinoso, and R. Aracil. Research and development of a pneumatic control for a parallel climbing robot. *In Proceeding of International Conference on Climbing and Walking Robots CLAWAR00*, pages 461–475, 2000.

[SSA+06]   J.M. Sabater, R.J. Saltarén, R. Aracil, E. Yime, and J.M. Azorın. Teleoperated parallel climbing robots in nuclear installations. *Industrial Robot: An International Journal*, 33(5):381–386, 2006.

[Ste65]   D. Stewart. A Platform with six degrees of freedom for flight simulation in pilot training. *Proceedings of Institution of Mechanical Engineers*, 180(15):371–378, 1965.

[Tay79]   R.H. Taylor. Planning and execution of straight line manipulator trajectories. *IBM Journal of Research and Development*, 23(4):424–436, 1979.

[TC00]   N. Tsagarakis and DG Caldwell. Improved modelling and assessment of pneumatic muscle actuators. *Robotics and Automation, 2000. Proceedings. ICRA'00. IEEE International Conference on*, 4, 2000.

[Tec09] Technosoft. http://www.technosoftmotion.com/products/OEM_PROD_IBL2403.htm. Web reference, May 2009.

[TL00] B. Tondu and P. Lopez. Modeling and control of McKibben artificial muscle robot actuators. *Control Systems Magazine, IEEE*, 20(2):15–38, 2000.

[TMB10] M. Tavakoli, L. Marques, and F. Bonsignorio. Biomimetic inspiration in climbing robots. In *Proceedings of the 13th International Conference on Advances in Climbing and Walking Robots, CLAWAR*, Japan, 31 August- 3 September 2010.

[TMdA06a] M. Tavakoli, L. Marques, and A.T. de Almeida. Design and simulation of a novel pole climbing and manipulating robot. In *Advances in Climbing and Walking Robots : Proceedings of the 9th International Conference*, Brussels, Belgium, September 2006. CLAWAR.

[TMdA06b] M. Tavakoli, L. Marques, and A.T. de Almeida. Pole climbing and manipulating robots: Assessment of different design categories. In *Proc. 37th Intl. Symp. on Robotics*, Munich, Germany, May 2006.

[TMdA08a] M. Tavakoli, L. Marques, and A.T. de Almeida. A comparison study on pneumatic muscles and electrical motors. In *2008 IEEE International Conference on Robotics and Biomimetics ROBIO 08*, Bangkok,Thailand, February 22 -25, 2009 2008.

[TMdA08b] M. Tavakoli, L. Marques, and A.T. de Almeida. *Propose of a Benchmark for Pole Climbing Robots*, volume 44 of *Springer Tracts in Advanced Robotics*, pages 215–222. Springer Berlin / Heidelberg, 2008.

[TMdA09] M. Tavakoli, L. Marques, and A.T. de Almeida. Self Calibration of Step-by-Step Based Climbing Robots. In *IEEE/RSJ International Conference on Intelligent Robots and Systems, IROS 2009*, MO,USA, October 11-15 2009.

[TMdAZ06] M. Tavakoli, L. Marques, A.T. de Almeida, and M.R. Zakerzadeh. Climbing robots for human-made 3d structures. In *Advances in Climbing and Walking Robots : Proceedings of the 9th International Conference*, Brussels, Belgium, September 2006. CLAWAR.

[TMMdA08] M. Tavakoli, A. Marjovi, L. Marques, and A.T. de Almeida. 3DCLIMBER: A climbing robot for inspection of 3D human made structures. In *IEEE/RSJ International Conference on Intelligent Robots and Systems, IROS 2008*, pages 4130–4135, Nice, France, 2008.

[TZV⁺04] M. Tavakoli, M.R. Zakerzadeh, G.R. Vossoughi, S. Bagheri, and H. Salarieh. A novel serial/parallel pole climbing/manipulating robot: Design, kinematic analysis and workspace optimization with genetic algorithm. In *21th Intl. Symp. on Automation and Robotics in Construction*, Jeju island, Korea, September 2004.

[TZVB05] M. Tavakoli, M.R. Zakerzadeh, G.R. Vossoughi, and S. Bagheri. A hybrid pole climbing and manipulating robot with minimum DOFs for construction and service applications. *Journal of Industrial Robot*, 32(2):171–178, March 2005.

[UB03] J.R. Usherwood and J.E.A. Bertram. Understanding brachiation: insight from a collisional perspective. *Journal of Experimental Biology*, 206(10):1631–1642, 2003.

[ULB03] J.R. Usherwood, S.G. Larson, and J.E.A. Bertram. Mechanisms of force and power production in unsteady ricochetal brachiation. *American journal of physical anthropology*, 120(4):364–372, 2003.

[VBT⁺04] G.R. Vossoughi, S. Bagheri, M. Tavakoli, M.R. Zakerzadeh, and M. Houseinzadeh. Design, modeling and kinematics analysis of a novel serial/parallel pole climbing and manipulating robot. *7th Biennial ASME Engineering Systems Design and Analysis conference, Manchester*, pages 19–22, 2004.

[VVHDL02] B. Verrelst, R. Van Ham, F. Daerden, and D. Lefeber. Design of a Biped Actuated by Pleated Pneumatic Artificial Muscles. *5th conderence on Climbing and Walking Robots and the Support Technologies for Mobile Machines*, 2002.

[VVvH⁺05] B. Vanderborght, B. Verrelst, R. van Ham, J. Vermeulen, and D. Lefeber. Dynamic Control of a Bipedal Walking Robot actuated with Pneumatic Artificial Muscles. *Proceedings of the 2005 IEEE International Conference on Robotics and Automation*, pages 1–6, 2005.

[web08] SolidWorks website. http://www.solidworks.com/. Web reference, May 2008.

[XBFK94] Y. Xu, H. Brown, M. Friendman, and T. Kanade. Control system of the self mobile space manipulator. *IEEE Trans. on Control Sys. Technology*, 2(3):207–219, 1994.

[YAH⁺04] B. Yazdani, M.N. Ahmadabadi, A. Harati, H. Moaveni, and N. Soltani. Design and development of a pole climbing robot mechanism. *the proceedings of Mechatronics and Robotics conference, Germany*, 2004.

[YHR01] M. Yim, S. Homans, and K. Roufas. Climbing with snake-robots. In *IFAC Workshop on Mobile Robot Technology*, Jejudo, Korea, 2001.

[YSD⁺99] W. Yan, L. Shuliang, X. Dianguo, Z. Yanzheng, S. Haoand, and G. Xuesban. Development and application of wall-climbing robots. In *Proc. IEEE Int. Conf. on Robotics and Automation*, pages 1207–1212, Detroit, USA, May 1999.

[YSHF08] H. Yoneda, K. Sekiyama, Y. Hasegawa, and T. Fukuda. Vertical ladder climbing motion with posture control for multi-locomotion robot. In *IEEE/RSJ International Conference on Intelligent Robots and Systems, 2008. IROS 2008*, pages 3579–3584, 2008.

[ZTVB04] M.R. Zakerzadeh, M. Tavakoli, G.R. Vossoughi, and S. Bagheri. Inverse Kinematic/Dynamic Analysis of a New 4-DOF Hybrid (Serial-Parallel) Pole Climbing Robot Manipulator. *Proceedings of the 7th International Conference on Climbing and Walking Robots (CLAWAR04)*, 2004.

[ZVB+04] MR Zakerzadeh, GR Vosoughi, S. Bagheri, M. Tavakoli, and H. Salarieh. Kinematics analysis of a new 4-DOF hybrid (Serial-Parallel) manipulator for pole climbing robot. *12th Mediterranean Conference on Control and Automation*, 2004.